TIME DOMAIN REFLECTOMETRY AS A METHOD FOR THE EXAMINATION OF DIELECTRIC RELAXATION PHENOMENA IN POLAR LIQUIDS

M. J. C. VAN GEMERT

STELLINGEN

1. De toepasbaarheid van de bestaande nauwkeurige TDR-technieken moet uit te breiden zijn tot relaxatiefrekwenties lager dan 10^7 Hz. In kombinatie met de door Hyde ontwikkelde laagfrekwent responsieapparatuur (werkend van 10^{-4} tot 10^6 Hz) bestaat hierdoor de mogelijkheid om op snelle wijze dielektrisch spektroskopisch onderzoek te verrichten voor frekwenties tussen 10^{-4} en $2\ 10^{10}$ Hz.

   P.J. Hyde, Proc. IEE, 117, 1819, (1970).

2. De mogelijkheid om uit de snijhoeken van het Cole-Cole plot en de ε'-as konklusies te kunnen trekken betreffende het asymptotisch gedrag van verschillende representaties van de dielektrische relaxatie in het tijdsdomein, vergroot de waarde van het Cole-Cole plot als grafische weergave van het dielektrische gedrag in het frekwentiedomein.

   Dit proefschrift, sektie 2.2.

3. De Kramers-Kronig relaties zijn een niet triviale konsekwentie van een fysisch schijnbaar triviale aanname.

4. De door Pichamuthu, Hassler en Coleman afgeleide relatie voor de opbouw van de stralingsdichtheid in een gepulste waterdamplaser, is door hen ten onrechte gebruikt om de gemeten afname van het laservermogen te interpreteren.

   J.P. Pichamuthu, J.C. Hassler, P.D. Coleman, Appl. Phys. Lett., 19, 510, (1971).

5. Bij theoretische studies betreffende spinheidsverdelingen ten gevolge van symmetrieverstorende substituenten in aromatische radikalen, dienen de invloeden van geometrische veranderingen van het molekuul in de beschouwingen te worden betrokken.

6. Ten onrechte nemen Hammond en Gallo in hun beschouwingen over de koncentratieafname van $Hg(6^3P_1)$-atomen in de afterglow van een Hg-Ar ontlading aan, dat de invloed van superelastische botsingen tussen elektronen en deze atomen verwaarloosd kan worden.

T.J. Hammond, C.F. Gallo, Appl. Optics, 11, 729, (1972).
J. Polman, P.C. Drop, J. Appl. Phys., 43, 1577, (1972).

7. De aanwijzingen dat de reflektiekoefficient van gewassen voor kortgolvige radargolven voornamelijk bepaald wordt door het zich boven de grond in de bladeren bevindende water, suggereert de mogelijkheid om op grote schaal met behulp van "Side Looking Radar" biomassa bepalingen te verrichten.

G.P. de Loor, AGARD conference proceedings No 90: Propagation limitations in remote sensing (1971), paper 12.
W.P. Waite, R.C. MacDonald, IEEE Trans., GE-19, 147, (1971).

8. De aanwezigheid van een defibrillator in een voetbalstadion is slechts dan zinvol wanneer eveneens de mogelijkheid is geschapen om een door ventrikelfibrillatie getroffen toeschouwer in leven te houden tot het moment dat hij met de defibrillator doeltreffender behandeld kan worden.

9. Wanneer Elizabethaanse luitmuziek op een moderne gitaar gespeeld wordt, is het aan te bevelen de g-snaar naar fis te verstemmen.

10. Het is te verwachten dat in het Nederlandse leger het rendement van de werkuren na de middagpauze zal toenemen indien de bar voor, tijdens en na de lunch gesloten zou blijven.

M.J.C. van Gemert, mei 1972

TIME DOMAIN REFLECTOMETRY AS A METHOD FOR THE EXAMINATION OF DIELECTRIC RELAXATION PHENOMENA IN POLAR LIQUIDS

PROEFSCHRIFT

TER VERKRIJGING VAN DE GRAAD VAN DOCTOR IN DE WISKUNDE EN NATUURWETENSCHAPPEN AAN DE RIJKS-UNIVERSITEIT TE LEIDEN, OP GEZAG VAN DE RECTOR MAGNIFICUS DR. W. R. O. GOSLINGS, HOOGLERAAR IN DE FACULTEIT DER GENEESKUNDE, VOLGENS BESLUIT VAN HET COLLEGE VAN DEKANEN TE VERDEDIGEN OP DINSDAG 6 JUNI 1972 TE KLOKKE 16.15 UUR

DOOR

MARTINUS JOHANNES COENRAAD VAN GEMERT

GEBOREN TE DELFT IN 1944

PROMOTOR: PROF. DR. C. J. F. BÖTTCHER

Aan mijn ouders
Aan Marian en Anja

CONTENTS

LIST OF SYMBOLS

A	frequency factor appearing in the Arrhenius equation, in Hz (Chapter 4)
A	parameter appearing in the non-ideal step function (Chapter 3)
a_0	$\lim_{\omega \to 0} f'_0(\omega)$, (section 2.2)
a_∞	$\lim_{\omega \to \infty} f'_\infty(\omega)$, (section 2.2)
C	distributed capacitance in Farad m^{-1}
$E(t)$	error voltage involved in $V_0(t)$ due to the unwanted step voltage (Chapter 3)
E_A	energy of activation appearing in the Arrhenius equation, in Kcal. mol^{-1} (Chapter 4)
$e(t)$	error signal involved in $R(t)$ due to the unwanted step voltage (Chapter 3)
$F(s)$	Laplace transform of the input voltage
$f_0(s)$	complex function appearing in the asymptotic behaviour of $\varepsilon(s)$ for $s \to 0$ (section 2.2)
$f_\infty(s)$	complex function appearing in the asymptotic behaviour of $\varepsilon(s)$ for $s \to \infty$ (section 2.2)
$f'(\omega)$	real part of $f(i\omega)$ (section 2.2)
$f''(\omega)$	imaginary part of $f(i\omega)$ (section 2.2)
G	distributed parallel conductance in $\Omega^{-1}\ m^{-1}$
$G(s)$	Laplace transform of the output voltage
$H(i\omega)$	transfer function of a linear and causal system
$h(t)$	system response to a delta function
I	current flowing through the conductors in Ampère m^{-2}
I_L	current flowing into a load impedance in Ampère m^{-2}
$I_n(x)$	modified Bessel function of the n-th order of argument x
$I_{\pm}$	current at the origin of the z-coordinate for the harmonic wave travelling into positive respectively negative direction, in Ampère m^{-2}
i	imaginary unit, $i = \sqrt{-1}$
L	distributed inductance in Henry m^{-1}
$\mathfrak{L}$	Laplace transform operator, defined by $\mathfrak{L}\{f(t)\} = \int_0^\infty dt\, e^{-st} \{f(t)\}$
$\mathfrak{L}^{-1}$	inverse Laplace transform operator, defined by $\mathfrak{L}^{-1}\{f(s)\} = \frac{1}{2\pi i} \int_{c-i\infty}^{c+i\infty} ds\, e^{st} \{f(s)\}$

M	total number of samples involved in $V_0(t)$
N	total number of samples involved in R(t)
O,o	order symbols used in the theory of asymptotic expansions (section 2.2)
P(t)	time domain reflectometry response to a heaviside step function
R	universal gas constant, in cal. mol^{-1}. K^{-1} (Chapter 4)
R	distributed series impedance in Ωm^{-1}
R(t)	time domain reflectometry response to a non-ideal step function
$R(\omega)$	frequency dependent amplitude of a complex function
$R_e(t)$	response to $V_e(t)$
r_o, r_i	radii of the outer and inner cylindrical conductors of a coaxial line, in m
s	variable in the complex frequency plane defined by $s = \gamma + i\omega$, γ is real and ω is the radial frequency
T	temperature, in ^oK
TDR	Time Domain Reflectometry
t	time, in sec (or picosec)
t(n)	actual time of the n-th sample
t_r	time reference
u(t - T)	translated heaviside step function
V	voltage between conductors, in Volts
V(t)	total voltage at the air-dielectric interface, in Volts
$V_{\pm}$	voltage at the origin of the z-coordinate for the harmonic wave travelling in positive respectively in negative direction, in Volts
$V_0(t)$	incident voltage, in Volts
$Z(i\omega)$	characteristic impedance of a dispersive coaxial line, in Ω
Z_0	characteristic impedance of an empty coaxial line, $Z_0 = 50\ \Omega$
α	empirical parameter appearing in the Cole-Cole relation, $0<\alpha< 1$
β	empirical parameter appearing in the Davidson-Cole relation, $0<\beta< 1$
$\Gamma(x)$	gamma function for argument x; $-\infty<x<\infty$
$\gamma(\omega)$	propagation constant of frequency ω
γ	real axis of the complex frequency s-plane, defined by $s = \gamma + i\omega$
Δ	error in the time reference procedure, in picosec (Chapter 3)
Δ_a	accidental part of Δ, in picosec (Chapter 3)
Δ_s	systematic part of Δ, in picosec (Chapter 3)
Δ_t	delay between the input voltage $V_0(t)$ and the output voltage R(t), in sec (Chapter 1)
$\Delta\Theta$	phase error of the reflection coefficient, in Deg/GHz
$\delta(t)$	Dirac delta function
$\varepsilon(i\omega)$	dimensionless complex dielectric permittivity, $\varepsilon(i\omega) = \varepsilon'(\omega) - i\varepsilon''(\omega)$

$\varepsilon'(\omega)$	real part of $\varepsilon(i\omega)$
$\varepsilon''(\omega)$	negative imaginary part of $\varepsilon(i\omega)$
$\underline{\varepsilon}$	permittivity of the vacuum, in Farad m^{-1}
ε_0	low-frequency dielectric permittivity
ε_∞	high-frequency dielectric permittivity
ζ	parameter denoting the low-frequency angle of the Cole-Cole plot with the ε' - axis, in units of $\pi/2$; $0 \leq \zeta \leq 2$ (section 2.2)
η	parameter, denoting the high-frequency angle of the Cole-Cole plot with the ε' - axis, in units of $\pi/2$; $0 \leq \eta \leq 2$ (section 2.2)
$\Theta(\omega)$	frequency dependent phase of a complex quantity, in radians or degrees
$\mu(i\omega)$	relative magnetic permeability of a material
$\underline{\mu}$	magnetic permeability of the vacuum, in Henry m^{-1}
ν	frequency, in Hz
ν_0	relaxation frequency denoted by $2\pi\nu_0\tau_0 = 1$, in Hz
ν_m	frequency limit, defined by $R(\nu) = 0$, $\nu > \nu_m$; in Hz
$\rho(i\omega)$	complex reflection coefficient
$\rho'(\omega)$	real part of $\rho(i\omega)$
$\rho''(\omega)$	imaginary part of $\rho(i\omega)$
$\rho(\infty) \equiv \rho(\varepsilon_\infty)$	$\lim_{\omega \to \infty} \rho(i\omega)$
$\rho(0) \equiv \rho(\varepsilon_0)$	$\lim_{\omega \to 0} \rho(i\omega)$
$\rho_1(\varepsilon) = \left(\frac{d\rho}{d\varepsilon}\right)$	$-1/[\sqrt{\varepsilon}(1+\sqrt{\varepsilon})^2]$
σ	low-frequency conductivity, in $\Omega^{-1}\ m^{-1}$
σ_c	conductance of the material of the conductors, in $\Omega^{-1}\ m^{-1}$
τ	transmission coefficient (section 1.2,3)
τ	time distance between two samples, in picosec
τ_r	rise time of the non-ideal step function defined by $V_0(\tau_r) = 1$ (Chapter 3)
τ_0	dielectric relaxation time
ω	angular frequency, in sec^{-1}

INTRODUCTION

The experimental investigation of dielectric relaxation phenomena is one of the oldest spectroscopic techniques, originating from the last decades of the former century[1]. Usually it is the aim of this type of spectroscopy to study the behaviour of electric dipoles in terms of absorption and dispersion from interactions of the material with an applied electro-magnetic field. Two properties are characteristic for dielectric spectroscopy in comparison to other spectroscopic methods. First, this spectroscopic method can generally be studied by classical physical methods, and second, it covers an unusually large frequency range, from about 10^{-4} Hz up to about 10^{11} Hz. Due to this enormous range, the evaluation of the dielectric permittivity of a polar medium, denoted by $\varepsilon(i\omega) = \varepsilon'(\omega) - i\varepsilon''(\omega)$, requires a number of laborious frequency domain techniques, each of them demanding a specialized knowledge in electrical engineering.

In general, dielectric permittivity is measured by determining, for all frequencies of interest, the impedance of a capacitor, or for high-frequencies, the impedance of a transmission line, filled with the dielectric material. For very low-frequencies, an alternative method is known[2,3], studying the transient response of a filled capacitor, in terms of its charge decay, to a step voltage excitation.

The extension of this "time domain" method to the microwave region has in recent years been enabled by the development of modern tunnel diodes and wide band sampling systems. In electronic and communication engineering a technique called "Time Domain Reflectometry" (TDR)[4] is in use since the early sixties and has been succesfully applied to the qualitative analysis of transmission line systems. The TDR-method has also been used for the quantitative measurement of electric circuit parameters[5] (network analysis).

In such a method a step voltage, which simultaneously contains all frequencies of interest, will be propagated in a low loss coaxial line. The shape of the step voltage remains constant as long as the transmission characteristic impedance and the propagation constant are unchanged. When the transmission line contains a section with a different characteristic impedance (for instance a section filled with a polar medium), part of the step voltage will be reflected at, and part of it will be transmitted through the discontinuity. The location of the discontinuity is then determined by the time difference between the incident and reflected pulses. When the discontinuity posesses a frequency dependent characteristic impedance, i.e. it is dispersive, the shape of the reflected pulse (and also of the transmitted pulse) is changed. The quantitative behaviour of the discontinuity, in terms of its frequency dependence, can then be determined by Fourier analysis of the incident and reflected voltages.

The possibility of applying time domain reflectometry to the quantitative study of dielectric permittivity was first indicated by Fellner-Feldegg[6,7], although other workers have independently reported in this field as well[8-10]. The interpretation and accuracy of TDR-measurements have recently been improved by Whittingham[11] and especially by Suggett, Quickenden-MacNess, Loeb and Young[12,13].

It should be noted that for measuring polar liquids, this technique has advantages above the point-by-point frequency domain methods, especially in the microwave region where savings in time and equipment are considerable. It also serves as an important technique to fill the measurement gap of about 10^8 - 3 10^9 Hz which exists in the frequency domain. This gap is more basically present for special polar media, such as pasta's and granular substances[14] (where an electrode system cannot be placed inside the material), than for polar liquids. However, two remarks should be made in this connection. The first is that one needs a fast digital computer and the second is that, in general, the accuracy of time domain methods is less, compared with frequency domain techniques. However, the computer has become a common piece of equipment nowadays, and in the microwave region the time domain technique is not necessarily inferior to the frequency domain method.

In this thesis the evaluation of the dielectric permittivity, from TDR-experiments, is discussed both theoretically and experimentally. Time domain reflectometry is essentially a method which:

(1) uses propagation characteristics (such as the characteristic impedance) as the object of the measurement and

(2) is based on the equivalence of the "time domain", and the "frequency domain" description of a linear and causal system.

Therefore introductions are given in Chapter 1 to the theory of transmission line propagation and to linear response theory.

In Chapter 2, the TDR-response is studied in the case of an ideal step function, for dielectrics with known characteristics in the frequency domain. First, numerical results are presented for a number of current descriptions of dielectric behaviour. Afterwards, the asymptotic behaviour of the TDR-step response has been related to the asymptotic behaviour of the permittivity in the Cole-Cole plot representation.

In Chapter 3 the experimental measurement procedure is outlined. It is shown how Fourier analysis of the actual output and input voltages (the input voltage consists of the response against a short circuit) may give the correct values of the dielectric parameters. Some deficiencies of the TDR-equipment and of the method of analysis are discussed. An analysis of the uncertanties involved in the experimental determination of the dielectric parameters, due to errors in the incident and reflected voltages, is also presented. The results of this analysis are that the un-

certanties in ε_o, ε_∞ and τ_o are about 5%, 20% and 7.5% respectively.

In Chapter 4 a number of experimental results are given. First, test experiments on some of the mono-alcohols are presented, which confirm the accuracy and applicability of the TDR-method. Since accurate dielectric measurements for propanol-1 are lacking for temperatures above 0^o C, this alcohol is studied in more detail. The results agree very well with data available for low-frequencies at lower temperatures. In the last part of Chapter 4, a study is presented of dielectric measurements on mixtures of some mono alcohols with carbon tetrachloride. Besides the influence of the carbon tetrachloride on the relaxation time characterizing the main dispersion range of the alcohols, the influence on the activation energy is discussed.

CHAPTER 1

DERIVATION OF THE RELATION BETWEEN THE TIME DOMAIN REFLECTOMETRY RESPONSE AND THE DIELECTRIC PERMITTIVITY

1.1 INTRODUCTION TO TIME DOMAIN REFLECTOMETRY

The time domain reflectometry system, as used in the determination of dielectric properties, is shown schematically in Figure 1.1. It consists of a step generator, producing a fast rise time step (about $35 \cdot 10^{-12}$ sec), a sampling system detecting the signal voltage between the coaxial conductors and transforming this high-frequency signal into a low-frequency output, an oscilloscope on which the low-frequency signal is displayed and the measuring cell consisting of a coaxial line filled with a polar liquid. The length of this cell is considered to be infinite for convenience.

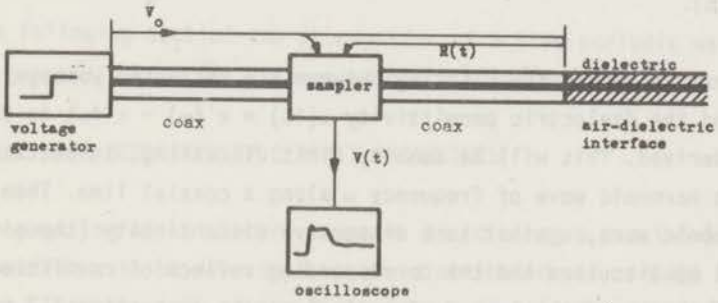

Figure 1.1 The experimental TDR-system.

The voltage step from the step generator is propagated along the coaxial line. The sum of the fast rise time step and the reflected voltage from the air-dielectric interface is detected and sampled by the sampling system and displayed on the oscilloscope. The total voltage, V(t), is then given by:

$$V(t) = V_0(t) + R(t)$$

where V(t) is the totally displayed voltage, $V_0(t)$ the voltage of the fast rise time step and R(t) the reflected voltage from the air-dielectric interface. A typical shape of V(t) is given in Figure 1.2, together with a reconstruction in terms of $V_0(t)$ and R(t). Because the behaviour of the system is studied in reflection, the signal detector is placed between the step generator and the cell, introducing a time delay Δ_t between the input $V_0(t)$ and the output R(t). For theoretical and practical rea-

sons, however, the situation shown in Figure 1.3 is to be used.

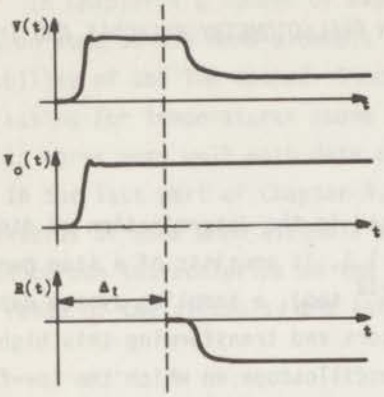

Figure 1.2 Typical wave form of V(t) and its reconstruction in terms of $V_0(t)$ and R(t).

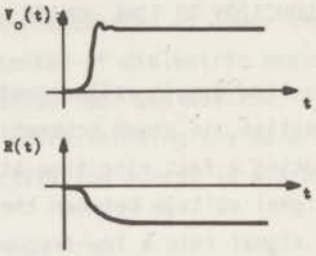

Figure 1.3 Response R(t) to input $V_0(t)$ when the response theory is to be used.

In the next sections, the relation between the reflected voltage in the time domain, R(t), and the dielectric permittivity $\varepsilon(i\omega) = \varepsilon'(\omega) - \varepsilon''(\omega)$ in the frequency domain will be derived. This will be done by first discussing, in section 1.2, the propagation of a harmonic wave of frequency ω along a coaxial line. Then the reflection of the harmonic wave, against some dispersive discontinuity (the air-dielectric interface), will be discussed and the corresponding reflection coefficient will be expressed as a function of the lumped circuit elements. In section 1.3 an introduction to linear response theory is given, discussing the integral relation between the system's transfer function in the frequency domain and the pulse response in the time domain. In particular it is shown how the transfer function can be obtained from the system's response, in the time domain, to some arbitrary input function. In section 1.4 the results from the foregoing discussions are applied to the determination of dielectric permittivity from TDR-experiments.

1.2 THEORY OF COAXIAL TRANSMISSION LINES

1.2,1 INTRODUCTION

In general a transmission line consists of two conductors separated by a dielectric material. Transmission of an electro-magnetic field is coupled with a voltage difference between and current flowing through the conductors. When measured at a transverse plane, the total currents in both conductors are of equal magnitude and of

opposite direction.

Although the conductors may be of any geometry and conducting material, the only line considered in this work is a coaxial line, consisting of an outer cylindrical conductor with radius r_0 and an inner cylindrical conductor with radius r_i, separated by some material (for instance air or a dielectric medium). In Figure 1.4, the geometry and sign conventions for voltage and current are indicated.

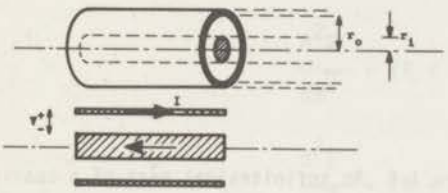

Figure 1.4 Geometry and sign conventions for voltage and current in a coaxial transmission line.

In the following section the propagation of a time periodic wave in a coaxial line will be treated, using the concept of circuit analysis.

1.2,2 A COAXIAL LINE DESCRIBED BY CIRCUIT PARAMETERS

The propagation of an electro-magnetic field along a coaxial line filled with a dielectric medium will be described by the distribution of voltage and current along the line. The behaviour of the dielectric medium is represented by the dielectric permittivity $\epsilon(i\omega)$ and the low-frequency conductivity σ, i.e. by the quantity $\epsilon(i\omega) - i\sigma/\omega$. The coaxial line is divided into infinitesimal parts of length dz. The voltage and current changes across a length dz are then represented by the voltage and current changes across a linear passive network, described by the usual parameters R ($\Omega\ m^{-1}$), C (Farad m^{-1}), L (Henry m^{-1}) and G ($\Omega^{-1}\ m^{-1}$) representing the distributed series resistance-, capacitance-, inductance- and parallel conductance per unith length of the coaxial line.

At a certain fixed frequency the values of the parameters R, C, L and G, which are constants everywhere along the line, are determined by geometry, dimension, material of the conductors and the dielectric medium only.

An infinitesimal part, length dz, of the line can then be represented as is shown in Figure 1.5. The voltage change across this length dz is:

$$\text{Voltage change} = \frac{\partial V}{\partial z}\,dz = -\,R\,dz\,I - L\,dz\,\frac{\partial I}{\partial t}$$

Similarly, the current change is given by:

$$\text{Current change} = \frac{\partial I}{\partial z}\,dz = -\,G\,dz\,V - C\,dz\,\frac{\partial V}{\partial t}$$

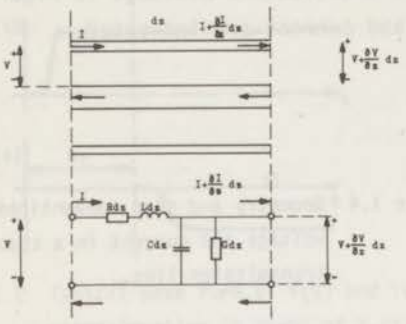

Figure 1.5 An infinitesimal part of a coaxial line and its circuit equivalence.

Dividing by dz gives the following equations which are known as the "telegraphy equations":

$$\frac{\partial V}{\partial z} = -\,R\,I - L\,\frac{\partial I}{\partial t} \tag{1.1}$$

$$\frac{\partial I}{\partial z} = -\,G\,V - C\,\frac{\partial V}{\partial t} \tag{1.2}$$

To obtain an equation containing voltage only, equation (1.1) is differentiated with respect to z and equation (1.2) with respect to t. By similar manipulations an equation containing current only is obtained. The results are:

$$\frac{\partial^2 V}{\partial z^2} = LC\,\frac{\partial^2 V}{\partial t^2} + (LG + RC)\,\frac{\partial V}{\partial t} + GR\,V \tag{1.3}$$

$$\frac{\partial^2 I}{\partial z^2} = LC\,\frac{\partial^2 I}{\partial t^2} + (LG + RC)\,\frac{\partial I}{\partial t} + RG\,I \tag{1.4}$$

It is very difficult to give a general solution of equations (1.3) and (1.4) if none of the circuit parameters L, C, R and G can be neglected[15]. However, when time periodic fields are involved, differentation with respect to time equals multiplication by $i\omega$.

The quantity ω is the radial frequency of the wave. Equations (1.1) - (1.4) can then be written as:

$$\frac{dV}{dz} = -(R + i\omega L)\, I \tag{1.5}$$

$$\frac{dI}{dz} = -(G + i\omega C)\, V \tag{1.6}$$

$$\frac{d^2V}{dz^2} = (R + i\omega L)\,(G + I\omega C)\, V \tag{1.7}$$

$$\frac{d^2I}{dz^2} = (R + i\omega L)\,(G + i\omega C)\, I \tag{1.8}$$

V and I are now complex functions of z only. Using the following abbreviation:

$$\gamma^2 = (R + i\omega L)\,(G + i\omega C) \tag{1.9}$$

the mathematical solutions of equations (1.7) and (1.8) yield:

$$V = V_+ e^{-\gamma z} + V_- e^{\gamma z} \tag{1.10}$$

$$I = I_+ e^{-\gamma z} + I_- e^{\gamma z} \tag{1.11}$$

V_+ denotes the voltage at z = 0 for the harmonic wave travelling in a positive direction, while V_- is the voltage at z = 0 for the harmonic wave travelling in the opposite direction. Combining equations (1.11) and (1.6) the following result is obtained:

$$V = Z(I_+ e^{-\gamma z} - I_- e^{\gamma z}) \tag{1.12}$$

$$Z = \sqrt{\frac{R + i\omega L}{G + i\omega C}} \tag{1.13}$$

The quantity Z, as defined by equation (1.13), is called the characteristic impedance of the line. It is defined as the ratio of voltage to current for the positively travelling wave and of voltage to minus current for the negatively travelling wave at any point of the transmission line. The characteristic impedance is in general complex, indicating that the line filled with a polar medium is dispersive. For an empty coaxial line G = 0 holds, while in practice R can be neglected with respect to ωL

indicating that an empty transmission line can often be considered as non-dispersive.

From transmission line theory, the following relation for the series impedance $R(\omega)$ can be derived[16,17]:

$$R(\omega) = \frac{\sqrt{\omega}}{2\pi} \frac{\sqrt{\mu\,\underline{\mu}}}{\sqrt{\sigma_c}} \left(\frac{1}{r_i} + \frac{1}{r_o} \right) \tag{1.14}$$

where $\underline{\mu}$ is the magnetic permeability of vacuum, μ the relative magnetic permeability of the conductors (which are presumed not to be ferro-magnetic, i.e. $\mu = 1$, σ_c the conductivity of the conductor material and r_i, r_o the radii of the inner- and outer conductors respectively. For L, C and G the calculations yield[16,17]:

$$L = \frac{\mu\,\underline{\mu}}{2\pi} \ln (r_o/r_i) \tag{1.15}$$

$$C = \frac{2\pi\underline{\varepsilon}}{\ln (r_o/r_i)} \epsilon(i\omega) \tag{1.16}$$

$$G = \frac{2\pi\sigma}{\ln (r_o/r_i)} \tag{1.17}$$

where $\underline{\varepsilon}$ is the dielectric permittivity of vacuum.

For an empty (commercially) coaxial line, i.e. a General Radio 50 Ω precision line, the values of the circuit elements are calculated, using the characteristics:

$$r_i = 3.075\ 10^{-3}\ \text{m}$$

$$r_o = 7.075\ 10^{-3}\ \text{m}$$

The conductors are made of messing, coated with silver. Due to the "skin-effect", the current through the conductors is flowing through the silver layer only. The conductance of silver is given by:

$$\sigma_c = 6.17\ 10^{7}\ \Omega^{-1}\ \text{m}^{-1}$$

Inserting these values into equations (1.14) and (1.16) and using

$$\underline{\mu} = 4\pi\ 10^{-7}\ \text{Henry m}^{-1}, \quad \underline{\varepsilon} = \frac{1}{36\pi}\ 10^{-9}\ \text{Farad m}^{-1}$$

The following results are calculated:

$$R(\omega) = 1.06\ 10^{-5}\ \sqrt{\omega} \qquad \Omega\ m^{-1} \tag{1.18}$$

$$L = 1.67\ 10^{-7} \qquad \text{Henry}\ m^{-1} \tag{1.19}$$

$$C = 6.67\ 10^{-11} \qquad \text{Farad}\ m^{-1} \tag{1.20}$$

$$G = 0 \qquad \Omega^{-1}\ m^{-1} \tag{1.21}$$

For the frequency band of interest, which is roughly 10^6 - 10^{10} Hz, the series impedance can be neglected with respect to ωL, as can be inferred from Table 1.1. From the results of this Table, it is clear that, for all frequencies of interest, one has:

$$R(\omega) << \omega L \tag{1.22}$$

TABLE 1.1

THE INFLUENCE OF $R(\omega)$ IN COMPARISON WITH ωL

ω	$R(\omega)$	ωL	$R(\omega)/\omega L$
$2\pi.\ 10^6$	$2.65\ 10^{-2}$	1.05	$2.5\ 10^{-2}$
$2\pi.\ 10^{10}$	2.65	$1.05\ 10^4$	$2.5\ 10^{-4}$

Combining this result with equation (1.13), the characteristic impedance Z is given by:

$$Z \equiv Z_0 = \sqrt{\frac{L}{C}} \tag{1.23}$$

1.2,3 REFLECTION AND TRANSMISSION AT AN IMPEDANCE DISCONTINUITY

When a transmission line contains an impedance change, part of the wave is reflected and the other part is transmitted. Across the discontinuity, which is first considered to be a load impedance Z_L, Kirchhoff's law requires that total voltage and current must be continuous. At the discontinuity, for which the coordinate z = 0 is

chosen, the total voltage consists of voltages from waves travelling in positive and negative directions, these voltages are denoted by V_+ and V_- respectively. The sum of V_+ and V_- must be equal to the total voltage V_L across the impedance Z_L:

$$V_+ + V_- = V_L \tag{1.24}$$

Similarly the total current I_L flowing into the load is equal to the sum of the currents from both waves:

$$I_+ + I_- = I_L \tag{1.25}$$

Using

$$\frac{V_+}{I_+} = -\frac{V_-}{I_-} = Z_0 \ , \ \frac{V_L}{I_L} = Z_L$$

equation (1.25) becomes:

$$\frac{V_+}{Z_0} - \frac{V_-}{Z_0} = \frac{V_L}{Z_L} \tag{1.26}$$

Defining the reflection coefficient ρ and the transmission coefficient τ as:

$$\rho = \frac{V_-}{V_+} \tag{1.27a}$$

$$\tau = \frac{V_L}{V_+} = 1 + \rho \tag{1.27b}$$

and combining equations (1.24) and (1.26), the following results are obtained:

$$\rho = \frac{Z_L - Z_0}{Z_L + Z_0} \tag{1.28}$$

$$\tau = \frac{2Z_L}{Z_L + Z_o} \tag{1.29}$$

Using the results given by equations (1.16) and (1.17) the characteristic impedance can be written as

$$Z_L = \sqrt{\frac{L}{C}} \quad \frac{\sqrt{i\omega}}{[i\omega\, \varepsilon(i\omega) + \sigma/\underline{\varepsilon}\,]^{\frac{1}{2}}} \tag{1.30}$$

where the property

$$\frac{G}{C} = \sigma/\underline{\varepsilon} \tag{1.31}$$

is used. Equation (1.30) is generally written as

$$Z_L = \frac{Z_0}{[\,\varepsilon(i\omega) + \frac{\sigma/\underline{\varepsilon}}{i\omega}\,]^{\frac{1}{2}}} \tag{1.32}$$

or, using the convention that the quantity $(\sigma/\underline{\varepsilon}i\omega)$ is implicitly involved in $\varepsilon(i\omega)$, the relation between Z_L and Z_0 becomes:

$$Z_L = \frac{Z_0}{\sqrt{\varepsilon}(i\omega)} \tag{1.33}$$

The reflection coefficient $\rho(i\omega)$ is now easily calculated from equations (1.26) and (1.33)

$$\rho(i\omega) = \frac{1 - \sqrt{\varepsilon}(i\omega)}{1 + \sqrt{\varepsilon}(i\omega)} \tag{1.34}$$

It is noted that in derivation of equation (1.34) it is assumed that the dielectric material has a magnetic permeability $\mu = 1$. For paramagnetic substances, however, the inductance per unit length is given by $\mu(i\omega)L$, and after similar arguments as given above, equation (1.34) becomes:

$$\rho(i\omega) = \frac{\sqrt{\mu}(i\omega) - \sqrt{\varepsilon}(i\omega)}{\sqrt{\mu}(i\omega) + \sqrt{\varepsilon}(i\omega)} \tag{1.35}$$

1.3 LINEAR RESPONSE THEORY

1.3,1 INTRODUCTION

Knowledge of the dynamic behaviour of a physical system can be obtained by studying the system's response to a disturbance of the equilibrium situation. This can be done for instance by switching on a time periodic-, pulse-, step-, noise-, or any other input function. This is schematically indicated in Figure 1.6 using the symbols f(t), g(t) for respectively input and output. The quantity S is used to denote the system's behaviour, transforming f(t) into g(t).

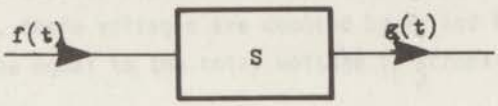

Figure 1.6 System S and its response g(t) to input f(t).

Two different response methods can be distinguished:

(1) The frequency domain method:
the input f(t), which is time periodic in this case, is applied adiabatically (which means that no transient behaviour is involved in g(t)) at $t = -\infty$. The system's response can then be studied at any time.

(2) The time domain method:
the input f(t), which is in general aperiodic in this case (although not necessarily, as for instance a rectangular periodic function) is switched on non adiabatically at some time t_0. The time domain method then studies the system's transient response for $t > t_0$ until equilibrium is reached. Examples of this method are pulse- and step response measurements.

Both methods determine the behaviour of the system completely (in a formal sense) and it is the aim of this section to discuss this similarity together with the link existing between the frequency and time domain methods.

The system S is assumed to be linear and causal, which means the following:

linear: the input f(t), consisting of the sum of any functions $f_1(t)$ and $f_2(t)$, results in an output g(t) which consists of the two independent responses $g_1(t)$ to $f_1(t)$ and $g_2(t)$ to $f_2(t)$.

causal: the input f(t), switched on at $t = 0$ cannot cause an output g(t) for $t < 0$.

This causality condition, which seems rather trivial, leads to the Kramers-Kronig relations[18-20], (see Appendix A).

1.3,2 INTEGRAL RELATION BETWEEN PULSE RESPONSE AND TRANSFER FUNCTION

The response of a linear causal system to a time periodic function is another time periodic function with the same period but (in general) different amplitude and phase. The following input is chosen first:

$$f(t) = \cos \omega t$$

The output is then given by, see Figure 1.7:

$$g(t) = R(\omega) \cos [\omega t + \Theta(\omega)]$$

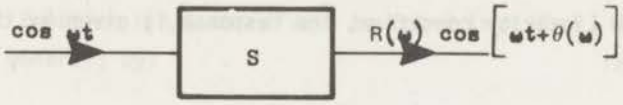

Figure 1.7 Response to a time periodic input.

The amplitude of the output, $R(\omega)$, and the phase difference between output and input, $\Theta(\omega)$, are both functions of the radial frequency ω.

Now the following input is chosen:

$$f(t) = \cos \omega t + i \sin \omega t = e^{i\omega t} \tag{1.36}$$

Using the linearity of the system, the following output is obtained:

$$g(t) = R(\omega) \cos [\omega t + \Theta(\omega)] + i\, R(\omega) \sin [\omega t + \Theta(\omega)]$$

which can be written as

$$g(t) = H(i\omega)\, e^{i\omega t} \tag{1.37}$$

$$H(i\omega) = R(\omega)\, e^{i\Theta(\omega)} \tag{1.38}$$

The complex function $H(i\omega)$ is called the "transfer function" or "system function". By definition it is the response to an exponential excitation, Figure 1.8

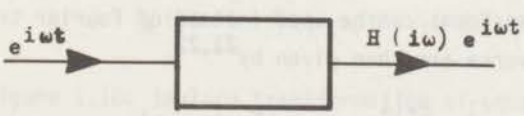

Figure 1.8 Definition of the transfer function $H(i\omega)$.

The next input to be chosen consists of the sum of an infinite number of exponentials, representing the Dirac pulse $\delta(t)$:

$$f(t) = \frac{1}{2\pi} \int_{-\infty}^{\infty} e^{i\omega t}\, d\omega = \delta(t) \qquad (1.39)$$

Again because of the linearity condition, the response is given by the integral of the individual responses:

$$g(t) = \frac{1}{2\pi} \int_{-\infty}^{\infty} H(i\omega)\, e^{i\omega t}\, d\omega = h(t) \qquad (1.40)$$

The symbol $h(t)$ is used to indicate the system's response to the unit pulse $\delta(t)$.

Mathematically, $h(t)$ is defined by equation (1.40) for all times $-\infty<t<\infty$ but due to the causality condition this reduces to $0<t<\infty$, see Figure 1.9

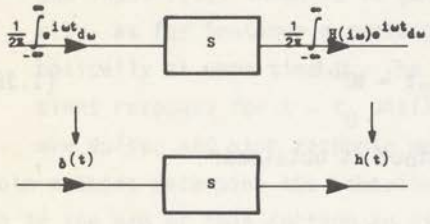

Figure 1.9 System response to a unit δ-function.

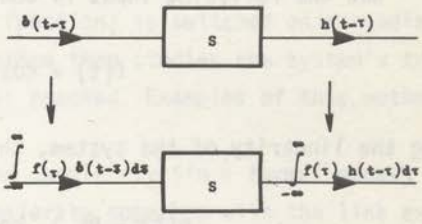

Figure 1.10 Input f(t) and output g(t) in terms of convolution with respectively δ(t) and h(t).

When equation (1.40) is to be inversed, difficulties may arise because of the requirements of $H(i\omega)$ and $g(t)$ for convergence of the Fourier transform. These difficulties are easily omitted, however, by extending the transfer function over the whole complex frequency plane, defining the complex frequencies by

$$s = \gamma + i\omega\,, \quad \gamma \text{ is real} \qquad (1.41)$$

This means that Laplace transforms can be used instead of Fourier transform methods. Equation (1.40) and its inverse are then given by[21,22]:

$$h(t) = \frac{1}{2\pi i} \int_{c-i\infty}^{c+i\infty} H(s)\, e^{st}\, ds \equiv \mathcal{L}^{-1}\{H(s)\} \qquad (1.42)$$

$$H(s) = \int_0^\infty h(t)\, e^{-st}\, dt \equiv \mathcal{L}\{h(t)\} \qquad (1.43)$$

It is noted that:

(1) the causality condition is automatically included in Laplace transforms and thus in equation (1.42)

(2) the transfer function $H(i\omega)$ can always be found from $H(s)$ (the reverse statement is not that general) by:

$$H(i\omega) = \lim_{\gamma \to 0} H(s) \qquad (1.44)$$

(3) the mathematical conditions to which $H(s)$ and $h(t)$ must obey to ensure the existence of the integrals (1.42) and (1.43) are fulfilled for all functions used in this work.

Details can be found in textbooks on Laplace transforms[23,24].

It can be concluded, from equations (1.42) and (1.43) and using (1.44) when necessary, that a linear causal system can be determined by means of the two response methods:

(1) the frequency domain method, by determination of $H(i\omega)$ for all ω.

(2) the time domain method, by determining $h(t)$ for all $t > 0$.

1.3,3 RESPONSE TO A GENERAL FUNCTION

The response $g(t)$ to some general input $f(t)$ is now calculated using the mathematical relations existing between $f(t)$ and $g(t)$.

Any function $f(t)$ can be written in terms of a convolution with the function $\delta(t)$[21],

$$f(t) = \int_{-\infty}^{\infty} f(\tau)\ \delta(t - \tau)\, d\tau \qquad (1.45)$$

In fact equation (1.45) is used as a definition of $\delta(t)$. The response $g(t)$ is then given by:

$$g(t) = \int_{-\infty}^{\infty} f(\tau)\ h(t - \tau)\, d\tau \qquad (1.46)$$

as is shown in Figure 1.10. Laplace transformation of equations (1.45) and (1.46) results into:

$$F(s) = F(s).1$$

$$G(s) = F(s).\ H(s) \tag{1.47}$$

where $F(s) = \mathcal{L}\{f(t)\}$ and $G(s) = \mathcal{L}\{g(t)\}$.

Introducing the causality condition, equation (1.46) becomes:

$$g(t) = \int_0^t f(\tau)\ h(t-\tau)\ d\tau = \int_0^t f(t-\tau)\ h(\tau)\ d\tau \equiv f(t) * h(t) \tag{1.48}$$

where it is noted that equation (1.47) is not changed by applying the causality contition. For completeness of this section it is noted that the equations (1.46) and (1.47) are integral equations of the convolution type and the Wiener-Hopf type respectively.

It can be concluded that

(1) equation (1.48) describes the linear time domain response g(t) to a general input f(t) in terms of a convolution of f(t) and h(t). It is important to note that it is not possible by simple methods, to find h(t) when g(t) is known.

(2) equation (1.47) describes the analogous situation in the frequency domain. Here it is very easy to find H(s) when G(s) and F(s) are known:

$$H(s) = \frac{G(s)}{F(s)} \tag{1.49}$$

and applying equation (1.49) one finds:

$$H(i\omega) = \frac{G(i\omega)}{F(i\omega)} \tag{1.50}$$

1.3,4 APPLICATION TO TIME DOMAIN REFLECTOMETRY

The results of the former section can now be applied to TDR. Then, the transfer function is given by $\rho(i\omega)$, the reflection coefficient of the system, where the system is defined as the air-dielectric interface involved in the coaxial line. Denoting the incident voltage by $V_0(t)$ and the reflected voltage by R(t), as shown in Figure 1.1, the relations between the time domain and the frequency domain response, as given for the general situation by equations (1.47) and (1.48), yield

$$R(t) = \int_0^t V_0(t-\tau)\ \ h(\tau)d\tau \tag{1.51}$$

and

$$G(s) = F(s).\ \rho(s) \tag{1.52}$$

with

$$G(s) = \mathcal{L}\{R(t)\} \; ; \; F(s) = \mathcal{L}\{V_0(t)\} \; ; \; \rho(s) = \mathcal{L}\{h(t)\}$$

It is instructive to consider the case of a heaviside step input. Then $V_0(t)$ is defined as

$$V_0(t) = \begin{cases} 1, & t > 0 \\ \frac{1}{2}, & t = 0 \\ 0, & t < 0 \end{cases} \tag{1.53}$$

Equations (1.51) and (1.52) then become:

$$R(t) = V_0 \int_0^t h(\tau)d\tau = V_0 P(t) \tag{1.54}$$

$$G(s) = V_0 \frac{1}{s} \rho(s) \tag{1.55}$$

$P(t)$ is the response to a unit heaviside step, for which the Laplace transform is $\frac{1}{s}$. The total displayed voltage $V(t)$ is in this case:

$$V(t) = V_0 + V_0 \, P(t) \tag{1.56}$$

The response $P(t)$ can be here interpreted as a reflection coefficient in the time domain. The unit step response $P(t)$ is then related to $\rho(s)$ by:

$$P(t) = \mathcal{L}^{-1}\left\{ \frac{1}{s} \rho(s) \right\} \tag{1.57}$$

When $V_0(t)$ is an experimental step, possessing a finite rise time, equation (1.47) remains unchanged but equation (1.48) cannot be simplified anymore:

$$R(t) = \int_0^t V_0(t - \tau) \; h(\tau)d\tau$$

This equation can be written in terms of a convolution between $V_0(t)$ and $P(t)$ as follows:

$$R(t) = V_0(t) \; * \; \frac{dP}{dt} \tag{1.58}$$

The total voltage $V(t)$ in terms of $V_0(t)$ and $P(t)$ is then given by:

$$V(t) = V_0(t) + V_0(t) \ * \ \frac{dP}{dt} \tag{1.59}$$

and the time domain response R(t) is related to $\rho(s)$ by:

$$R(t) = \mathcal{L}^{-1} \{ F(s) \ \rho(s) \} \tag{1.60}$$

$$\rho(s) = \frac{G(s)}{F(s)} \tag{1.61}$$

Using equations (1.34) and (1.61), the dielectric permittivity can be found from the equation

$$\varepsilon(i\omega) = \left(\frac{1 - \rho(i\omega)}{1 + \rho(i\omega)} \right)^2$$

or

$$\varepsilon(i\omega) = \left(\frac{F(i\omega) - G(i\omega)}{F(i\omega) + G(i\omega)} \right)^2 \tag{1.62}$$

ERRATUM

† The direct determination of ε_∞, as suggested by Fellner-Feldegg, is not based upon an exact mathematical method, resulting into large errors.

*See Appendix A where the Cole-Cole equation is discussed in connection with causality.

CHAPTER 2

CALCULATIONS OF THE TDR-RESPONSE TO A HEAVISIDE STEP FUNCTION FOR DIELECTRICS WITH KNOWN CHARACTERISTICS IN THE FREQUENCY DOMAIN

2.1 NUMERICAL CALCULATIONS[25]

2.1,1 INTRODUCTION

In the first paper on TDR, Fellner-Feldegg[6] obtained the dielectric permittivity, from the experimental results, by assuming the TDR-decay to be the Laplace transform of the dielectric permittivity (in a qualitative sense). For a Debye permittivity relation, defined by[26]

$$\varepsilon(s) = \varepsilon_\infty + \frac{\varepsilon_0 - \varepsilon_\infty}{1 + s\tau_0} \qquad (2.1)$$

where ε_∞, ε_0 are the high- and the low-frequency limits of $\varepsilon(s)$, and τ_0 is the relaxation time involved, the step response P(t) is then assumed to be of the following form

$$P(t) = \frac{1 - \sqrt{\varepsilon_0}}{1 + \sqrt{\varepsilon_0}} + \left[\frac{1 - \sqrt{\varepsilon_0}}{1 + \sqrt{\varepsilon_0}} - \frac{1 - \sqrt{\varepsilon_\infty}}{1 + \sqrt{\varepsilon_\infty}}\right] e^{-t/\tau_0} \qquad (2.2)$$

where τ_0 is again the dielectric relaxation time. It was pointed out by Whittingham[11], however, that equation (2.2) does not represent the correct TDR-response, because P(t) is the step response of the reflection coefficient $\rho(i\omega)$ instead of the dielectric permittivity $\varepsilon(i\omega)$. This is confirmed by Figure 2.1 where the Argand diagram of $\rho(i\omega)$ (for a Debye dispersion) is shown. Very clearly this diagram is not a semicircle. Then in a second paper with Barnett, Fellner-Feldegg[27] calculated P(t) numerically for a Debye permittivity relation and suggested that τ_0 should be determined by means of graphs,to be used when the values of ε_∞ and ε_0 are known (in his first paper, Fellner-Feldegg showed how ε_0 and ε_∞[†] can be found directly from a TDR-curve). Such graphs, for a Debye permittivity, were given in their paper.

It will be shown in the following sections, where the work of Fellner-Feldegg and Barnett is extended, that the dielectric parameters of a polar medium should not be estimated in the time domain, but instead in the frequency domain.The extension of the work of Fellner-Feldegg and Barnett will consist of a numerical calculation of the step responses P(t) for a dielectric material behaving according to the permittivity relations of Cole and Cole[28], defined by[*]:

$$\varepsilon(s) = \varepsilon_\infty + \frac{\varepsilon_0 - \varepsilon_\infty}{1 + (s\tau_0)^{1-\alpha}}, \quad 0<\alpha<1 \tag{2.3}$$

and of Davidson and Cole[29,30], defined by:

$$\varepsilon(s) = \varepsilon_\infty + \frac{\varepsilon_0 - \varepsilon_\infty}{(1 + s\tau_0)^{\beta}}, \quad 0<\beta<1 \tag{2.4}$$

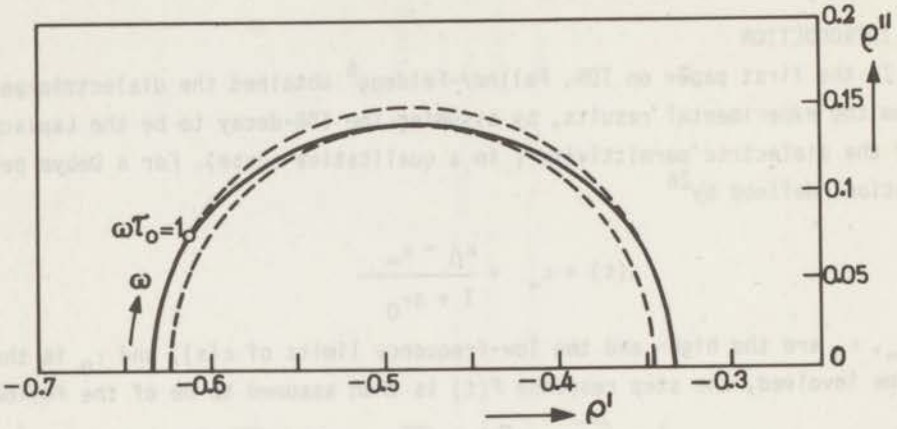

Figure 2.1 Argand diagram of $\rho(i\omega)$ for a Debye dispersion, $\varepsilon_0 = 20$ and $\varepsilon_\infty = 4$.

Apart from proving the impossibility of a direct evaluation of the dielectric parameters in the time domain, such calculations also provide qualitative information about accuracy, general behaviour and trends in TDR-experiments. In fact, some of the results obtained gave rise to a more systematic analysis of the asymptotic behaviour of P(t) in connection with the asymptotic behaviour of $\varepsilon(i\omega)$ in the Cole-Cole plot representation.

2.1,2 RELATIONS FROM ANALYTICAL CALCULATIONS

The general purpose of this section is the calculation of the step response P(t), defined by equation (1.57):

$$P(t) = \mathcal{L}^{-1}\left\{\frac{1}{s}\,\rho(s)\right\} \tag{1.57}$$

$$\rho(s) = \frac{1 - \sqrt{\varepsilon(s)}}{1 + \sqrt{\varepsilon(s)}} \tag{1.34}$$

for the three relations (2.1), (2.3) and (2.4) describing the frequency behaviour of $\varepsilon(s)$. An analytical evaluation of equation (1.57), by means of contour integration is

extremely difficult because $\rho(s)$ is a very complicated function in s. However, due to standard boundary value conditions, existing for Laplace transforms, it is possible to calculate P(t) and its derivative with respect to time, at t = 0 and t = ∞. The calculations are based upon the following theorems:

$$\lim_{t \downarrow 0} P(t) = \lim_{s \to \infty} s \, \mathcal{L} \{P(t)\} \tag{2.5}$$

$$\lim_{t \to \infty} P(t) = \lim_{s \to 0} s \, \mathcal{L} \{P(t)\} \tag{2.6}$$

Using equations (1.57) and (1.34) the following boundary value conditions are obtained for any dielectric permittivity $\varepsilon(s)$:

$$P(0) = \rho(\infty) = \frac{1 - \sqrt{\varepsilon_\infty}}{1 + \sqrt{\varepsilon_\infty}} \tag{2.7}$$

$$P(\infty) = \rho(0) = \frac{1 - \sqrt{\varepsilon_0}}{1 + \sqrt{\varepsilon_0}}, \quad \sigma = 0 \tag{2.8}$$

$$P(\infty) = \rho(0) = -1, \quad \sigma \neq 0 \tag{2.9}$$

In principle, equations (2.7) and (2.8) show the possibility of a direct determination of ε_∞ and (when $\sigma = 0$) of ε_0. When the low-frequency conductivity σ is not negligible, the static permittivity cannot be determined by straightforward methods in the time domain (however, this is also true in the frequency domain).

It is also possible to calculate the derivative of P(t), at t = 0, using equation (2.5) again, now written as:

$$\lim_{t \downarrow 0} \frac{dP}{dt} = \lim_{s \to \infty} \mathcal{L} \left\{ \frac{dP}{dt} \right\} \tag{2.10}$$

$$\mathcal{L} \left\{ \frac{dP}{dt} \right\} = s \, \mathcal{L}\{ P(t)\} - P(0) \tag{2.11}$$

Equation (2.11) follows immediately from Laplace transform theory. Combination of equations (2.10) and (2.11) gives:

$$\left(\frac{dP}{dt} \right)_{t=0} = \lim_{s \to \infty} s\{ \rho(s) - \rho(\infty) \} \tag{2.12}$$

Using the equations (1.34) and (2.1), (2.3) and (2.4) respectively, the following results are obtained:

(1) Debye
$$\left(\frac{dP}{dt}\right)_{t=0} = - \frac{(\varepsilon_0 - \varepsilon_\infty) + \sigma\tau_0/\varepsilon}{\tau_0 \sqrt{\varepsilon_\infty}\,(1 + \sqrt{\varepsilon_\infty})^2} \tag{2.13}$$

(2) Cole-Cole
$$\left(\frac{dP}{dt}\right)_{t=0} = - \infty \tag{2.14}$$

(3)Davidson-Cole
$$\left(\frac{dP}{dt}\right)_{t=0} = - \infty \tag{2.15}$$

2.1,3 NON-CONDUCTING DIELECTRIC MATERIALS

In this section the results from the calculations of P(t) will be presented assuming the behaviour of the permittivity in the frequency domain to be according to the equations (2.1), (2.3) and (2.4). The calculations are carried out assuming:

(1) a heaviside step input and
(2) an infinitely long dielectric sample enclosed in a perfectly conducting coaxial line.

In Appendix B some details are given on the numerical evaluation of the inverse Laplace transform; equation (1.57).

DEBYE DIELECTRIC PERMITTIVITY. Fellner-Feldegg and Barnett[27] have calculated P(t) for various combinations of ε_0 and ε_∞ and they have given graphs from which the corresponding values of τ_0 can be determined when ε_0 and ε_∞ are known.

When the time derivative of P(t) at t = 0 can be found, the relaxation time τ_0 can also be calculated from equation (2.13) with $\sigma = 0$, but this procedure cannot be very accurate in practice because it is related to the behaviour of P(t) for very small values of t and this part of the step response cannot be found very well experimentally due to the finite rise time of the voltage step*.

However, when it is known that a dielectric material behaves according to a Debye dispersion, the parameters ε_0, ε_∞ and τ_0 can be found in the time domain. This is demonstrated in Figure 2.2 where some of the results are shown together with the corresponding Cole-Cole plots and the Argand diagrams of $\rho(i\omega)$. The tangents (dP/dt) at t = 0 are calculated from equation (2.13) with $\sigma = 0$.

*This procedure may be applied experimentally when τ_0 is very large.

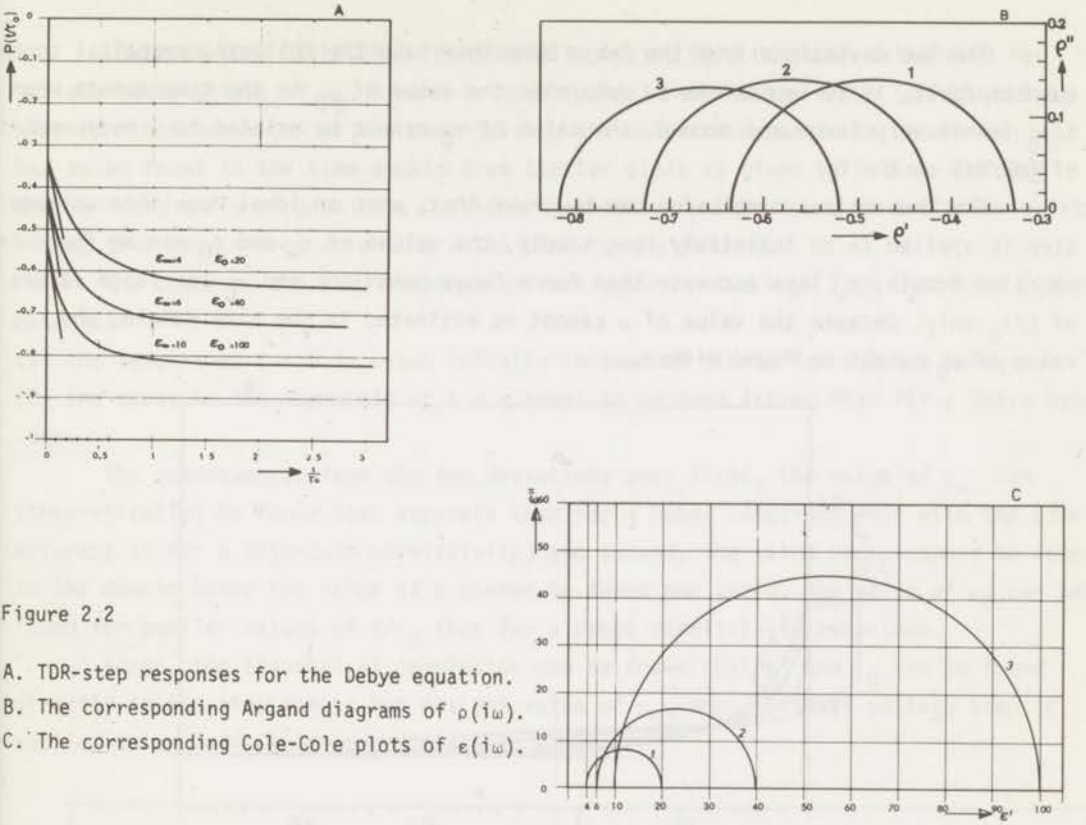

Figure 2.2

A. TDR-step responses for the Debye equation.
B. The corresponding Argand diagrams of $\rho(i\omega)$.
C. The corresponding Cole-Cole plots of $\varepsilon(i\omega)$.

COLE-COLE DIELECTRIC PERMITTIVITY. For a number of combinations of ε_0, ε_∞ and α, the step response P(t) is calculated. Some of the results are shown in Figure 2.3. It is not very useful to follow Fellner-Feldegg and Barnett in their procedure of the determination of τ_0, since not only ε_∞ and ε_0 must then be known but also the value of the empirical parameter α. No criterion in the time domain can be found from which the value of α can be deduced, as can be seen from the graphs of Figure 2.3.

The shape of P(t) for a dielectric material behaving according to the Cole-Cole equation, differs significantly in two ways from that of a Debye material:

(1) the tangent at t = 0 is finite when a Debye permittivity is involved and minus infinite for a Cole-Cole dielectric material.

(2) the decay to the asymptote at t = ∞ is much slower than for a Debye behaviour.

The two deviations from the Debye behaviour have the following practical consequences, first, it is impossible to determine the value of ε_0 in the time domain when t/τ_0 is not very large and second, the value of τ_0 cannot be related to a measurement of (dP/dt) at t = 0.

The theoretical conclusion can be drawn that, when an ideal heaviside voltage step is applied to an infinitely long sample, the values of ε_∞ and ε_0 can be found in the time domain, ε_∞ less accurate than for a Debye behaviour and ε_0 for large values of t/τ_0 only. Because the value of α cannot be estimated in the time domain, the value of ε_0 cannot be found either.

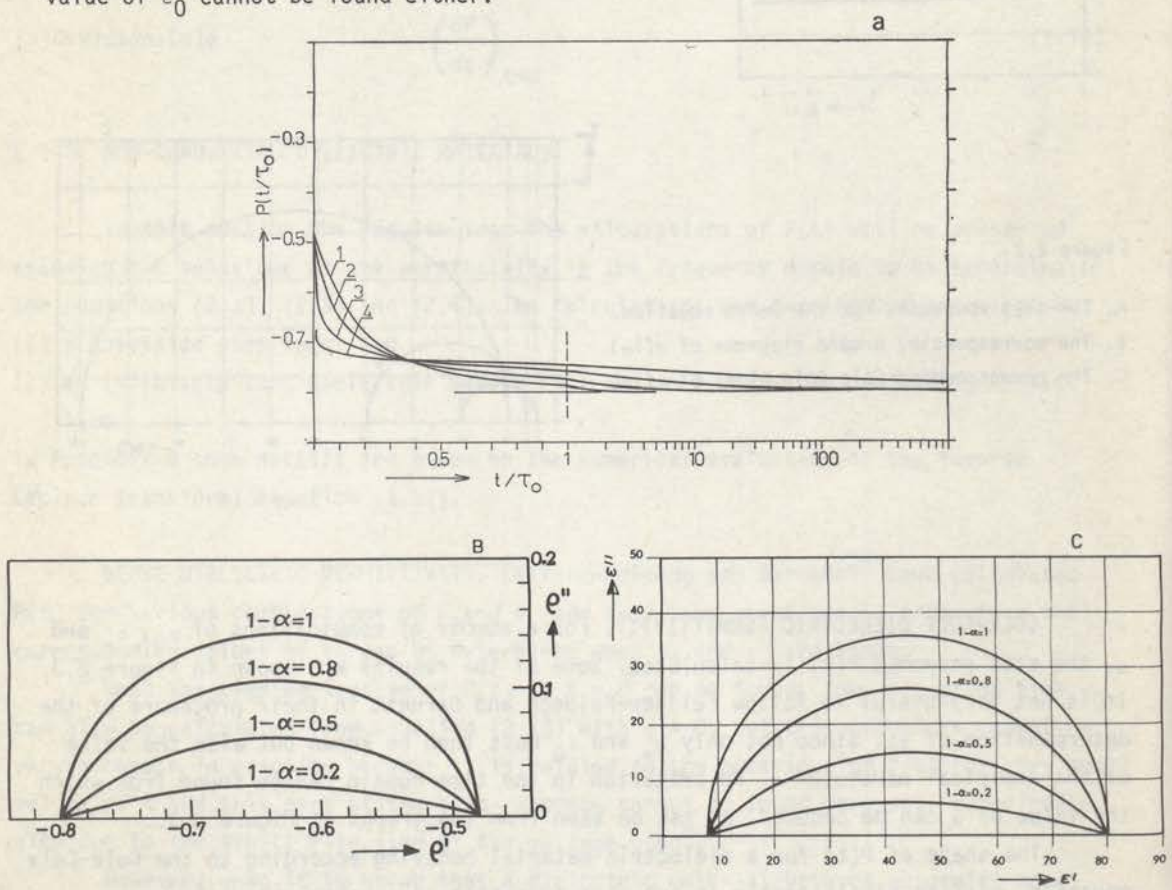

Figure 2.3

A. TDR-step responses for the Cole-Cole equation,
ε_0 = 80 and ε_∞ = 8.

1 $1 - \alpha = 1$
2 $1 - \alpha = 0.8$
3 $1 - \alpha = 0.5$
4 $1 - \alpha = 0.2$

B. The corresponding Argand diagrams of $\rho(i\omega)$.
C. The corresponding Cole-Cole plots of $\varepsilon(i\omega)$.

DAVIDSON-COLE DIELECTRIC PERMITTIVITY. Again, P(t) has been calculated for various combinations of ε_0, ε_∞ and β. Some typical results are shown in Figure 2.4. Also for this behaviour of the permittivity the value of β has to be known when τ_0 has to be found in the time domain from similar plots as given by Fellner-Feldegg and Barnett, and analogous to a Cole-Cole permittivity behaviour, no criterion exists in the time domain from which the value of β can be deduced.

The shape of the step response differs again in two ways from that of a Debye material:

(1) the tangent at t = 0 is minus infinity instead of finite for a Debye behaviour

(2) the decay to the asymptote at t = ∞ seems to be even faster than for a Debye behaviour.

The consequences from the two deviations are: first, the value of ε_∞ can (theoretically) be found less accurate than for a Debye behaviour (but with the same accuracy as for a Cole-Cole permittivity) and second, the value of τ_0 cannot be found in the domain since the value of β cannot be found and third, the value of ε_0 can be found for smaller values of t/τ_0 than for a Debye permittivity behaviour.

Again, the theoretical conclusion can be drawn that ε_∞ and ε_0 can be found directly in the time domain but not the value of τ_0, when an ideal voltage step is applied to an infinitely long dielectric sample.

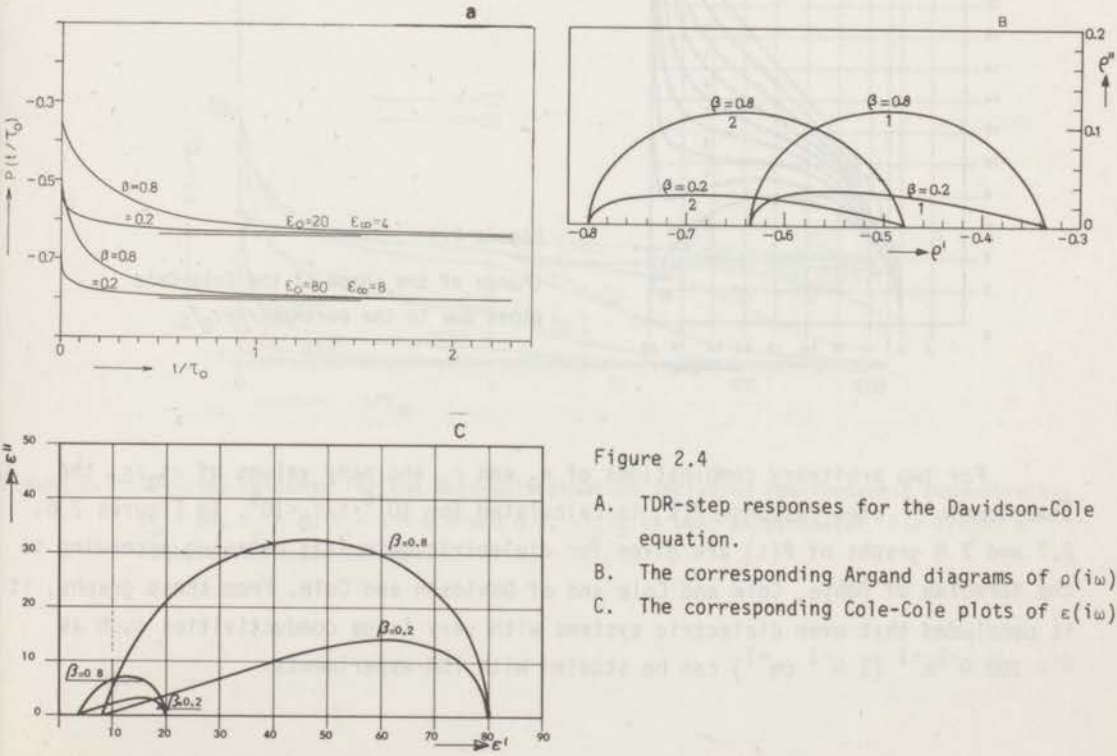

Figure 2.4

A. TDR-step responses for the Davidson-Cole equation.

B. The corresponding Argand diagrams of $\rho(i\omega)$.

C. The corresponding Cole-Cole plots of $\varepsilon(i\omega)$.

2.1,4 CONDUCTING DIELECTRIC MATERIALS

When the low-frequency conductivity σ cannot be neglected, i.e., when

$$\frac{1}{\omega}\,\frac{\sigma}{\underline{\varepsilon}} \simeq \varepsilon''(\omega) \tag{2.16}$$

Or, using $\omega\tau_0 = 1$, when:

$$\sigma\tau_0/\underline{\varepsilon} \simeq \frac{\varepsilon_0 - \varepsilon_\infty}{2} \tag{2.17}$$

the shape of P(t) changes significantly. However, the Cole-Cole plot in the frequency domain changes as well, vide Figure 2.5.

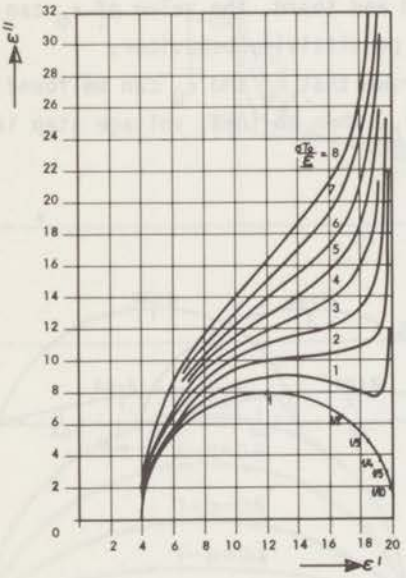

Figure 2.5

Change of the shape of the Cole-Cole plots due to the parameter $\sigma\tau_0/\underline{\varepsilon}$.

For two arbitrary combinations of ε_0 and ε_∞ and many values of $\sigma\tau_0/\underline{\varepsilon}$, the time domain step response P(t) is calculated for $10^{-4}<t/\tau_0<10^{6}$. In Figures 2.6, 2.7 and 2.8 graphs of P(t) are given for dielectric materials behaving according to the formulae of Debye, Cole and Cole and of Davidson and Cole. From these graphs, it is concluded that even dielectric systems with very large conductivities such as $\sigma = 100\ \Omega^{-1}m^{-1}$ ($1\ \Omega^{-1}\ cm^{-1}$) can be studied with TDR-experiments.

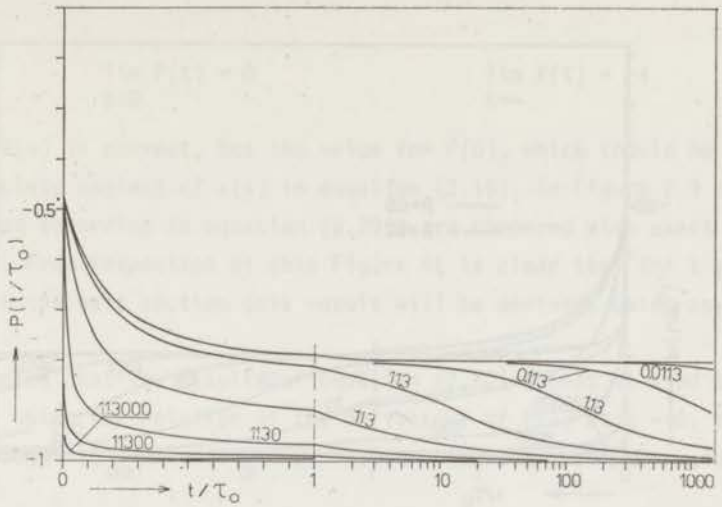

Figure 2.6 TDR-step response for the Debye equation including low-frequency conductivity; $\varepsilon_0 = 80$, $\varepsilon_\infty = 8$, $\sigma\tau_0/\varepsilon$ is used as parameter. For $t/\tau_0 > 1$ a logarithmic scale is used.

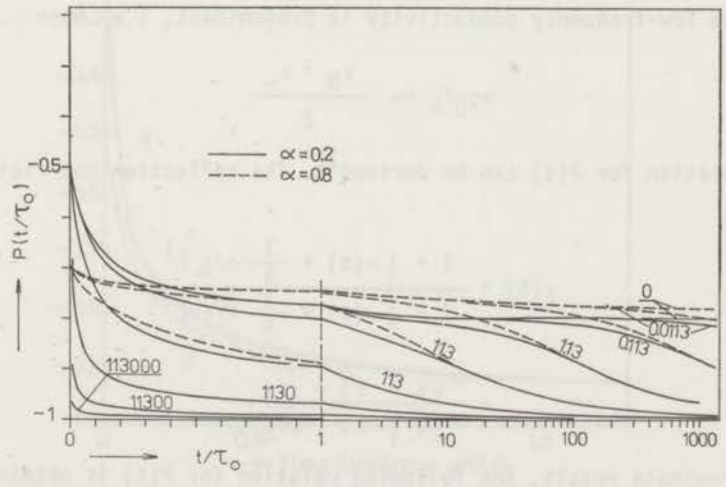

Figure 2.7 TDR-step response for the Cole-Cole equation including low-frequency conductivity; $\varepsilon_0 = 80$, $\varepsilon_\infty = 8$, $1 - \alpha = 0.8$ and 0.2, $\sigma\tau_0/\varepsilon$ is used as parameter. For $t/\tau_0 > 1$ a logarithmic scale is used.

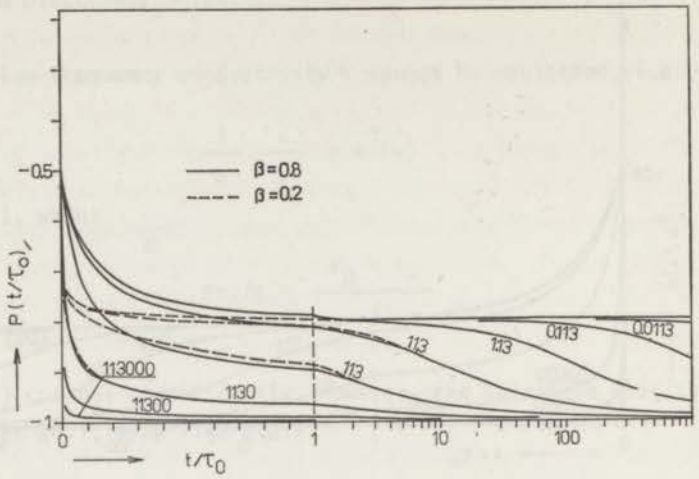

Figure 2.8 TDR-step response for the Davidson-Cole equation including low-frequency conductivity; $\varepsilon_0 = 80$, $\varepsilon_\infty = 8$, $\beta = 0.8$ and 0.2, $\sigma\tau_0/\underline{\varepsilon}$ is used as parameter. For $t/\tau_0 > 1$ a logarithmic scale is used.

When the low-frequency conductivity is predominant, i.e. when:

$$\sigma\tau_0/\underline{\varepsilon} >> \frac{\varepsilon_0 - \varepsilon_\infty}{2} \tag{2.18}$$

an analytic relation for P(t) can be derived[31]. The reflection coefficient $\rho(s)$ then becomes:

$$\rho(s) = \frac{1 - \left[\varepsilon(s) + \frac{1}{s}\sigma/\underline{\varepsilon}\right]^{\frac{1}{2}}}{1 + \left[\varepsilon(s) + \frac{1}{s}\sigma/\underline{\varepsilon}\right]^{\frac{1}{2}}}$$

$$= \frac{\sqrt{s} - \sqrt{s + \sigma/\underline{\varepsilon}}}{\sqrt{s} + \sqrt{s + \sigma/\underline{\varepsilon}}} \tag{2.19}$$

From this approximate result, the following relation for P(t) is obtained

$$P(t) = -1 + e^{-xt}\left[I_0(xt) + I_1(xt)\right] \tag{2.20}$$

$$x = \sigma/2\underline{\varepsilon} \tag{2.21}$$

In this equation, I_0, I_1 are modified Bessel functions. The behaviour of P(t), according to equation (2.15) is for very small and very large times respectively:

$$\lim_{t \downarrow 0} P(t) = 0 \qquad \lim_{t \to \infty} P(t) = -1 \tag{2.22}$$

The value for $P(\infty)$ is correct, but the value for $P(0)$, which should be $\rho(\infty)$ is not, due to the complete neglect of $\varepsilon(s)$ in equation (2.19). In Figure 2.9 two curves of $P(t)$, calculated according to equation (2.20), are compared with exact curves, obtained numerically. From inspection of this Figure it is clear that for $t > \tau_0$ both curves are similar. In the next section this result will be derived, using asymptotic techniques.

It is noted that the results of equation (2.20) cannot be used to measure the value of σ, by using the relation of the derivative of $P(t)$ at $t = 0$, as was suggested by Fellner-Feldegg[6,7]. A curve-fitting procedure would probably work for this determination.

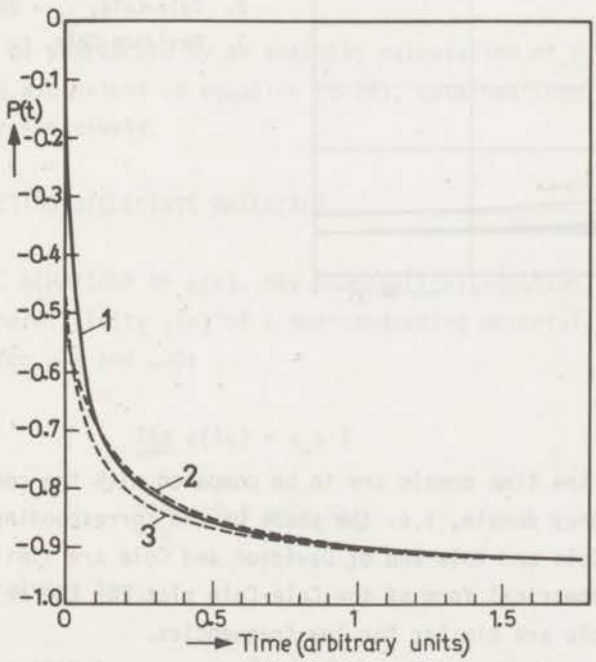

Figure 2.9 Some curves of the TDR-step response for a very large value of $\sigma/\underline{\varepsilon}$.
1. $P(t)$ calculated from equation (2.20)
2. $P(t)$ for a Debye equation, $\varepsilon_0 = 20$, $\varepsilon_\infty = 10$
3. $P(t)$ for a Debye equation, $\varepsilon_0 = 80$, $\varepsilon_\infty = 8$

2.2 ASYMPTOTICAL CALCULATIONS[32]

2.2,1 INTRODUCTION

In section 2.1 some results of P(t), from numerical calculations, were presented, using three current, partly empirical relations to represent the behaviour of dielectric material. One of the interesting features is that the behaviour of P(t), for $t \to 0$, is similar for the permittivity relations of Cole and Cole and of Davidson and Cole, while the behaviour of P(t) for $t \to \infty$ is similar for the relations of Debye and of Davidson and Cole, as is shown in Figure 2.10.

Figure 2.10 TDR-step response P(t)

1. Debye, $\varepsilon_0 = 20$, $\varepsilon_\infty = 4$
2. Cole-Cole, $\varepsilon_0 = 20$, $\varepsilon_\infty = 4$, $1 - \alpha = 0.6$
3. Davidson-Cole, $\varepsilon_0 = 20$, $\varepsilon_\infty = 4$, $\beta = 0.6$

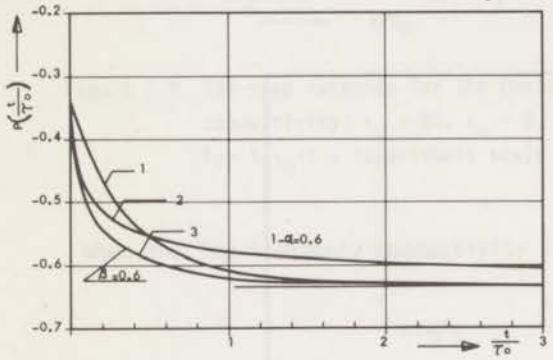

These similarities in the time domain are to be compared with the corresponding similarities in the frequency domain, i.e. the shape of the corresponding Cole-Cole plots for the relations of Cole and Cole and of Davidson and Cole are similar for high-frequencies while the geometrical form of the Cole-Cole plot for the relations of Debye and of Davidson and Cole are similar for low-frequencies.

These similarities between the asymptotic behaviour of P(t) and the (geometrical) asymptotic behaviour of $\varepsilon(i\omega)$ in the Cole-Cole plot representation, for three specific dielectric permittivity equations, suggest the possibility that for any dielectric permittivity the asymptotic behaviour of P(t) may yield information about the asymptotic behaviour of $\varepsilon(i\omega)$ in terms of the geometry in the Cole-Cole plot representation and vice versa.

It must be noted, that knowledge about these features is rather formal a priori, although it can serve as useful theoretical background knowledge. It will be shown,

however, that under some circumstances it gives information about the accuracy of dielectric parameters obained from TDR-experiments.

In this section the mathematical relations existing between the asymptotic behaviour of the time domain step response P(t) and the asymptotic behaviour of the complex dielectric permittivity $\varepsilon(s)$ are derived, in section 2.2,2 for the low-frequency conductivity being negligible, and in section 2.2,3 for this conductivity being considerable.

By definition, P(t) and $\varepsilon(i\omega)$ are related by equations (1.57) and (1.34)

$$P(t) = \mathcal{L}^{-1}\left\{ \frac{1}{s}\, \rho(s) \right\} \tag{1.57}$$

$$\rho(s) = \frac{\sqrt{s} - \sqrt{s\,\varepsilon(s) + \sigma/\underline{\varepsilon}}}{\sqrt{s} + \sqrt{s\,\varepsilon(s) + \sigma/\underline{\varepsilon}}} \tag{1.34}$$

The problem will be approached by an analytic calculation of P(t) for $t \to 0$ and $t \to \infty$, from power series expansions of equation (1.34), obtained from expressions of $\varepsilon(i\omega)$ for $\omega \to 0$ and $\omega \to \infty$ respectively.

2.2,2 NON-CONDUCTING DIELECTRIC MATERIALS

ASYMPTOTIC BEHAVIOUR OF $\varepsilon(s)$. Any mathematical equation, representing the complex dielectric permittivity $\varepsilon(s)$ of a non-conducting material, must have real and limiting values for $\omega \to \infty$ and $\omega \to 0$:

$$\lim_{\omega \to \infty} \varepsilon(i\omega) = \varepsilon_\infty \geq 1 \tag{2.23}$$

$$\lim_{\omega \to 0} \varepsilon(i\omega) = \varepsilon_0 > \varepsilon_\infty \tag{2.24}$$

Further more one always has:

$$\omega\, \varepsilon''(\omega) > 0 \tag{2.25}$$

The Cole-Cole plot gives the graph for $\varepsilon''(\omega)$ as a function of $\varepsilon'(\omega)$. If the angles made by this plot with the ε'-axis at the high- and the low-frequency ends are denoted by $\phi_\infty = \frac{1}{2}\pi\eta$ and $\phi_0 = \frac{1}{2}\pi\zeta$ respectively, one has:

$$\lim_{\omega \to \infty} \frac{\varepsilon''(\omega)}{\varepsilon'(\omega) - \varepsilon_\infty} = \operatorname{tg} \tfrac{1}{2}\pi\eta \ , \quad 0 \leq \eta \leq 2 \tag{2.26}$$

$$\lim_{\omega\to\infty} \frac{\varepsilon''(\omega)}{\varepsilon_0 - \varepsilon'(\omega)} = \operatorname{tg} \tfrac{1}{2}\pi\zeta, \quad 0\leq\zeta\leq 2 \tag{2.27}$$

The restrictions on η and ζ are derived from the restriction $\omega\varepsilon''(\omega)>0$.

Without loss of generality $\varepsilon(s)$ can formally be written in two forms[33]:

$$\varepsilon(s) = \varepsilon_\infty + s^{-\eta} f_\infty(s) \tag{2.28}$$

and

$$\varepsilon(s) = \varepsilon_0 - s^{\zeta} f_0(s) \tag{2.29}$$

In the following, equation (2.28) will be used for $s\to\infty$ and equation (2.29) for $s\to 0$. Equation (2.28) gives for ε' and ε'':

$$\varepsilon'(\omega) = \varepsilon_\infty + \omega^{-\eta}[f'_\infty(\omega) \cos \tfrac{1}{2}\pi\eta + f''_\infty(\omega) \sin \tfrac{1}{2}\pi\eta] \tag{2.30}$$

$$\varepsilon''(\omega) = \omega^{-\eta}[f'_\infty(\omega) \sin \tfrac{1}{2}\pi\eta - f''_\infty(\omega) \cos \tfrac{1}{2}\pi\eta] \tag{2.31}$$

where $f'_\infty(\omega)$ and $f''_\infty(\omega)$ denote the real and imaginary parts of $f_\infty(i\omega)$. Substituting these expressions in equation (2.26) one obtains

$$\lim_{\omega\to\infty} \frac{f'_\infty(\omega) \sin \tfrac{1}{2}\pi\eta - f''_\infty(\omega) \cos \tfrac{1}{2}\pi\eta}{f'_\infty(\omega) \cos \tfrac{1}{2}\pi\eta + f''_\infty(\omega) \sin \tfrac{1}{2}\pi\eta} = \operatorname{tg} \tfrac{1}{2}\pi\eta \tag{2.32}$$

Analogously, for $\omega\to 0$ is found:

$$\lim_{\omega\to 0} \frac{f'_0(\omega) \sin \tfrac{1}{2}\pi\zeta - f''_0(\omega) \cos \tfrac{1}{2}\pi\zeta}{f'_0(\omega) \cos \tfrac{1}{2}\pi\zeta + f''_0(\omega) \sin \tfrac{1}{2}\pi\zeta} = \operatorname{tg} \tfrac{1}{2}\pi\zeta \tag{2.33}$$

From equations (2.32) and (2.33) it follows that:

$$\lim_{\omega\to\infty} \frac{f''_\infty(\omega)}{f'_\infty(\omega)} = 0 \tag{2.34}$$

$$\lim_{\omega\to 0} \frac{f''_0(\omega)}{f'_0(\omega)} = 0 \tag{2.35}$$

The causality condition requires further that $\varepsilon(s)$, and thus also $f_\infty(s)$ and $f_0(s)$ are analytic functions for the right hand side of the complex frequency plane, i.e. for $\operatorname{Re}[s]>0$.

In general, three kinds of asymptotic behaviour of $f(i\omega)$ may be distinguished.

These cases will be discussed for $f_\infty(i\omega)$:

(1) $$\lim_{\omega\to\infty} f'_\infty(\omega) = a_\infty \tag{2.36}$$

where a_∞ is a finite real number. It then follows from equation (2.34)

$$\lim_{\omega\to\infty} f''_\infty(\omega) = 0 \tag{2.37}$$

and equation (2.28) can be written in the form:

$$\varepsilon(s) = \varepsilon_\infty + a_\infty s^{-\eta} + o[s^{-\eta}], \quad s\to\infty \tag{2.38}$$

where the order symbol o has been used. From equation (2.25) it follows that

$$a_\infty > 0 \tag{2.39}$$

(2) $$\lim_{\omega\to\infty} f'_\infty(\omega) = \infty \tag{2.40}$$

In this case equation (2.34) implies the restriction that $f_\infty(s)$ must go to infinity with a slower rate than any power of s:

$$f_\infty(s) = o[s^\lambda], \quad s\to\infty, \text{ for any } \lambda>0 \tag{2.41}$$

where $f_\infty(s)$ may for instance be a logarithmic like function, such as log s , log log s, etc.

(3) $$\lim_{\omega\to\infty} f'_\infty(\omega) = 0 \tag{2.42}$$

or $$\lim_{\omega\to\infty} \mathrm{Re}\left[\frac{1}{f_\infty(i\omega)}\right] = \infty \tag{2.43}$$

we now use the property that equation (2.34) is equivalent with

$$\lim_{\omega\to\infty} \frac{\mathrm{Im}\,[\,1/f_\infty(i\omega)\,]}{\mathrm{Re}\,[\,1/f_\infty(i\omega)\,]} = 0 \tag{2.44}$$

This relation is obeyed when

$$[f_\infty(s)]^{-1} = o[s^\lambda], \quad s\to\infty, \text{ for any } \lambda>0 \tag{2.45}$$

e.g. when $[f_\infty(s)]^{-1}$ goes to infinity as logs, log log s, etc.

For $\lim_{s\to 0} f_0(s)$ the same three cases can be distinguished as for $\lim_{s\to\infty} f_\infty(s)$. The conditions obtained for $f_0(s)$ are then:

$$f_0(s) = o\,[\,s^{-\lambda}\,] \quad , \quad s\to 0 \quad , \quad \text{for any } \lambda>0 \tag{2.46}$$

$$[f_0(s)]^{-1} = o\,[\,s^{-\lambda}\,] \quad , \quad s\to 0 \quad , \quad \text{for any } \lambda>0 \tag{2.47}$$

ASYMPTOTIC BEHAVIOUR OF $\rho(s)$. Because the function $\rho(\varepsilon)$, defined by equation (1.34) with $\sigma = 0$, is analytic for all $\varepsilon(i\omega)$, a Taylor expansion around some specific value ε_ω is possible:

$$\rho(\varepsilon) - \rho(\varepsilon_\omega) = \rho_1(\varepsilon_\omega)\,(\varepsilon - \varepsilon_\omega) + o\,[\,(\varepsilon - \varepsilon_\omega)\,] \tag{2.48}$$

$$\rho(\varepsilon_\omega) = \frac{1 - \sqrt{\varepsilon_\omega}}{1 + \sqrt{\varepsilon_\omega}} \tag{2.49}$$

$$\rho_1(\varepsilon_\omega) = \frac{-1}{\sqrt{\varepsilon_\omega}\,(1 + \sqrt{\varepsilon_\omega})^2} \tag{2.50}$$

Combination of equation (2.48) with equations (2.28) and (2.29) leads to:

$$\rho(s\to\infty) - \rho(\varepsilon_\infty) = \rho_1(\varepsilon_\infty)s^{-\eta}\, f_\infty(s) + o\,[\,s^{-\eta}\, f_\infty(s)\,] \tag{2.51}$$

$$\rho(s\to 0) - \rho(\varepsilon_0) = -\,\rho_1(\varepsilon_0)s^{\zeta}\, f_0(s) + o\,[\,s^{\zeta} f_0(s)\,] \tag{2.52}$$

For the cases $\lim_{s\to\infty} f_\infty(s) = a_\infty$ and $\lim_{s\to 0} f_0(s) = a_0$, one obtains:

$$\rho(s\to\infty) - \rho(\varepsilon_\infty) = \rho_1(\varepsilon_\infty)\, a_\infty s^{-\eta} + o\,[\,s^{-\eta}\,] \tag{2.53}$$

$$\rho(s\to 0) - \rho(\varepsilon_0) = -\,\rho_1(\varepsilon_0)a_0 s^{\zeta} + o\,[\,s^{\zeta}\,] \tag{2.54}$$

It is interesting to note, that, since both $\rho_1(\varepsilon_\infty)$ and $\rho_1(\varepsilon_0)$ will always be finite, it follows from comparison of equations (2.51) and (2.52) with equations (2.28) and (2.29) that the Argand diagram of $\rho(i\omega) = \rho'(\omega) + i\rho''(\omega)$ intersects the negative part of the ρ'-axis under the same angles $\frac{1}{2}\pi\eta$ and $\frac{1}{2}\pi\zeta$ as the Cole-Cole plot of $\varepsilon(i\omega)$. This property can be observed from Figures (2.2b), (2.3b) and (2.4b).

ASYMPTOTIC BEHAVIOUR OF $P(t)$. For $t = 0$, the behaviour of $P(t)$ is given by equation (2.7):

$$P(0) = \rho(\infty) \tag{2.7}$$

To find the relation with the asymptotic behaviour of the dielectric permittivity the time derivative of P(t) at t = 0 is considered, which is given by equation (2.12):

$$\left(\frac{dP}{dt}\right)_{t=0} = \lim_{s\to\infty} s\,[\,\rho(s) - \rho(\infty)] \tag{2.12}$$

Applying equation (2.51) one obtains:

$$\left(\frac{dP}{dt}\right)_{t=0} = \rho_1(\varepsilon_\infty) \lim_{s\to\infty} s^{1-\eta} f_\infty(s) \tag{2.55}$$

Using the restrictions on $f_\infty(s)$, as given by equations (2.41) and (2.45), it is found that $(dP/dt) = 0$ at $t = 0$, for $\eta>1$, and $(dP/dt) = -\infty$ for $\eta<1$ (the minus sign is involved because $\rho_1<0$). For $\eta = 1$, i.e. when the Cole-Cole plot intersects the ε'-axis perpendicularly at the high-frequency side, the value of (dP/dt) at $t = 0$ depends on $f_\infty(s)$ for $s\to\infty$. If this limiting value is finite, (dP/dt) at $t = 0$ will also be finite, and equal to

$$\left(\frac{dP}{dt}\right)_{t=0} = -\frac{a_\infty}{\sqrt{\varepsilon_\infty}\,(1+\sqrt{\varepsilon_\infty})^2} \tag{2.56}$$

For $\lim_{s\to\infty} f_\infty(s) = \infty$ or $\lim_{s\to\infty} f_\infty(s) = 0$ respectively, the derivative at $t = 0$ will also become infinite or zero.

For $t\to\infty$ the behaviour of P(t) can be derived from the low-frequency behaviour of $\mathcal{L}\{P(t)\}$. First we consider the case of equation (2.54) i.e. the case of $\lim_{s\to0} f_0(s) = a_0$:

$$\mathcal{L}\{P(t)\} = s^{-1}\rho(s) = \frac{\rho(\varepsilon_0)}{s} - \rho_1(\varepsilon_0)a_0 s^{\zeta-1} + o\,[\,s^{\zeta-1}\,] \quad , \quad s\to0 \tag{2.57}$$

From this follows[34]:

$$P(t) = \rho(\varepsilon_0) - \frac{\rho_1(\varepsilon_0)a_0}{\Gamma(1-\zeta)} t^{-\zeta} + o\,[\,t^{-\zeta}\,] \quad , \quad t\to\infty$$

$$= \rho(\varepsilon_0) + \frac{a_0}{\Gamma(1-\zeta)\sqrt{\varepsilon_0}\,(1+\sqrt{\varepsilon_0})^2} t^{-\zeta} + o\,[\,t^{-\zeta}\,] \,,\ t\to\infty \tag{2.58}$$

From the sign of the gamma function[35], it follows that for $0<\zeta<1$ the step response $P(t)$ will approach its limiting value $P(\infty) = \rho(\varepsilon_0)$ from the positive side, for $1<\zeta<2$ from the negative side. In the cases $\zeta = 1$ and $\zeta = 2$, when the low-frequency side of the Cole-Cole plot respectively intersects the ε'-axis perpendicularly and touches the ε'-axis, the term in $t^{-\zeta}$ in the series development of $P(t) - P(\infty)$ vanishes because of the result[35] $\Gamma^{-1}(-n) = 0$, $n = 0,1.....$. The series development will than be dominated by the next term, which can be either positive or negative. When the series development for $\varepsilon(s\to 0)$ contains only integer powers of s, all terms in the corresponding series of $P(t) - P(\infty)$ will vanish, and $P(t)$ will approach its asymptotic value faster than any power of t^{-1}. Consider now $\lim_{s\to 0} f_0(s)$ is zero or infinite:

$$\mathcal{L}\{P(t)\} = \frac{\rho(\varepsilon_0)}{s} - \rho_1(\varepsilon_0)\, f_0(s)\, s^{\zeta-1} + o\left[f_0(s)\, s^{\zeta-1}\right] \quad , \quad s\to 0 \tag{2.59}$$

The function $P(t) - P(\infty)$, $t\to\infty$, is now dominated by the term $-\rho_1(\varepsilon_0)\, \mathcal{L}^{-1}\{f_0(s)\, s^{\zeta-1}\}$. From the restrictions on $f_0(s)$, i.e. equations (2.46) and (2.47), it follows that for $s\to 0$, $f_0(s)\, s^{\zeta-1}$ goes to zero faster than any $s^{\zeta-1-\lambda}$ and slower than any $s^{\zeta-1+\lambda}$, $\lambda>0$ (the value of λ cannot be zero, since then a logarithmic function for $f_0(s)$ is not possible). Now it is known[36], that the asymptotic expansion of a function for $t\to\infty$ corresponds to an asymptotic expansion of its Laplace transform at a finite point where the transformed function has a singularity. Thus the rate by which the step response $P(t)$ approaches its asymptotic value in the case of equation (2.59), will be faster than any $t^{-\zeta+\lambda}$, and slower than any $t^{-\zeta-\lambda}$, $\lambda>0$, as long as ζ is a fractional number. If ζ is an integer, $P(t)$ can only be derived in this way to go to its asymptotic value for $t\to\infty$ faster than any $t^{-\zeta+\lambda}$. The results are summarized in Table 2.1.

TABLE 2.1

ASYMPTOTIC BEHAVIOUR OF $P(t) - P(\infty)$ FOR $t\to\infty$

	$P(t) - P(\infty)$ goes to zero		sign of the dominating term
	faster than	slower than	
$\zeta = 0$		$t^{-\lambda}$	+
$0 < \zeta < 1$	$t^{-\zeta+\lambda}$	$t^{-\zeta-\lambda}$	+
$\zeta = 1$	$t^{-1+\lambda}$		$\pm$
$1 < \zeta < 2$	$t^{-\zeta+\lambda}$	$t^{-\zeta-\lambda}$	-
$\zeta = 2$	$t^{-2+\lambda}$		$\pm$

For non-conducting materials, the asymptotic behaviour of P(t) appears to be comparable with the asymptotic behaviour of the "after-effect"* function, as is discussed by Bordewijk and Van Gemert[33]. This is due to the fact that the asymptotic behaviours of $\varepsilon(s)$ and $\rho(s)$ are similar.

APPLICATIONS. Because many experiments are analyzed in terms of the analytic relations proposed by Debye, Cole and Cole and Davidson and Cole[37-40], in this section the results of the calculations given above will be applied to these relations. It appears that the three relations can be expanded into power series of s and of s^{-1}, so that the relations derived for $\lim_{s\to 0} f_0(s) = a_0$ and $\lim_{s\to\infty} f_\infty(s) = a_\infty$ can be used. The values of the relevant parameters are summarized in Table 2.2.

TABLE 2.2

PARAMETERS CHARACTERIZING THE ASYMPTOTIC BEHAVIOUR IN THE FREQUENCY DOMAIN FOR THE CASES OF DEBYE, COLE-COLE AND DAVIDSON-COLE

	expression for $\varepsilon(i\omega)$	η	a_∞	ζ	a_0
Debye	$\varepsilon_\infty + \frac{\varepsilon_0 - \varepsilon_\infty}{1 + i\omega\tau_0}$	1	$(\varepsilon_0-\varepsilon_\infty)\tau_0^{-1}$	1	$(\varepsilon_0-\varepsilon_\infty)\tau_0$
Cole-Cole	$\varepsilon_\infty + \frac{\varepsilon_0 - \varepsilon_\infty}{1 + (i\omega\tau_0)^{1-\alpha}}$	$1-\alpha$	$(\varepsilon_0-\varepsilon_\infty)\tau_0^{-(1-\alpha)}$	$1-\alpha$	$(\varepsilon_0-\varepsilon_\infty)\tau_0^{1-\alpha}$
Davidson-Cole	$\varepsilon_\infty + \frac{\varepsilon_0 - \varepsilon_\infty}{(1 + i\omega\tau_0)^{\beta}}$	β	$(\varepsilon_0-\varepsilon_\infty)\tau_0^{-\beta}$	1	$\beta(\varepsilon_0-\varepsilon_\infty)\tau_0$

Using the results from this Table and inserting the parameters into equations (2.55) and (2.56), exact agreement is obtained with the results given by equations (2.13) - (2.15).

For $t\to\infty$, it is clear that the dominating term in P(t) - P(∞) is positive for a Cole-Cole relation, and goes to zero as fast as $t^{-(1-\alpha)}$. For the relations of Debye and Davidson-Cole, the subsequent terms in the series expansion of $\varepsilon(s)$ become important. For the Debye relation the expansion is given by

$$\varepsilon(s\to 0) - \varepsilon_0 = (\varepsilon_0 - \varepsilon_\infty) \sum_{n=1}^{\infty} (-s\tau_0)^n \qquad (2.60)$$

*The after-effect function, $\phi(t)$, is defined by the following equation: $-\frac{d\phi(t)}{dt} = \mathcal{L}^{-1}\left\{\frac{\varepsilon(s) - \varepsilon_\infty}{\varepsilon_0 - \varepsilon_\infty}\right\}$

for the Davidson-Cole relation, it is given by:

$$\varepsilon(s\to 0) - \varepsilon_0 = (\varepsilon_0 - \varepsilon_\infty)\sum_{n=1}^{\infty} \frac{\beta(\beta+1)(\beta+2)\ldots(\beta+n-1)}{n!}(-s\tau_0)^n \quad (2.61)$$

Because all powers are integer, this is also true for the expansion of $\rho(s\to 0)$. Therefore in the case of Debye and Davidson-Cole, P(t) will go to its limiting value $P(\infty)$ faster than any power of t^{-1}.

The rate of which P(t) goes to $P(\infty)$ in the cases of Debye and Davidson-Cole, can be obtained by developing the expression $s^{-1}[\rho(s) - \rho(\varepsilon_0)]$ around the point where it has a singularity, i.e. around the point $s_0 = -1/\tau_0$:

$$s^{-1}[\rho(s) - \rho(\varepsilon_0)] =$$

$$\frac{1}{s}\left[\frac{1 - \sqrt{\varepsilon_\infty + (\varepsilon_0 - \varepsilon_\infty)(1+s\tau_0)^{-\beta}}}{1 + \sqrt{\varepsilon_\infty + (\varepsilon_0 - \varepsilon_\infty)(1+s\tau_0)^{-\beta}}} - \frac{1-\sqrt{\varepsilon_0}}{1+\sqrt{\varepsilon_0}}\right]$$

$$= \frac{2\sqrt{\varepsilon_0} - 2\sqrt{\varepsilon_\infty + (\varepsilon_0 - \varepsilon_\infty)(1+s\tau_0)^{-\beta}}}{s(1+\sqrt{\varepsilon_0})\left[1 + \sqrt{\varepsilon_\infty + (\varepsilon_0 - \varepsilon_\infty)(1+s\tau_0)^{-\beta}}\right]}$$

$$= \frac{2\tau_0^{\beta/2}}{s(1+\sqrt{\varepsilon_0})}\left[\frac{\sqrt{\varepsilon_0}(s-s_0)^{\beta/2} - \sqrt{(\varepsilon_0 - \varepsilon_\infty) + \varepsilon_\infty\tau_0^\beta(s-s_0)^\beta}}{\tau_0^{\beta/2}(s-s_0)^{\beta/2} + \sqrt{(\varepsilon_0 - \varepsilon_\infty) + \varepsilon_\infty\tau_0^\beta(s-s_0)^\beta}}\right]$$

Now the following property is used:

$$F(s) = F(s_0) + [F(s) - F(s_0)]$$

where $F(s) = s^{-1}[\rho(s) - \rho(\varepsilon_0)]$ and $s_0 = -\tau_0^{-1}$.

The result is

$$\frac{2\tau_0}{1+\sqrt{\varepsilon_0}} +$$

$$+\left[\frac{2\tau_0^{\beta/2}(s-s_0)^{\beta/2}\left[1+\sqrt{\varepsilon_0} - \tau_0(s-s_0)\right] + \tau_0(s-s_0)\sqrt{\varepsilon_0 - \varepsilon_\infty + \varepsilon_\infty\tau_0^\beta(s-s_0)^\beta}}{s(1+\sqrt{\varepsilon_0})\left[\tau_0^{\beta/2}(s-s_0)^{\beta/2} + \sqrt{\varepsilon_0 - \varepsilon_\infty + \varepsilon_\infty\tau_0^\beta(s-s_0)^\beta}\right]}\right]$$

which can be written as:

$$\frac{2\tau_0}{1+\sqrt{\varepsilon_0}} - \frac{\tau_0^{\beta/2}\,(1+\sqrt{\varepsilon_0})\,(s-s_0)^{\beta/2} + o[\,(s-s_0)^{\beta/2}]}{1/\tau_0\,(1+\sqrt{\varepsilon_0})\,\sqrt{\varepsilon_0-\varepsilon_\infty} + o[\,1\,]} =$$

$$= \frac{2\tau_0}{1+\sqrt{\varepsilon_0}} - \frac{2\tau_0^{1+\beta/2}}{\sqrt{\varepsilon_0-\varepsilon_\infty}}\,(s-s_0)^{\beta/2} + o[\,(s-s_0)^{\beta/2}]\quad s\to s_0 \qquad (2.62)$$

It follows that the asymptotic behaviour of $P(t) - P(\infty)$ is given by[34]:

$$P(t) - P(\infty) = \frac{\Gamma(\frac{3}{2}\beta)\,\sin\frac{1}{2}\pi\beta}{\sqrt{\varepsilon_0-\varepsilon_\infty}}\,(t/\tau_0)^{-(1+\frac{1}{2}\beta)}\,e^{-t/\tau_0} + o[\,e^{-t}\,t^{-(\frac{1}{2}\beta+1)}] \qquad (2.63)$$

where the result $\Gamma^{-1}(-\beta/2) = \Gamma(\frac{3}{2}\beta)\sin\frac{\pi}{2}\beta$ is used. For the Debye relation one has $\beta = 1$, and equation (2.63) becomes

$$P(t) - P(\infty) = \frac{1}{2\sqrt{\pi(\varepsilon_0-\varepsilon_\infty)}}\,(t/\tau_0)^{-3/2}\,e^{-t/\tau_0} + o[\,e^{-t}\,t^{-3/2}] \qquad (2.64)$$

2.2,3 DIELECTRIC MATERIALS WITH LARGE CONDUCTIVITY

When the conductivity of the material is considerable, the quantity in the frequency domain obtained experimentally is $\varepsilon(i\omega) + \sigma/\underline{\varepsilon}i\omega$, and a Cole-Cole plot can be obtained by plotting the negative imaginary part of this quantity against the real part. According to equation (1.34), the asymptotic behaviour of $P(t)$ for $t\to 0$ will now be determined by the high-frequency side of the Cole-Cole plot obtained in this way, and the same cases can be distinguished as in the case of non-conducting materials. The results are similar to the results obtained for the special cases of Debye, Cole-Cole and Davidson-Cole as given in section 2.1.

The low-frequency side of the Cole-Cole plot now does not intersect the real axis, however, since $\varepsilon(i\omega) + \frac{\sigma/\varepsilon}{i\omega}$ has a pole for $s = 0$. The quantity $s^{-1}[\rho(s) - \rho(\varepsilon_0)]$ can now be developed around $s = 0$ in the following way, using $\rho(\varepsilon_0) = -1, \sigma \neq 0$:

$$s^{-1}[\,\rho(s) - \rho(\varepsilon_0)\,] = \frac{1}{s}\left[\frac{\sqrt{s} - \sqrt{s\,\varepsilon(s) + \sigma/\underline{\varepsilon}}}{\sqrt{s} + \sqrt{s\,\varepsilon(s) + \sigma/\underline{\varepsilon}}} + 1\right] =$$

$$= \frac{1}{s}\left[\frac{2\sqrt{s}}{\sqrt{s} + \sqrt{s}\,\varepsilon(s) + \sigma/\underline{\varepsilon}}\right] =$$

$$= 2\sqrt{\underline{\varepsilon}/s\sigma} + o\left[s^{-\frac{1}{2}}\right] \quad , \quad s \to 0 \tag{2.65}$$

Then it follows:

$$P(t) - P(\infty) = \frac{2}{\Gamma(\frac{1}{2})}\sqrt{\frac{\underline{\varepsilon}}{t\sigma}} + o\left[t^{-\frac{1}{2}}\right] \quad , \quad t \to \infty$$

$$= 2\sqrt{\frac{\underline{\varepsilon}}{\pi\sigma}}\, t^{-\frac{1}{2}} + o\left[t^{-\frac{1}{2}}\right] \quad , \quad t \to \infty \tag{2.66}$$

For the case $\varepsilon(s) = 1$, in section 2.1,4 it was found that

$$P(t) = -1 + e^{-xt}\left[I_0(xt) + I_1(xt)\right] \tag{2.20}$$

where $x = \sigma/2\underline{\varepsilon}$ and I_0 and I_1 are modified Bessel functions. Taking the asymptotic developments for these modified Bessel functions[41], the following series development for P(t) is obtained:

$$P(t) = -1 + e^{-xt}\left[\frac{e^{xt}}{\sqrt{2\pi xt}}\left(1 + \frac{1}{8xt} + \ldots.\right) + \frac{e^{xt}}{\sqrt{2\pi xt}}\left(1 - \frac{3}{8xt} + \ldots.\right)\right]$$

$$= -1 + 2\sqrt{\frac{\underline{\varepsilon}}{\pi\sigma}}\, t^{-\frac{1}{2}} + o\left[t^{-\frac{1}{2}}\right] \quad , \quad t \to \infty \tag{2.67}$$

which is in agreement with equation (2.66)

2.3 DISCUSSION AND CONCLUSIONS

In section 2.1 of this Chapter, the step response P(t) is calculated numerically for dielectric materials behaving according to the relations of Debye, Cole and Cole and of Davidson and Cole.

The main conclusion is that a direct evaluation of the dielectric parameters

in the time domain (except ε_0 in most cases) as proposed by Fellner-Feldegg and Barnett[27], is in general impossible, since the shape of the TDR-response does not show enough characteristic features from which the value of certain parameters can be estimated (for instance the value of $1 - \alpha$ or β in the permittivity relations of Cole-Cole and Davidson-Cole). Instead, Fourier analysis of the time domain results is necessary for the evaluation of τ_0, α or β and ε_∞.

When low-frequency conductivity is involved, it is shown that ε_0 can be determined when $\sigma\tau_0/\underline{\varepsilon} < 0.1$. The evaluation of σ from the derivative of P(t) at t = 0 is impossible, even in the situation that the low-frequency conductivity is predominant. It is suggested, however, that a determination of σ , from TDR-experiments, may be possible by curve-fitting methods, although it is noted that the value of σ can be very easily obtained from standard techniques.

In section 2.2 of this Chapter the asymptotic behaviour of the step response P(t) is compared with the asymptotic behaviour of the complex permittivity, where the relation with the angles of intersection in the Cole-Cole plot is emphasized.

For $t \to 0$, the point of interest is the derivative (dP/dt) at t = 0. It appears that if the value of this derivative is finite, the angle of intersection at the high-frequency side of the Cole-Cole plot will be $\pi/2$. If the derivative is zero, the angle of intersection will be greater than, or equal to $\pi/2$. If the derivative is infinite, it will be smaller than or equal to $\pi/2$. These results are of importance, experimentally, in terms of accuracy of TDR-experiments, because in an experimental situation for which the value of (dP/dt) at t = 0 is infinite, the accuracy of the high-frequency points of $\varepsilon(i\omega)$ is less than for situations where (dP/dt) at t = 0 is finite.

For $t \to \infty$, the first question of interest is, if there is a considerable low-frequency conductivity. If this conductivity may be neglected, the limiting value of P(t) amounts to $P(\infty) = \rho(\varepsilon_0)$, and the rate by which this limiting value is approached, is related to the angle of intersection at the low-frequency side of the Cole-Cole plot. An exponential rate may be found if the angle of intersection is $\pi/2$ or if the Cole-Cole plot grazes the ε'-axis. If the asymptotic value is approached as fast as $t^{-\zeta}$, $0<\zeta<1$, it follows that the angle of intersection at the low-frequency side of the Cole-Cole plot amounts to $\frac{1}{2}\pi\zeta$. In these respects the asymptotic behaviour of P(t) for non-conducting materials appears to be comparable with the asymptotic behaviour of the after-effect function[33].

If the low-frequency conductivity is considerable, one has $P(\infty) = -1$, and this value is approached as fast as $t^{-\frac{1}{2}}$. Instead of using a curve-fitting technique, the low-frequency conductivity can also be determined from the coefficient of the term in $t^{-\frac{1}{2}}$, for instance by plotting P(t) against $t^{-\frac{1}{2}}$.

An important consequence is that for compounds with a considerable low-frequency conductivity, and for compounds where the low-frequency side of the Cole-Cole plot cuts the ε'-axis non-perpendicularly, as for instance in the case of the Cole-Cole equation, it will be difficult to obtain a complete TDR-response, since in these cases the asymptotic value is approached at a relatively slow rate. This introduces the risk of large errors, when in these cases the TDR-signal is Fourier transformed to obtain values of ε' and ε'' in the frequency domain.

CHAPTER 3

EXPERIMENTAL PROCEDURE

3.1 EXPERIMENTAL EQUIPMENT

A schematic representation of the experimental equipment was given in Figure 1.1. In Figure 3.1 the experimental equipment as used in this work is shown. It incorporates the Hewlett-Packard 180 B Time Domain Reflectometry system (12.4 GHz), consisting of the 180 C mainframe, the 1815 B Plug-in unit, the 1817 A picosec Sampling Head and the 1106 A 20 picosec Tunnel Diode Mount. Part of the coaxial lines are of 7 mm precision lines as delivered by Hewlett-Packard, connected together with Amphenol APC-7 type connectors. The other part, including the measurement cell, is made of 14 mm precision coaxial line from General Radio (GR-900 system). The equipment used for thermostatic purposes consists of a dewar placed around the measurement cell, filled with water at the desired temperature. The temperature of the dielectric liquid under test was measured directly as it was enclosed in the coaxial line.

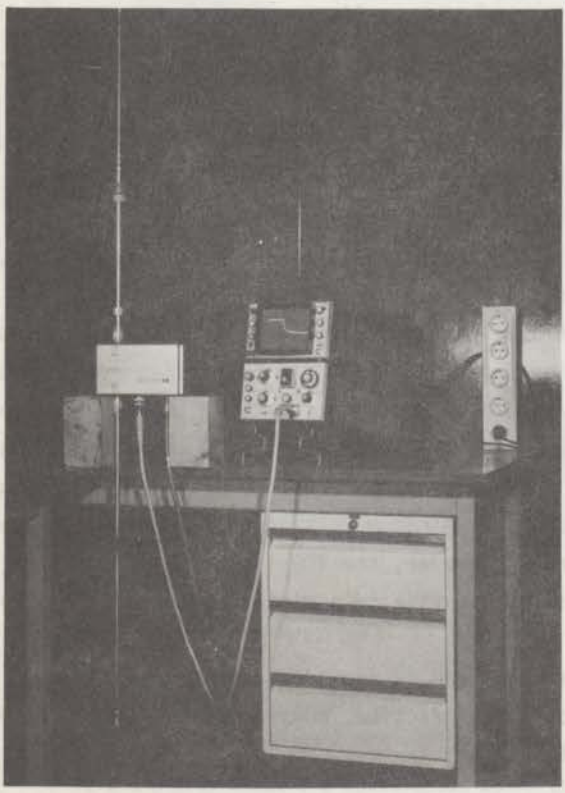

Figure 3.1 A

The experimental equipment.

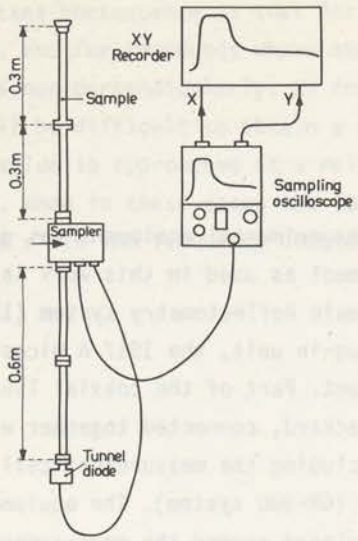

Figure 3.1 B

The experimental equipment.

The TDR-equipment operates as follows. A slow voltage ramp is propagated via the coaxial cable to the tunnel diode. This ramp will then open the tunnel diode from which a very fast step voltage (rise time about 35.10^{-12} sec) arises. This voltage is propagated again via the sampling system, to the air-dielectric interface where part of it will be reflected and the other part will be transmitted into the dielectric material. A short circuit is placed at the end of the cell which means that the voltage between the inner- and the outher conductor will only change its sign at that point and is propagated back through the interface to the sampling gate. In this thesis, the first reflection against the air-dielectric interface is analysed only, which means that the TDR-decay is assumed to be finished before the second reflection reaches the interface as well (infinite line). This gives a limitation, to lower frequencies, of the dielectric relaxation phenomena which can be studied by TDR. Using a cell length of about 0.33 meter and assuming a dielectric material with $\varepsilon_\infty = 3$, the maximum decay time is about 3.8 nanosec. Using the fact that the TDR-decay is finished, with sufficient accuracy, after $3\tau_0$, the maximum relaxation time measurable with the TDR-equipment is then about 1.3 nanosec or the minimum relaxation frequency, is about $\nu_0 = 0.12$ GHz. For reasons discussed later, however, the TDR-system is used with a maximum decay time of about 1.8 nanosec, giving rise to a minimum relaxation frequency of about 0.26 GHz.

The limitation at the higher frequency end is caused, in principle, by the finite rise time of the step function only. In practice, however, this is not the only limitation as will be discussed in section 3.3.

The measurement cell* used for the experiments is shown in Figure 3.2. It consists of a General Radio precision coaxial line (GR-900 system) with a thin mica bead (about 0.3 mm thick) to hold the liquid and at the end a short circuit which can be removed in order to fill the cell. Because the TDR-equipment from Hewlett-Packard is constructed for amphenol coaxial lines, an adapter has to be used to link the two coaxial systems.

In the paper by Loeb et al[13], it is suggested that minimum trouble from unwanted reflections against discontinuities (connectors, sampler, tunnel diode) will arise during the decay of the TDR-response when about 0.6 m coax is placed between tunnel diode and sampling system and also about 0.3 m (without connectors) between sampling system and the air-dielectric interface. All experiments , described in this thesis, have been carried out using the above improvement of the TDR-system.

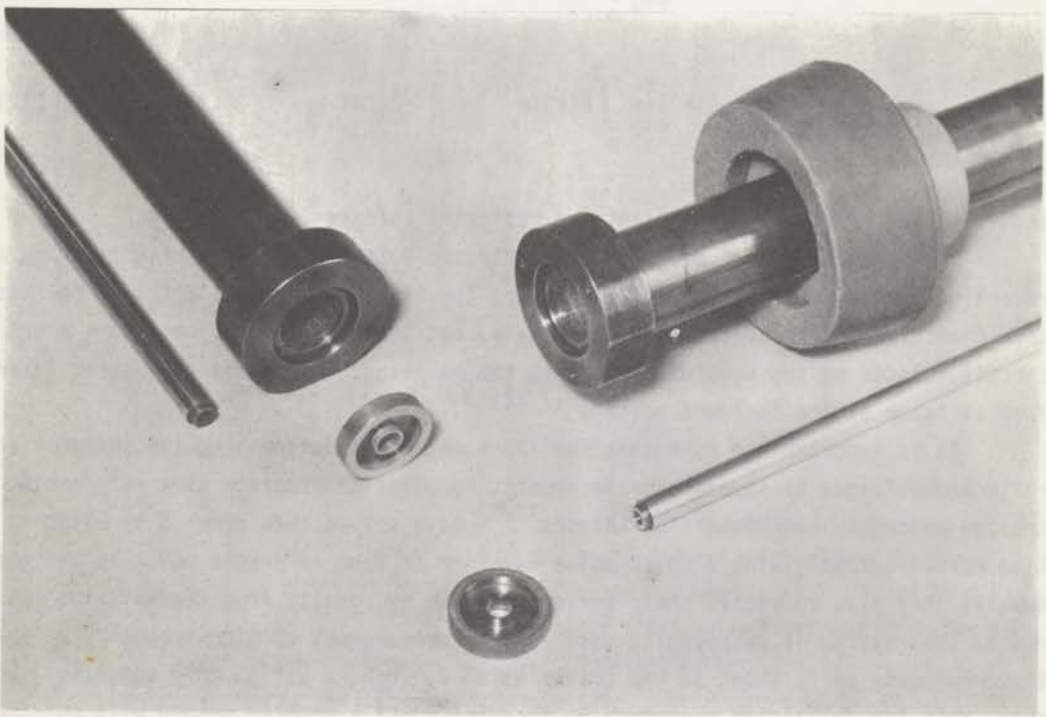

Figure 3.2 The measurement cell.

*The cell and mica beads are constructed by P. Leemans.

3.2 MEASUREMENT PROCEDURE

In section 1.4 it is concluded that the dielectric permittivity can be calculated from the Fourier transforms of the incident and reflected voltages, by the relation

$$\varepsilon(i\omega) = \left(\frac{F(i\omega) - G(i\omega)}{F(i\omega) + G(i\omega)} \right)^2 \tag{3.1}$$

where

$$F(i\omega) = \lim_{\gamma \to 0} \int_0^\infty V_0(t)\, e^{-(\gamma + i\omega)t}\, dt \tag{3.2}$$

$$G(i\omega) = \lim_{\gamma \to 0} \int_0^\infty R(t)\, e^{-(\gamma + i\omega)t}\, dt \tag{3.3}$$

and $V_0(t)$ and $R(t)$ are the incident and reflected voltages respectively.

The measurement procedure of the reflected voltage $R(t)$ is straightforward by recording the TDR-response on a XY-recorder. The incident voltage, $V_0(t)$ is not measured directly as it passes the sampling gate, but instead, the response to a short circuit, placed at the same distance from the sampling gate as the dielectric interface is taken as the incident voltage[6,7,12,13].

It is important to note that the above method of determining the incident and reflected voltages by separate measurements, requires an accurate time referencing of the two voltages. Suggett and colleagues[12,13] have solved this problem by using a time marker system giving a sharp spike waveform at some reference point in the time domain. They also corrected their reflection data by results from transmission measurements. This system is succesfully used for the measurement of high-frequency relaxation phenomena up to about 15 GHz (water at 5^o C, Loeb et al[13]). They suggested, however, that for relaxation phenomena up to about 1 GHz a simpler method will suffice. This reference method is shown in Figure 3.3. The shape of the reflected voltage (against the short circuit as well as against the dielectric interface) is then extrapolated to the top of the pulse. This position in time is used as the time reference $t = t_r$, for both voltages. All experiments described in this thesis have been carried out using the above reference procedure. It will be discussed in more detail in section 3.3.

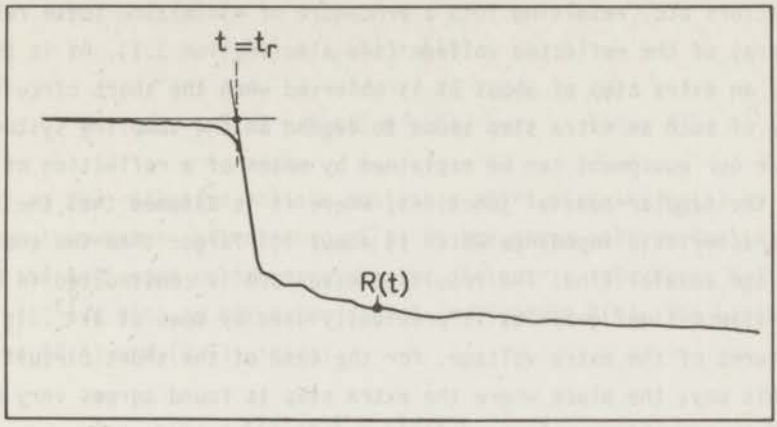

Figure 3.3 Definition of the time reference point $t = t_r$.

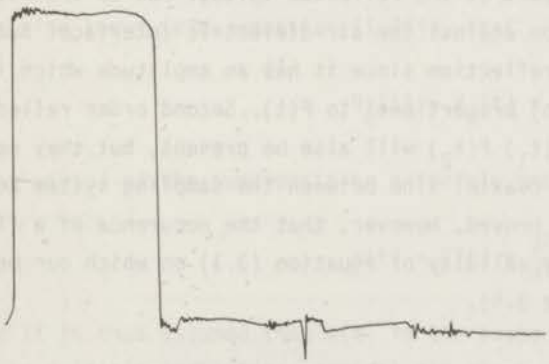

Figure 3.4

A. TDR-response against a short circuit, showing the unwanted step voltage.

B. Distance-time graph of the response against a short circuit, using 50 Ω for the coaxial lines and 55 Ω for the sampling system.

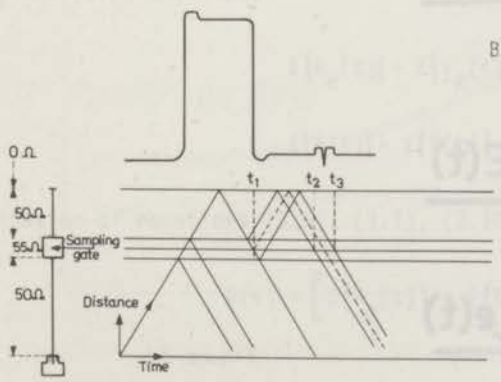

In their paper, Loeb et al[13] have payed much attention to unwanted reflections against connectors etc. resulting into a procedure of minimizing these reflections during the decay of the reflected voltage (see also section 3.1). As is shown in Figure 3.4, however, an extra step of about 5% is observed when the short circuit is applied. The occurence of such an extra step seems to depend on the sampling system used. The step found for our equipment can be explained by means of a reflection of the step voltage against the sampler-coaxial junctions, where it is assumed that the sampler system has a characteristic impedance which is about 10% larger than the characteristic impedance of the coaxial line. The resulting wave form is constructed in Figure 3.4 B, using the "distance-time" graph as is previously used by Loeb et al[13]. It appears that the main features of the extra voltage, for the case of the short circuit, can be explained in this way; the place where the extra step is found agrees very well with the dimensions of the sampling system.

An important feature of this extra step is, that the wave front has reflected only once against the short circuit. Therefore, if the short circuit is replaced by the air-dielectric interface, that part of the reflected voltage due to the extra step, depends only on one single reflection against the air-dielectric interface. Such a reflection is called a first order reflection since it has an amplitude which is (to an excellent degree of approximation) proportional to P(t). Second order reflections, with an amplitude proportional to $P(t_1)\ P(t_2)$ will also be present, but they occur at rather large times due to the 0.3 m coaxial line between the sampling system and the air-dielectric interface. It can be proved, however, that the occurence of a first order reflection does not affect the validity of equation (3.1) on which our measurement procedure is based (vide Figure 3.5).

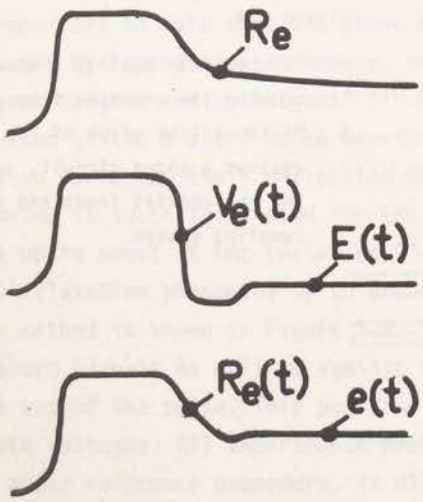

Figure 3.5
Definition of some symbols.

By definition one has:

$$V_0(t) = V_e(t) + E(t) \tag{3.4}$$

$$R(t) = R_e(t) + e(t) \tag{3.5}$$

where $V_0(t)$ is the reflected voltage against a short circuit, $V_e(t)$ is the incident pulse (without unwanted reflections), $E(t)$ is the error voltage due to the unwanted step, $R(t)$ the reflected voltage against the dielectric interface, $R_e(t)$ the exact response to $V_e(t)$ and $e(t)$ is the error signal involved in $R(t)$. The Laplace transform of equations (3.4) and (3.5) yields:

$$F(s) = \mathcal{L}\{V_e(t)\} + \mathcal{L}\{E(t)\} \tag{3.6}$$

$$G(s) = \mathcal{L}\{R_e(t)\} + \mathcal{L}\{e(t)\} \tag{3.7}$$

It is also known (e.g. equation (1.74)), that

$$R_e(t) = V_e(t) * \frac{dP}{dt} \tag{3.8}$$

and by virtue of the superposition principle one has

$$e(t) = E(t) * \frac{dP}{dt} \tag{3.9}$$

where it is thus assumed that $e(t)$ is the response to $E(t)$, which is only correct when no multiple reflections against the short circuit and air-dielectric interface are present in $E(t)$ and $e(t)$ respectively. Taking the Laplace transform of equations (3.8) and (3.9) one finds

$$\mathcal{L}\{R_e(t)\} = \mathcal{L}\{V_e(t)\} \cdot \Sigma(s) \tag{3.10}$$

$$\mathcal{L}\{e(t)\} = \mathcal{L}\{E(t)\} \cdot \Sigma(s) \tag{3.11}$$

Combination of equations (3.6), (3.7), (3.10) and (3.11) finally gives

$$G(s) = \left[\mathcal{L}\{V_e(t)\} + \mathcal{L}\{E(t)\}\right] \cdot \Sigma(s) = F(s) \cdot \Sigma(s)$$

or

$$\rho(s) = \frac{G(s)}{F(s)} \tag{3.12}$$

It is thus shown by equation (3.12), that the dielectric permittivity is obtained by calculating the Fourier transforms of the reflected pulses against the air-dielectric interface and the short circuit, even when a first order reflection against the interface is present.

It is clear from the discussion given above that the total length of the TDR-decay may not exceed the total length of the unwanted first order step, since otherwise the response R(t) is not the exact response to the step voltage $V_0(t)$ anymore and errors may be involved (see also the discussion in the next section about the errors in that situation).

The evaluation of the real and negative imaginary parts of the dielectric permittivity from the incident and reflected TDR-curves occurs as follows*. The shapes of the voltages are recorded on a XY-recorder and sampled (by hand). The time reference procedure is carried out as indicated in Figure 3.3. Then the actual times of all samples, using $t = t_r$ for the two reference points are calculated by:

$$t(n) = n\tau + t(1) - t_r \tag{3.13}$$

where t(n) is the actual time of the n-th sample, τ is the difference in time between two samples, t(1) is the actual time of the first sample and t_r is the reference time, see Figure 3.6.

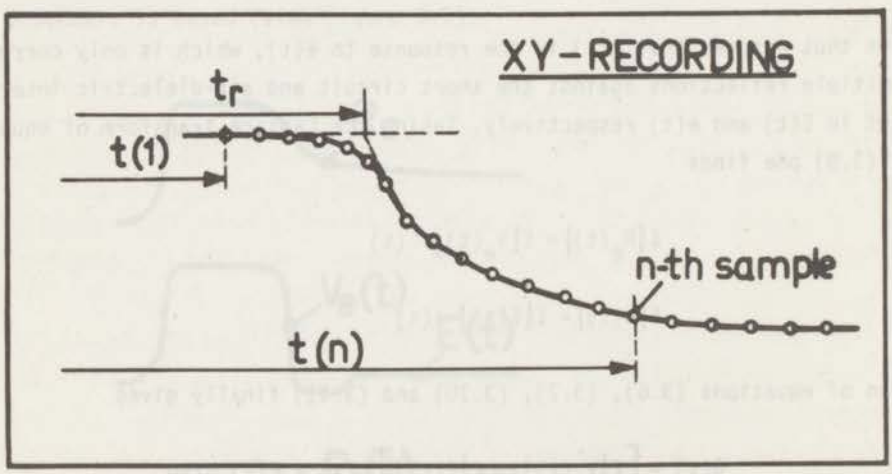

Figure 3.6 Definition of the symbols used for the calculation of the actual time t(n).

*This procedure has been suggested to the author by Mrs. P.A. Quickenden and Dr. A. Suggett during a short stay at their Laboratory (Unilever Research Laboratories, Sharnbrook, England).

After punching the data on cards the Fourier transform of the data is calculated[12] using Samulon's[42] modification of Shannon's[43] sampling theorem

$$F(i\omega) = \frac{\tau}{1 - e^{-i\omega\tau}} \sum_{n=1}^{N} [f(n\tau + \tau) - f(n\tau)]\, e^{-i\omega(n\tau + \tau)} \qquad (3.14)$$

where N is the number of samples used (which is about 300 for this work). Then the permittivity is calculated directly from equation (3.1) and the dielectric parameters are evaluated from the Cole-Cole plot of ε'' versus ε'.

The calibration of the TDR-traces in terms of actual time versus distance on the XY-recording (i.e. determination of τ) has been carried out by using the calibration lines on the oscilloscope. This is a fairly accurate procedure[44]. Due to the jitter, no other method seemed to be more accurate (a brief discussion of the jitter phenomenon is given in section 3.3).

The computer programs, as used by the author, are given in Appendices B and C.

3.3 ERROR ANALYSIS

3.3,1 INTRODUCTION

In the subsequent steps of evaluating the real and imaginary parts of the dielectric permittivity from TDR-measurements, as discussed in the former section, several errors may be involved. Due to these errors uncertanties arise in the parameters characterizing the dielectric relaxation behaviour, e.g. in ε_0, ε_∞ and τ_0, for a single relaxation time (Debye behaviour).

It is the purpose of this section to discuss the uncertanties involved in the determined parameters ε_0, ε_∞ and τ_0 in connection with inaccuracies involved in R(t) and $V_0(t)$. Due to the complexity of the problem, it will not be possible to give a detailed mathematical analysis. In most cases, however, an order of magnitude can be estimated.

In this section, the important error sources potentially present in $V_0(t)$ and R(t) will be defined and in section 3.3,2 their influences upon the values of ε_0, ε_∞ and τ_0 will be discussed.

In Figure 3.7 a schematic graph of $V_0(t)$ and R(t) is shown (for a better understanding of the purposes of this section, both curves are distorted). It is assumed that the XY-recorded curves run from C to E for R(t) and from D to F for $V_0(t)$. Very clearly the curve $V_0(t)$, as drawn in Figure 3.7, should have been recorded from point G instead of D.

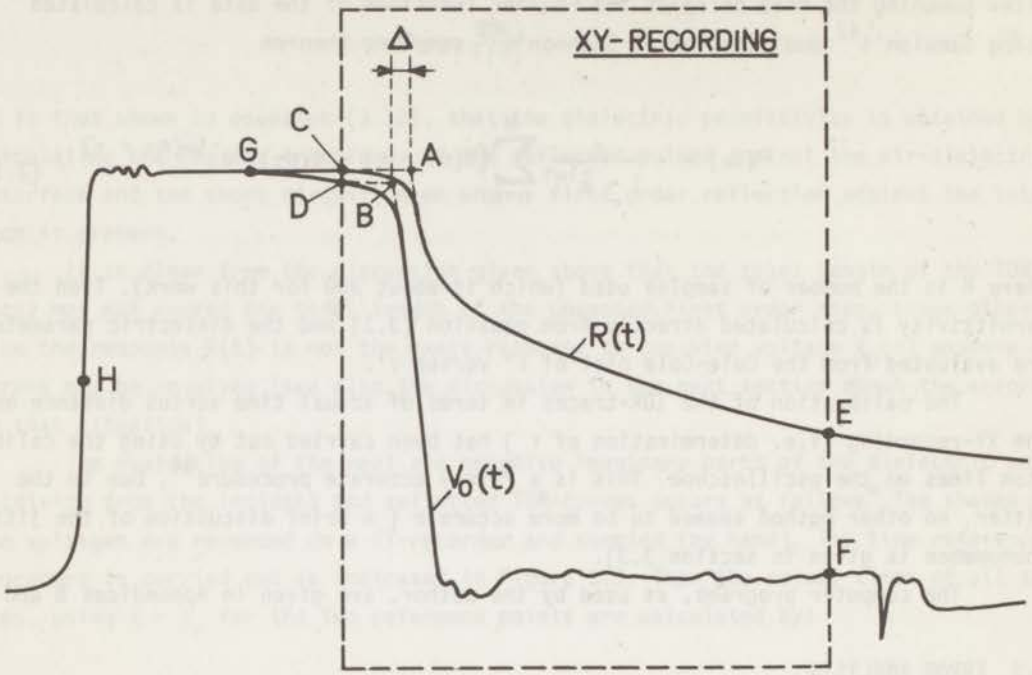

Figure 3.7 Definition of some possible uncertainties involved in XY-recorded TDR-curves.

In this graph, the time reference procedure is carried out, resulting in the reference points A and B for R(t) and $V_0(t)$ respectively. Because the total response curves are drawn, the two points H, which coincide on the two input ramp voltages, can be considered as exact time references, and it is therefore clear that the actual times of points A and B are not equal. This time difference, indicated by Δ , is the timing error which is potentially involved in the time reference procedure.

It is already noted, that the point D is not the best point to represent the first sample of curve $V_0(t)$. It is assumed, however, that the experimental conditions are such that on the XY-recording the point $V_0(1)$ corresponds to point D. Therefore this value of $V_0(1)$ is in error. The last point of $V_0(t)$,i.e. $V_0(N\tau)$ corresponds to point F. It can be observed from Figure 3.7 that the value of $V_0(N\tau)$ is in error as well, since F is chosen, for instance, on the top of a little "bubble" (these bubbles originate from unwanted reflections against connectors, sampler, tunnel diode etc). The possible errors in $V_0(1)$ and $V_0(N\tau)$ result into a possible error in $\rho(0)$. It must be mentioned that, in principle, the same uncertanties are present in the curve R(t), but their influence upon $\rho(0)$ is considerably smaller. However, in section 3.3,2 an "overall" error in $\rho(0)$ is discussed and the origin of this error is not of importance

in that discussion.

So far, two sources of errors are mentioned, both of which may influence the whole shape of the Cole-Cole plot and thus the values of all parameters to be obtained. However, there are at least three other potential errors. The first may appear in the situation that the dielectric material under test posesses such a large relaxation time that the curve R(t) has not reached its equilibrium value at $t = N\tau$, as is also shown in Figure 3.7. In that case, the value of $\rho(0)$ and thus of ε_0 is in error and very certainly the value of τ_0 as well (but not the value of ε_∞). The second may be due to the sampled representation of the steepest part of $V_0(t)$ which consists of about ten points in an actual recording. Refering to Shannon's sampling theorem[43], the question may then arise wether this discrete representation of $V_0(t)$ is sufficiently complete to give accurate values for the high-frequency part of the Fourier spectrum of $V_0(t)$. The third potential error consists of horizontal jitter of the TDR-curve as it is displayed on the oscilloscope screen. This jitter consists of uncontrollable and unpredictable horizontal movements of the signal which, unfortunately, are inherent to the use of sampling-oscilloscopes. Since the scan time of the XY-recording takes one minute, and during this scan time the displayed curve cannot be observed, it is clear that the jitter may be a rather hidden source of error.

Summarizing, the most important errors, to be discussed in the next section, are

(1) a time reference error
(2) an error in $\rho(0)$
(3) a not completed TDR-decay
(4) failure of Shannon's sampling theorem for the steepest part of $V_0(t)$?
(5) horizontal jitter of the TDR-curves

3.3,2 DISCUSSION OF THE ERRORS

The basis equations, to be used in this discussion are:

$$R(t) = \mathcal{L}^{-1}\{F(s)\,\rho(s)\} \tag{3.15}$$

$$\rho(i\omega) = -\frac{\sum_n [R(n\tau + \tau) - R(n\tau)]\, e^{-i\omega(n\tau + \tau)}}{\sum_m [V_0(m\tau + \tau) - V_0(m\tau)]\, e^{-i\omega(m\tau + .\tau)}} \tag{3.16}$$

$$\varepsilon(i\omega) = \left(\frac{1 - \rho(i\omega)}{1 + \rho(i\omega)}\right)^2 \tag{3.17}$$

When possible, the consequences of the errors involved in R(t) and $V_0(t)$ are directly translated into their equivalences in the frequency domain, i.e. into errors involved in $\varepsilon(i\omega)$ or $\rho(i\omega)$, but unfortunately this procedure cannot be carried out for all cases of interest. An alternative approach is then the construction of the Cole-Cole plot of $\varepsilon(i\omega)$ from simulated and Fourier transformed curves $V_0(t)$ and R(t). The parameters $\varepsilon_0, \varepsilon_\infty$ and τ_0 are then evaluated in the usual way. For those simulations, the application of a heaviside step function is not very useful, but the following non-ideal step function suffice:

$$V_0(t) = 1 - \frac{\sin (At + \phi)}{\sin \phi} \, e^{-t A \operatorname{cotg} \phi} \tag{3.18}$$

where $\phi = 0.785$. The values for A have been chosen in such a way that the rise time τ_r, defined by $V_0(\tau_r) = 1$, is equal to

$$\tau_r = \tau_0 \quad \text{for } A = 2.357$$

$$\tau_r = 0.1 \ \tau_0 \quad \text{for } A = 23.57$$

The Laplace transform of equation (3.18) yields

$$F(s) = \frac{1}{s} - \frac{2A \operatorname{cotg} \phi + s}{(s + A \operatorname{cotg} \phi)^2 + A^2} \tag{3.19}$$

A graph of equation (3.18), together with the corresponding response R(t) for a Debye dispersion is given in Figure 3.8.

For some of the discussions, it is necessary to compare results obtained from theoretical curves, such as Figure 3.8, with the corresponding results for experimental curves, such as Figure 3.9. To do so, it is assumed, from comparison of Figures 3.8 and 3.9 that the theoretical rise time τ_r corresponds approximately to 60 picosec experimentally.

In the following parts the influences upon the values of $\varepsilon_0, \varepsilon_\infty$ and τ_0, of the errors involved in R(t) and $V_0(t)$, are discussed.

(1) A TIME REFERENCE ERROR. When a timing error Δ is involved, the reflection coefficient, $\rho'(i\omega)$, is given by

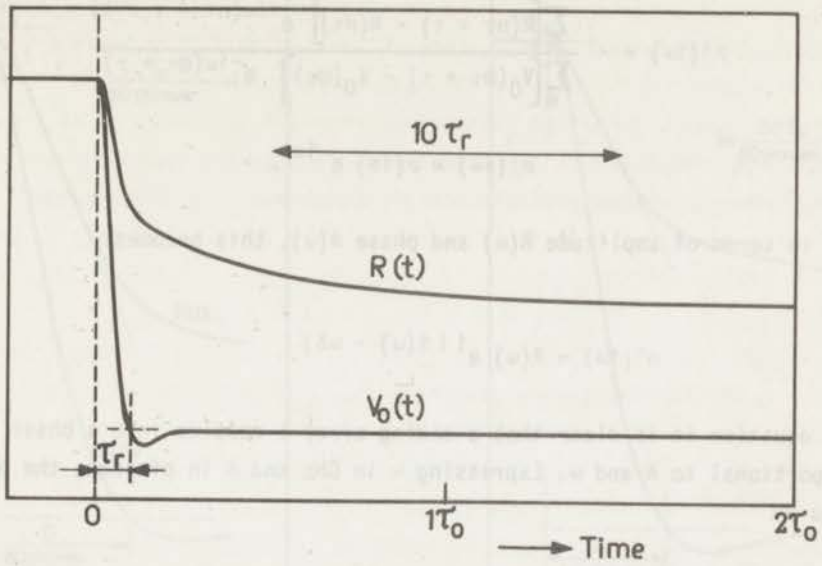

Figure 3.8 Curves $V_0(t)$ and the response R(t) for a Debye equation, $\varepsilon_0 = 20$, $\varepsilon_\infty = 4$.

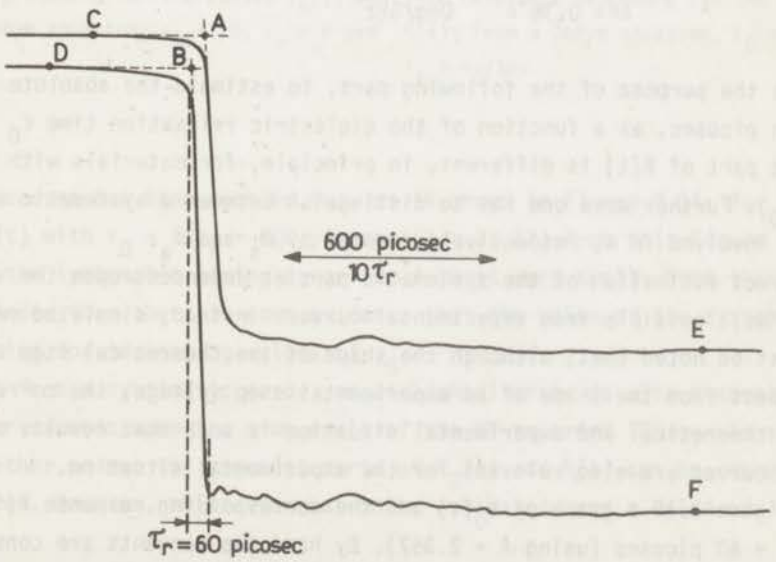

Figure 3.9 Experimental curves $V_0(t)$ and R(t) for methanol, T = 22 °C, $\varepsilon_0 = 33$, $\varepsilon_\infty = 5$, $\nu_0 = 3$ GHz ($\tau_0 = 53$ picosec).

$$\rho'(i\omega) = - \frac{\sum_n \left[R(n\tau + \tau) - R(n\tau)\right] e^{-i\omega(n\tau + \tau + \Delta)}}{\sum_m \left[V_0(m\tau + \tau) - V_0(m\tau)\right] e^{-i\omega(m\tau + \tau)}}$$

or $$\rho'(i\omega) = \rho(i\omega)\, e^{-i\omega\Delta}$$

Writing ρ in terms of amplitude $R(\omega)$ and phase $\theta(\omega)$, this becomes:

$$\rho'(i\omega) = R(\omega)\, e^{i\,[\,\theta(\omega) - \omega\Delta\,]} \tag{3.20}$$

From this equation it is clear that a timing error Δ results into a phase error with a value proportional to Δ and ω. Expressing ν in GHz and Δ in picosec, the phase error is denoted by

$$\text{phase error} = 2\pi\nu\ \Delta\ 10^{-3}$$

or, expressing this error in "Degrees/GHz", the result is:

$$\Delta\theta = 0.36\ \Delta \qquad \text{Deg/GHz} \tag{3.21}$$

It is the purpose of the following part, to estimate the absolute value of Δ, expressed in picosec, as a function of the dielectric relaxation time τ_0 (note that the steepest part of R(t) is different, in principle, for materials with different values of τ_0). Further more one has to distinguish between a systematic and an accidental part involved in Δ, respectively denoted by Δ_s and Δ_a.

A direct estimation of the systematic part as dependent upon the value of τ_0, is not very well possible from experimental curves. Instead, simulated results will be used. It must be noted that, although the shape of the theoretical step as such differs in some respect from the shape of an experimental step voltage, the correspondence between the theoretical and experimental situation is such that results obtained from theoretical curves are also relevant for the experimental situation.

In Figure 3.10 a graph of $V_0(t)$ and the corresponding response R(t) is given for $\tau_r = \tau_0 = 60$ picosec (using A = 2.357). By hand the tangents are constructed and it is observed that a systematic timing error is involved. The value of Δ_s is estimated, from this graph as

$$\Delta_s \simeq 2.5 \text{ picosec} \quad (\tau_0 = 60 \text{ picosec})$$

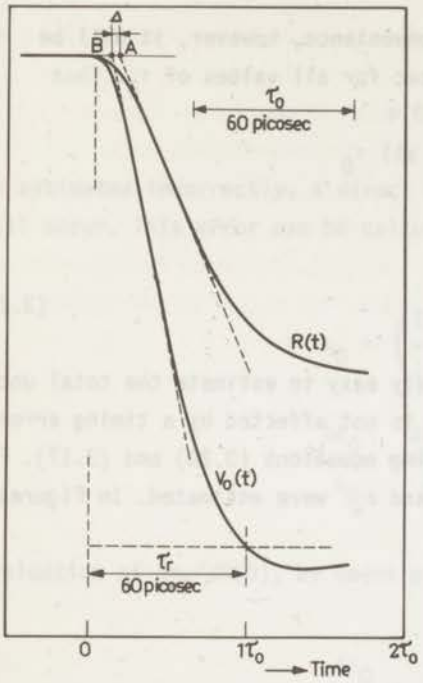

Figure 3.10

Time reference procedure for the curves $V_0(t)$ and R(t); From a Debye equation, $\varepsilon_0 = 20$, $\varepsilon_\infty = 4$ and $\tau_r = \tau_0$.

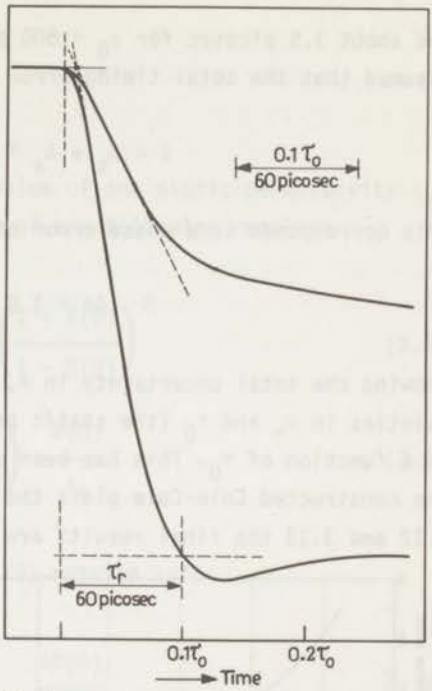

Figure 3.11

Time reference procedure for the curves $V_0(t)$ and R(t); From a Debye equation, $\varepsilon_0 = 20$, $\varepsilon_\infty = 4$ and $\tau_r = \tau_0/10$.

The same procedure has been carried out, as is shown in Figure 3.11, for graphs of $V_0(t)$ and R(t) with $\tau_0 = 10\tau_r = 600$ picosec (A = 23.57). From this Figure it can be observed that the systematic timing error is at least very small. From these results it can be concluded that there is some evidence that the value of the systematic part of Δ is decreasing for increasing values of τ_0.

Apart from a systematic error, an accidental error is also present. The value of this error depends upon the time scale of the XY-recorded TDR-curves and also upon the fact whether or not the steepest parts of $V_0(t)$ and R(t) can be represented by straight lines. However, this error has to be estimated, and a value of

$$\Delta_a = 1.5 \text{ picosec}$$

is chosen (this value corresponds to 0.25 mm in an actual XY-recorded curve).

From the foregoing results, it can be concluded that the total possible error in the time reference procedure is of the order of 4 picosec for $\tau_0 \simeq 60$ picosec

and about 1.5 picosec for $\tau_0 \simeq 600$ picosec. For convenience, however, it will be assumed that the total timing error equals 4 picosec for all values of τ_0. Thus

$$\Delta = \Delta_s + \Delta_a \simeq 4 \text{ picosec for all } \tau_0$$

This corresponds to a phase error of

$$\Delta\theta \simeq 1.5 \quad \text{Deg/GHz} \tag{3.22}$$

Knowing the total uncertainty in Δ, it is relatively easy to estimate the total uncertainties in ε_∞ and τ_0 (the static permittivity ε_0 is not affected by a timing error), as a function of τ_0. This has been done by combining equations (3.20) and (3.17). From the constructed Cole-Cole plots the values of τ_0 and ε_∞ were estimated. In Figures 3.12 and 3.13 the final results are given.

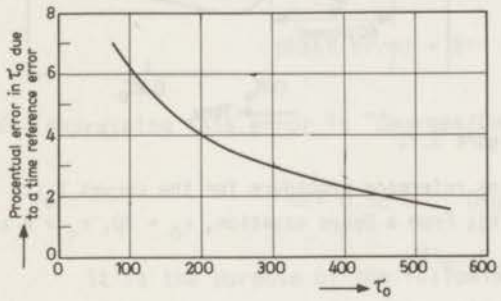

Figure 3.12

Procentual error in τ_0 or ν_0 as depending on τ_0, due to a time reference error.

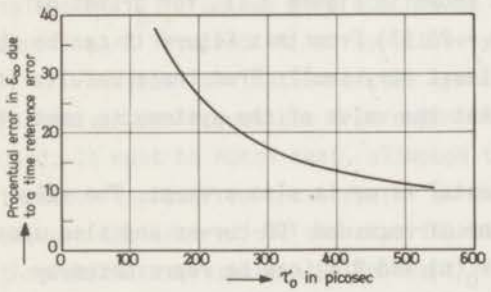

Figure 3.13

Procentual error in ε_∞ as depending on τ_0, due to a time reference error.

(2) AN INCORRECT ESTIMATION OF $\rho(0)$. When the value of $\rho(0)$, given by

$$\rho(0) = -\frac{\sum_n \{R(n\tau + \tau) - R(n\tau)\}}{\sum_m \{V_0(m\tau + \tau) - V_0(m\tau)\}} = -\frac{R(N\tau) - R(\tau)}{V_0(M\tau) - V_0(\tau)}$$

or

$$\rho(0) = -R(\omega = 0)$$

is estimated incorrectly, a direct error in the value of the static permittivity ε_0 will occur. This error can be calculated by means of the following results:

$$\varepsilon_0 = \left(\frac{1 - \rho(0)}{1 + \rho(0)}\right)^2 = \left(\frac{1 + R(0)}{1 - R(0)}\right)^2 \tag{3.23}$$

$$\frac{\Delta\varepsilon_0}{\varepsilon_0} = \frac{\Delta R(0)}{R(0)} \left(\frac{d\varepsilon_0}{dR(0)}\right) \frac{R(0)}{\varepsilon_0} \tag{3.24}$$

Evaluation of $d\varepsilon_0/dR(0)$, by means of equation (3.23) results into:

$$\frac{\Delta\varepsilon_0}{\varepsilon_0} = \left[\frac{4\ R(0)}{1 - R(0)^2}\right] \frac{\Delta R(0)}{R(0)} \tag{3.25}$$

In Figure 3.14, the multiplication factor $4\ R(0)/[\,1 - R(0)^2]$ is plotted versus R(0) (and also versus ε_0). From this graph it is clear that some uncertainty in R(0) causes a considerable larger uncertainty in ε_0 (for $\varepsilon_0 \approx 20$ and $\Delta R(0)/R(0) \approx 1\%$ it follows that $\Delta\varepsilon_0/\varepsilon_0 \approx 4\%$).

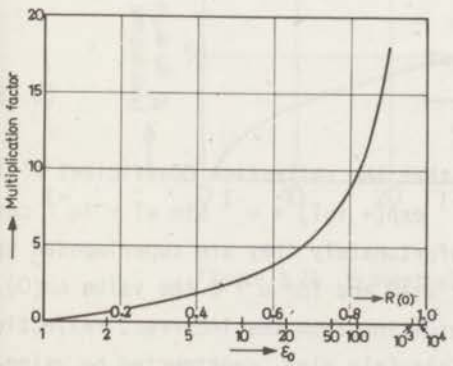

Figure 3.14

Graph of the multiplication factor $4R(0)/\{1-R(0)^2\}$.

The uncertainty in τ_0 due to an error in $\rho(0)$ cannot be calculated very easily for the general situation that this error is caused by uncertainties in the first and last samples of $V_0(t)$ and $R(t)$. This problem can perhaps be solved by means of simulations, but this research has not been carried out yet. It is possible, however, to give an order of magnitude for the uncertainty in τ_0 due to an uncertainty in the last samples only. In that case, the measured reflection coefficient $\rho'(i\omega)$, may consist of the exact $\rho(i\omega)$ and an error term $\Delta\rho(i\omega)$ which can be approximated by the Fourier transform of a step function with amplitude $\Delta\rho(0)$, starting at the actual time T of the last samples, i.e.

$$\Delta\rho(i\omega) = \lim_{\gamma \to 0} \mathcal{F}^{-1}\{\Delta\rho(0)\, u(t - T)\} \tag{3.26}$$

where $u(t - T)$ is the translated heaviside step, defined by:

$$u(t - T) = \begin{cases} 1 & t > T \\ 0.5 & t = T \\ 0 & t < T \end{cases} \tag{3.27}$$

Then $\rho(i\omega)$ is given by

$$\Delta\rho(i\omega) = \Delta\rho(0)\, \frac{e^{-i\omega T}}{i\omega} \tag{3.28}$$

It should be noted that equation (3.28) is only correct for $\omega >> 0$, because $\Delta\rho(i\omega) \to -i\infty$ when $\omega \to 0$ instead of $\Delta\rho(i\omega) \to \Delta\rho(0)$. However, using equation (3.28) the new reflection coefficient becomes:

$$\rho'(i\omega) = \rho(i\omega) + \Delta\rho(0)\, \frac{e^{-i\omega T}}{i\omega} \tag{3.29}$$

From inspection of equation (3.29), it is clear that the reflection coefficient $\rho'(i\omega)$ will contain oscillations, due to the term $(i\omega)^{-1} \exp(-i\omega T) = \omega^{-1} \sin \omega T - i\omega^{-1} \cos \omega T$ The oscillations as such can be smoothed, but unfortunately they are superimposed upon an average error which has the value $\Delta\rho(0)/\omega$ for $\omega >> 0$ and for $\omega \simeq 0$ the value $\Delta\rho(0)$.

The uncertainty in the value of τ_0, as resulting from the incorrect reflection coefficient $\rho'(i\omega)$ has been estimated from the Cole-Cole plot, constructed by using equation (3.17). It is assumed, that the total uncertainty in $\rho(0)$, as resulting from incorrect values of the samples of $V_0(t)$ and $R(t)$, is about 0.5%. Then, the error in the value of τ_0 is about 5% (for $\varepsilon_0 = 20$, $\varepsilon_\infty = 4$ and $T = 5\ \tau_0$). Thus:

$$\frac{\Delta\tau_0}{\tau_0} \simeq 5\% \quad \text{for} \quad \frac{\Delta\rho(0)}{\rho(0)} \simeq 0.5\%$$

Further more the total inaccuracy of $\rho(0)$ is estimated to be

$$\frac{\Delta\rho(0)}{\rho(0)} \simeq 1\%$$

resulting into an error in ε_0 as given by equation (3.25) with $\Delta R(0)/R(0) = 1\%$:

$$\frac{\Delta\varepsilon_0}{\varepsilon_0} \simeq \frac{4\,R(0)}{1 - R(0)^2}\,, \qquad \frac{\Delta R(0)}{R(0)} = 1\%$$

or

$$\frac{\Delta\varepsilon_0}{\varepsilon_0} \simeq \frac{1 - \varepsilon_0}{\sqrt{\varepsilon_0}} \quad |\%| \tag{3.30}$$

In Figure 3.15 the result is plotted (Figure 3.15 is the same as Figure 3.14, but with a linear scale in ε_0).

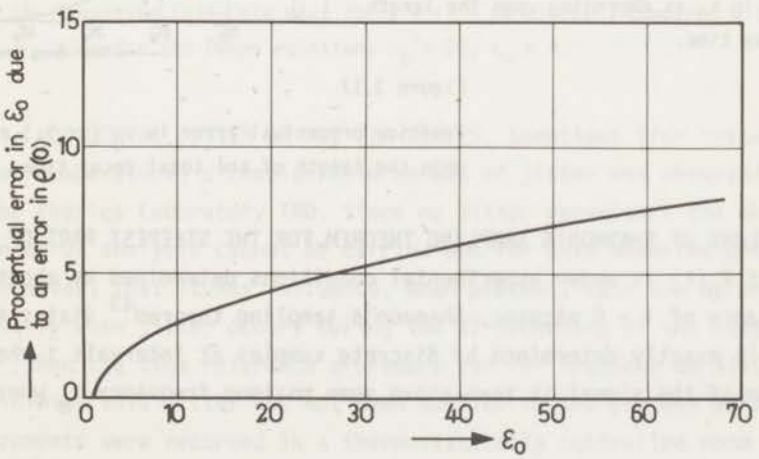

Figure 3.15 Procentual error in ε_0 due to an error in $\rho(0)$.

The influence of an error in the first samples (see Figure 3.7) has some effect upon the possible error in ε_∞. This error in ε_∞ is than also given by Figure 3.14. Using $\varepsilon_\infty \simeq 3$ and $\Delta R(\infty) \simeq 0.5\%$, the error involved in ε_∞ will be of the order of 0.5%. This

is negligible compared with errors involved in ε_∞ from other sources (for instance a timing error).

(3) A NOT COMPLETED DECAY. The influence upon the values of ε_0, ε_∞ and τ_0 when a not completed TDR-decay is Fourier analysed is very easily studied by means of simulated graphs. In Figures 3.16 and 3.17 the results are presented for the errors in ε_0 and τ_0 as a function of the total decay time (expressed in units of τ_0). It is noted that the point t = 0 for the simulated TDR-curves is rather close to the time reference point used experimentally. The results from the simulations are therefore representative for experimental purposes.

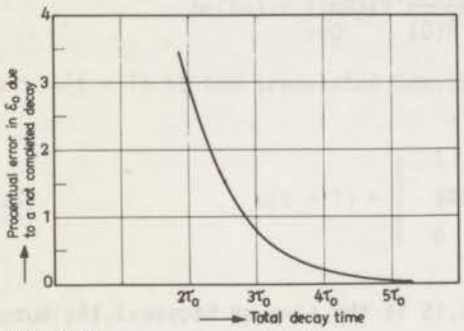

Figure 3.16

Procentual error in ε_0 as depending upon the length of the total decay time.

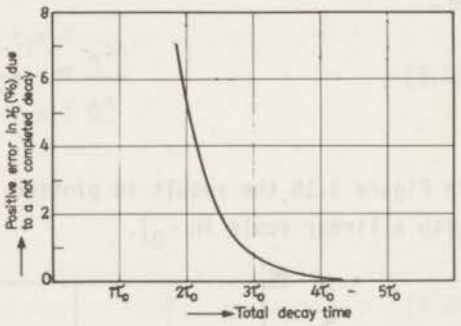

Figure 3.17

Positive procentual error in ν_0 (or τ_0) as depending upon the length of the total decay time.

(4) FAILURE OF SHANNON'S SAMPLING THEOREM FOR THE STEEPEST PART OF $V_0(t)$? The steepest part of $V_0(t)$ is under experimental conditions determined by about ten samples, at a distance of τ = 6 picosec. Shannon's sampling theorem[43] states that the complete curve is exactly determined by discrete samples at intervals τ when the Fourier spectrum of the signal is zero above some maximum frequency ν_m where ν_m and τ are related by

$$\nu_m = \frac{1}{2\tau} \tag{3.31}$$

or, using $\tau = 6\ 10^{-12}$:

$$\nu_m = 80\ \text{GHz} \tag{3.32}$$

According to this value of ν_m, it is assumed that Shannon's criterion is sufficiently obeyed. Nevertheless a simulation is carried out with $\tau = \tau_r$, thus $\tau \approx 60$ picosec for experimental conditions (the steepest part of $V_0(t)$ is then represented by only one sample). The resulting Cole-Cole plot is presented in Figure 3.18, from which it can be seen that the value of τ_0 is about 0.8% lower and the value of ε_∞ is about 5% larger. Compared with the extreme large value of the interval τ, it can be stated that no difficulties are to be expected from deviations of Shannon's theorem.

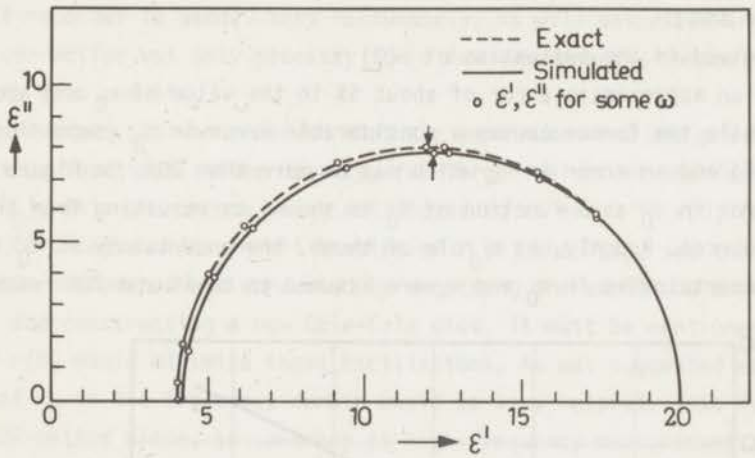

Figure 3.18 Resulting Cole-Cole plot for $\tau = \tau_r = 60$ picosec, compared with the exact plot for the Debye equation, $\varepsilon_0 = 20$, $\varepsilon_\infty = 4$.

(5) HORIZONTAL JITTER OF THE TDR-CURVES. Sometimes (for instance after a change of the room temperature) a considerable amount of jitter was observed for the TDR-equipment at the Physics Laboratory TNO. Since no jitter parameters can be predicted a priori, an error analysis cannot be carried out for this unwanted phenomenon. It is certain, however, that it has influence, when present, upon the accuracy of at least τ_0, especially when jitter occurs during the XY-recording of the steepest part of the TDR-curve (then the time reference procedure can for instance be disturbed). A procedure to minimize this jitter has not been applied in the present work[45,10] but the TDR-measurements were recorded in a thermostatically controlled room and after each scan the position of the TDR-curve was compared with respect to its original position and when the difference was too large, a new curve was recorded. Nevertheless, some slight movements had to be accepted sometimes.

It is important to note, that this unwanted jitter is the reason that, when a XY-recording method is used (with a scan time of one minute) the more advanced method of time referencing, using a delay line which produces a sharp spike, does not give better results than the reference method described in this thesis[44]. This is of course

not true when a C.A.T. data logging system is available since very fast scan times (of about 1/30 sec) can then be used.

3.3,3 DISCUSSION OF THE RESULTS

From the foregoing analysis it is clear that at least two sources of error are of importance in the TDR-experiments:

(1) a timing error between the short circuit response curve relative to the dielectric response curve and

(2) the error involved in the evaluation of $\rho(0)$

The latter causes an approximate error of about 5% in the value of τ_0 and about 5% in the value of ε_0 while the former causes a considerable error in τ_0 (depending upon the value of τ_0 itself) and an error in ε_∞ which may be more than 20%. In Figure 3.19 the total possible error in τ_0 as a function of τ_0 is shown, as resulting from the two mentioned error sources. Roughly, as a rule of thumb, the uncertainty in τ_0 is about 7.5%, while the uncertainties in ε_0 and ε_∞ are assumed to be 5% and 20% respectively.

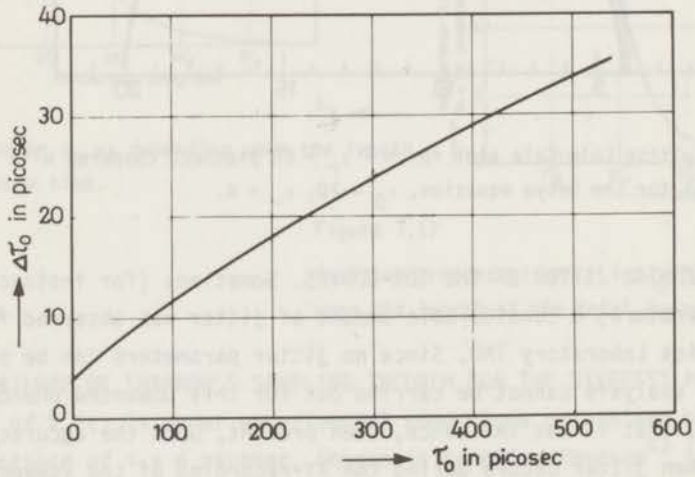

Figure 3.19 Total error in τ_0 as depending upon τ_0, for a timing error and an error in $\rho(0)$.

Apart from the possible errors in ε_0 and ε_∞ which are slightly larger than from frequency domain experiments, the total error in τ_0 is of the same order.

The two error mechanisms, mentioned above, sometimes give rise to a necessary correction of the originally constructed Cole-Cole plot. When very obviously a timing error is involved, the reflection coefficient $\rho(i\omega) = R(\omega) \exp(i\theta)$ has to be corrected. Because a timing error does not affect the amplitude R, the phase $\theta(\nu)$ is corrected by $\Delta\theta$ Degrees/GHz, until the Cole-Cole plot has a more acceptable shape. This procedure

is correct when the value of ε_∞ is known (as for instance for the results given in the paper by Suggett et al[12] and in some of the test experiments described in the next Chapter) or when one or more high-frequency points in the Cole-Cole plot are known[13]. When, however, no high-frequency data is present, this correction procedure is rather arbitrary. It must be noted, however, that the procedure as such has an exact mathematical basis and also that it is necessary when the time reference method, as described in this work, is used (because of the jitter in combination with the large scan time of one minute, this is very obviously the only time reference method possible when a XY-recorder is used). Very fortunately, as will described in the next Chapter, a phase correction was only necessay for a few experiments, indicating that this method gives very good results.

More often, it was observed that the amplitude- and the phase curves were oscillating, sometimes rather heavily, for larger values of the frequency (in general for $\nu > 2\ \nu_0$), this phenomenon being attributed to an error in $\rho(0)$ (and very probably also due to uncertainties in all samples of $V_0(t)$ and $R(t)$, see the paper by Loeb et al[13]). This phenomenon was corrected by smoothing the amplitude and the phase curves, by hand, and constructing a new Cole-Cole plot. It must be mentioned that a correct value of $\rho(0)$ would minimize these oscillations. As was suggested earlier[25], a measurement of ε_0 in the frequency domain would be very helpful. This is not a restriction of the TDR-method since, in contrary to high-frequency measurements, a determination of ε_0 is standard and takes very little time.

The fact that a small error in $\rho(0)$ generates considerable errors in ε_0 and τ_0 is the reason that the curves $V_0(t)$ and $R(t)$ cannot be used at actual times t larger than the maximum time of the first order unwanted step, since then errors in $\rho(0)$ of the order of 5% may appear and very obviously this would lead to a complete distorted shape of the Cole-Cole plot. It is relatively easy,however, to change the equipment for a measurement of relaxation times larger than about 600 picosec ($\nu_0 < 0.25$ GHz), by lengthening the coaxial line between sampler and air-dielectric interface, since the unwanted step has the same length in time as the step voltage itself, see Figure 3.4.

Although the error analysis given in this Chapter is by no means complete, it nevertheless gives some idea of the accuracy to be expected in the values of the dielectric parameters obtained from TDR-experiments.

It should also be noted that the use of reflection and transmission methods and a C.A.T. a very accurate time referencing, to 0.1 picosec[44], can be obtained. An accurate value of $\rho(0)$, within about 0.2%, is than also possible.

Finally, to end this Chapter an example of the method of analysis is given. In Figure 3.20 the experimental TDR-curves of a 1:1 volume mixture of Heptanol-1 and carbon tetrachloride (see section 4.3) are shown. After sampling (by hand) and Fourier transforming the data, the Cole-Cole plot shown in Figure 3.21 is obtained. From this

plot it is clear that at least oscillations are involved. The amplitude and phase curves are then constructed, as shown in Figure 3.22. In this Figure the smoothed curves and the phase curve resulting from $\Delta\theta$ = -1 Deg/GHz are also shown. From these curves, the final Cole-Cole plot is obtained which is shown in Figure 3.23.

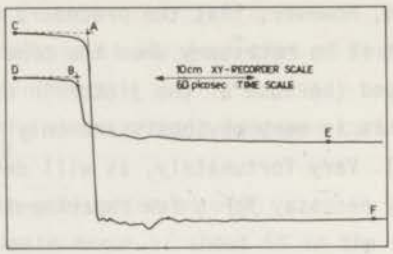

Figure 3.20 Experimental TDR-curves for 1:1 volume mixture of heptanol-1 and carbon tetrachloride, T = 33 °C.

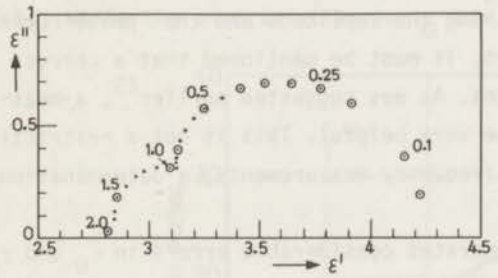

Figure 3.21

Direct obtained Cole-Cole plot without any corrections.

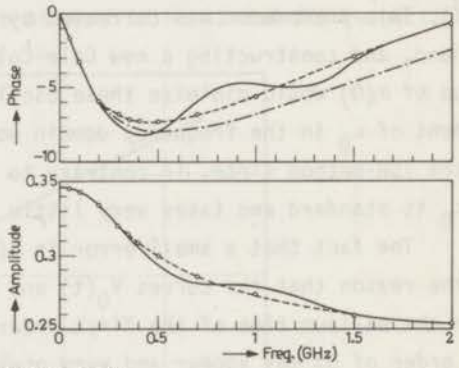

Figure 3.22

Amplitude and phase curves.

——— original curves

– – – smoothed curves

– · – corrected phase curve $\Delta\theta$ = -1 Deg/GHz.

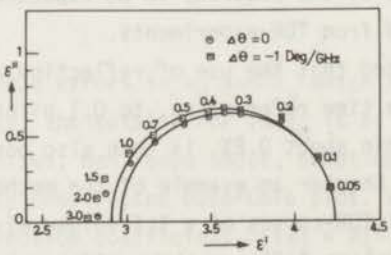

Figure 3.23 Corrected Cole-Cole plot, smoothed and $\Delta\theta$ = -1 Deg/GHz.

CHAPTER 4

TDR-MEASUREMENTS ON SOME NORMAL ALCOHOLS AND ON SOLUTIONS OF NORMAL ALCOHOLS IN CARBON TETRACHLORIDE

4.1 INTRODUCTION

Studies by various physico-chemical methods (e.g. IR, NMR, dielectric spertroscopy) of the molecular motions in polar liquids have indicated the significance of hydrogen bonding in these systems. From such studies one might hope to obtain information concerning the energy and average lifetime of the hydrogen bond and its influence upon the structure of the polar liquid.

Two types of hydrogen bonds may be distinguished: the intramolecular and the intermolecular bonds, the latter being the only relevant type in our case.

Intermolecular hydrogen bonds can occur between identical molecules, leading to association and between different molecules, leading to complex formation. In the case of association a second distinction can be made between

(1) compounds where only one group in each molecule can act as a hydrogen bond donor or acceptor, leading to associates with a restricted number of molecules (multimers), and

(2) compounds where more than one group can occur as a hydrogen bond donor or acceptor, leading to a three-dimensional network involving the whole liquid.

If the association is restricted to multimers of a limited size, the structure may be characterized by means of the various types of multimer structure and by the equilibrium constants. Examples are the carboxylic acids, hydrogen cianide and the mono alcohols.

For the mono alcohols no general agreement has yet been obtained concerning the structure of the multimers[51,52], despite investigations carried out with a great number of techniques. Dieletric relaxation is one such techniques by which many experiments have been reported. For the normal alcohols it has been shown that (at least) three relaxation ranges[52-54] are involved of which the low-frequency range is the dominant one. This range can be characterized, within measurement accuracy, by one single relaxation time, which varies with temperature as in a rate process. The activation energy depends strongly on the number of carbon atoms, the structure of the carbon skeleton[55] and the location of the hydroxyl group in the carbon chain[56,57]. A further interesting feature is that mixtures of alcohols with strongly different activation energies also show a main dispersion range characterized by one single relaxation time[58].

Another possible variation of the system, which may for instance influence the activation energy, is a dilution of the alcohol by a non-polar solvent. One reason for

a dielectric investigation of such mixtures may be the interest in the high-frequency dispersion ranges of the alcohols[59-61]. In that case the alcohols are diluted by a polar solvent to such a degree that the low-frequency dispersion range vanishes. It is also of interest to carry out a systematic investigation on the influence of non-polar solvents to the value of the main relaxation time. Here, only a few data are available.

Moriamez[62] found an increase of the activation energy for dilution of 2-ethylhexanol-1 with paraffin. An analogous result was found by Sagal[63] for mixtures of ethanol and cyclohexane. From the measurements of Denney and Ring[64], however, it follows that mixtures of propanol-1 and 2-methylpentane show a decrease in activation energy[51]. Very recently, Van den Berg[65] studied mixtures of butanol with carbon tetrachloride and with hexane, the former leading to an increase in activation energy and frequency factor (see the next section), while for the latter mixture the values of these quantities do not change significantly.

A systematic investigation on this subject may therefore be of great importance. A study should then be made of a great number of alcohols diluted into a variety of non-polar solvents. Such experiments, carried out with the conventional frequency domain methods, require much work and time. With the aid of time domain reflectometry, however, it is possible to perform the experiments within a reasonable timescale.

In section 4.2 the results of test measurements on some of the mono alcohols are presented, while in section 4.3 the results are given of measurements on alcohol/carbon tetrachloride mixtures.

4.2 TEST MEASUREMENTS ON SOME NORMAL ALCOHOLS

Since both Fellner-Feldegg[6] and Suggett and colleagues[12,13] have chosen the normal alcohols as test specimens for their TDR-experiments, we have used the same compounds for this purpose.

The alcohols were obtained from Merck N.V. The liquids were dried on $CaSO_4$ (about 24 hours) and distilled shortly before the measurements. The boiling points proved to be in agreement with literature values[47].

In Table 4.1 the results from measurements on ethanol, propanol, butanol and heptanol are summarized. Some experiments were carried out at the "Unilever Research Laboratories" in England. They are labelled with an "E", while the experiments carrried out at the "Physisch Laboratorium TNO" in Den Haag are labelled with an "H". The measurement procedure, used in the former experiments[12,13] differs slightly from the procedure described in Chapter 3: the TDR-curves were recorded with a C.A.T. and the measuring cell consisted of an Amphenol coaxial line of 20 cm length. Table 4.1 also indicates when smoothing (see section 3.3) has been necessary (denoted by a +). When the phase had to be corrected, the value for $\Delta\theta$ is also given. In Appendix D some of the

Cole-Cole plots are shown.

TABLE 4.1

TDR-MEASUREMENTS ON THE MONO ALCOHOLS

Compound	T	ε_0	ε_∞	ν_0	τ_0	H/E	smoothed	$\Delta\theta$
Ethanol	2.0	28.3	4.7	0.48	332	H	+	-2
	24.0	24.75	4.55	0.902	176	H	+	-1
Propanol	4.5	23.22	4.23	0.263	605	H		
	19.8	21.3	4.22	0.394	404	H	+	
	25.9	20.6	4.25	0.495	322	H		
	44.5	18.9	4.7	0.78	204	H	+	
	51.5	18.95	4.78	1.16	137	H	+	-0.5
	69.5	15.5	4.3	1.90	84	H	+	
Butanol	19.2	17.1	3.3	0.293	543	E	+	-1
	22.5	17.4	3.3	0.31	513	E†	+	-1
	26.5	17.2	2.8	0.336	474	H		
	30.0	16.7	3.3	0.42	379	H		
	46.5	15.8	2.35	0.65	245	H	+	+2
Heptanol	30.5	10.9	2.85	0.195	816	H		
	41.8	9.95	2.65	0.31	513	H		
	77.0	7.2	4.0	1.25	127	H		

† XY-recorded TDR-curves

In Figures 4.1 - 4.4 the results of the TDR-measurements are compared with frequency domain measurements referred to the literature. The results of Fellner-Feldegg and Suggett et al are also shown. From these Figures it can be concluded that the results obtained from TDR-experiments, using the procedure indicated in Chapter 3, are in excellent agreement with those from frequency domain measurements. This is consistent with the conclusion of Suggett and colleagues. The results obtained by Fellner-Feldegg are less consistent (except his values for ε_0) as is to be expected considering his less acceptable method of analysis.

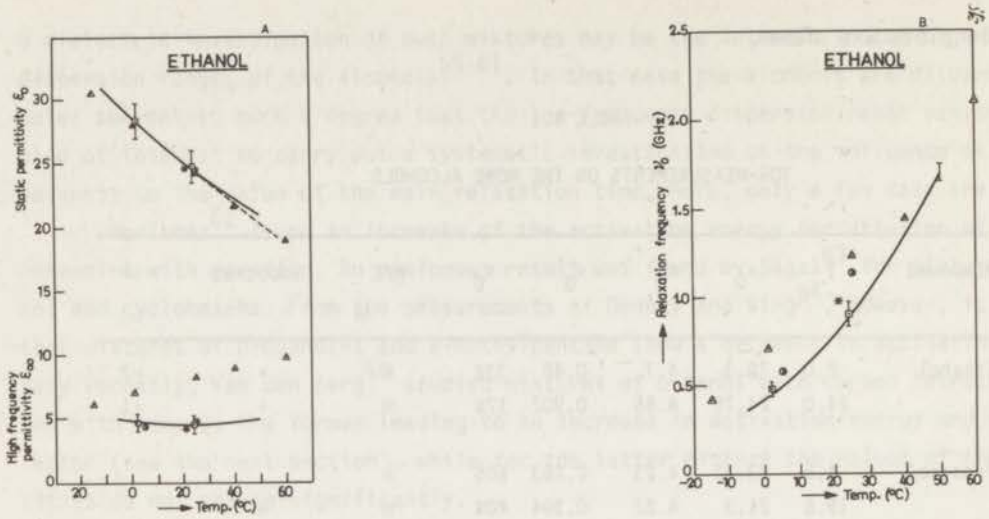

Figure 4.1

Values of ε_0, ε_∞ and ν_0 as depending on temperature for ethanol.
——— M.W. Sagal[63] ; – – – P. Huyskens et al[69] ; ✱, E.H. Grant, Proc. Phys. Soc., B70, 937, (1957) ; ⊡, This work ; ◑, A. Suggett et al[12,13] ; ▲, H. Fellner-Feldegg[6].

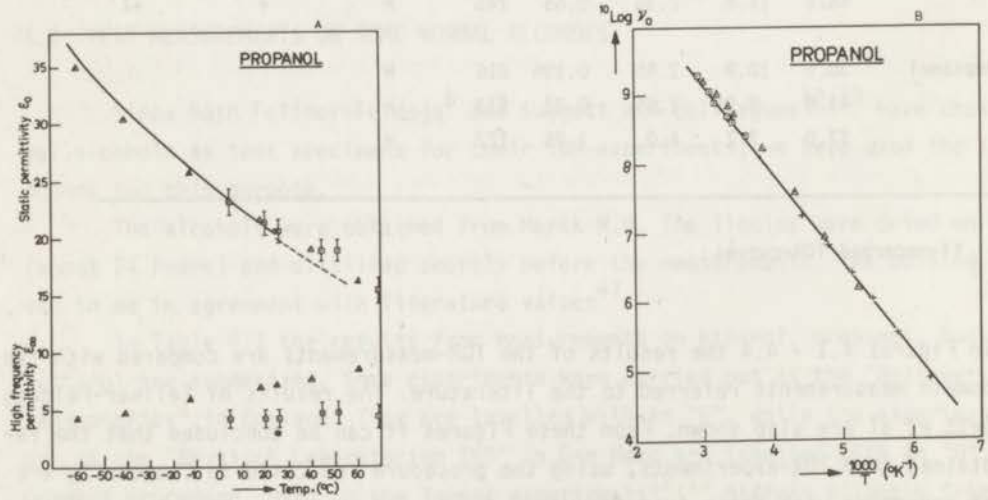

Figure 4.2 Values of ε_0, ε_∞ and ν_0 as depending on temperature for propanol-1.
——— D.W. Davidson, R.H. Cole[29] ; – – – P. Huyskens et al[69] ; ⊡, This work ; ◑, A. Suggett et al[12,13] ; ▲, H. Fellner-Feldegg[6].

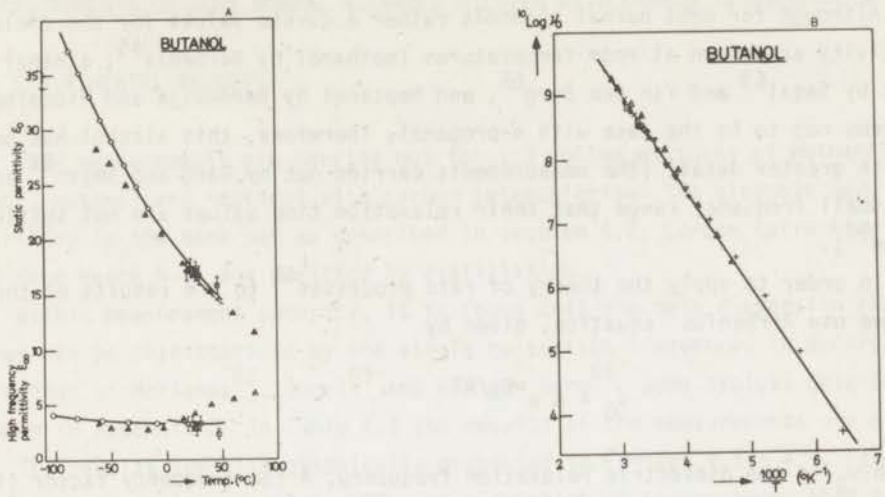

Figure 4.3

Values of ε_0, ε_∞ and ν_0 as depending on temperature for butanol-1.
——— M.W. Sagal[63] ; —0— W. Dannhauser, R.H. Cole, J. Chem. Phys., 23, 1762, (1955) ;
— + — H. A. Rizk, N. Youssef, Z. Phys. Chem. N.F., 58, 100, (1968) ; ▽, J.F. v.d. Berg[65] ;
⊡, This work, H, and ◈, This work, E[45] ; ◑, A. Suggett et al[12,13] ; Δ, H. Fellner-Feldegg[6].

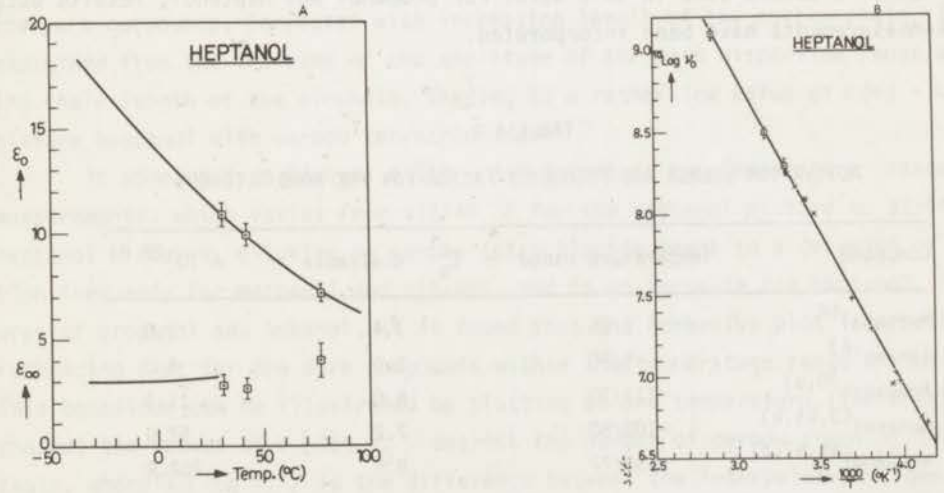

Figure 4.4

Values of ε_0, ε_∞ and ν_0 as depending on temperature for heptanol-1.
——— J. Middelhoek[57] and P. Bordewijk[51] ; X, J. Middelhoek[57] ; +, P. Bordewijk[51] ;
⊡, This work.

Although for most normal alcohols rather accurate values for the dielectric permittivity are known at room temperatures (methanol by Barbenza[66], ethanol by Sagal[63], butanol by Sagal[63] and Van den Berg[65], and heptanol by Bordewijk and Middelhoek[51,57]), this seems not to be the case with n-propanol. Therefore, this alcohol has been measured with greater detail (the measurements carried out by Garg and Smyth[67] are over such a small frequency range that their relaxation time values are not sufficiently accurate[56]).

In order to apply the theory of rate processes[68] to the results of the measurements, we use Arrhenius' equation, given by

$$\nu_0 = A\, e^{-E_A/RT} \qquad (4.1)$$

in which ν_0 is the dielectric relaxation frequency, A the frequency factor (in Hz), E_A the activation energy (in Kcal/mole), R the universal gas constant (in cal/mole ^oK) and T the absolute temperature (in ^oK). When a plot of log ν_0 versus T^{-1} is constructed, the derivative of this function (assuming the Arrhenius equation to hold) yields the activation energy while the frequency factor can be found from the value of log ν_0 for $T = \infty$.

In Table 4.2 the values for E_A and A, mainly from literature results, are given for the normal alcohols used in this work. For propanol and heptanol, results obtained from TDR-measurements have been incorporated.

TABLE 4.2

ACTIVATION ENERGY AND FREQUENCY FACTOR FOR THE MONO ALCOHOLS

Compound	Temperature range	E_A [c] Kcal/mole	A 10^{-12} [d]
Methanol[66]	5/55	3.4	1.0
Ethanol[63]	-5/50	5.0	4.0
Propanol[30,a)]	-113/70	6.0	11.3
Butanol[63,65,b)]	-100/50	7.2	57.0
Heptanol[51,57,a)]	-33/77	8.6	262.0

a) This work. b) W. Dannhauser, R.H. Cole, J. Chem. Phys., 23, 1762, (1955)
c) Inaccuracy about 5%. d) Inaccuracy about 50%.

4.3 MEASUREMENTS ON SOME NORMAL ALCOHOLS DILUTED WITH CARBON TETRACHLORIDE

4.3,1 EXPERIMENTAL RESULTS

TDR- measurements are carried out for 1:1 volume mixtures of methanol, ethanol, propanol, butanol and heptanol with carbon tetrachloride. The alcohols were obtained and purified in the same way as described in section 4.2. Carbon tetrachloride was obtained from Merck N.V. and purified by distillation.

Within measurement accuracy, it is found that the main dispersion range of these mixtures can be characterized by one single relaxation frequency, in accordance with the findings of Moriamez[62], Sagal[63] and Van den Berg[65]. Some typical Cole-Cole plots are shown in Appendix D. In Table 4.3 the results of the measurements are summarized.

The results are also graphically presented in Figures 4.5 - 4.9. Figures 4.5 A - 4.9 A give the obtained values of ε_0 as a function of temperature. When possible these results are compared with literature values obtained from the work of Huyskens and co-workers[69]. As was to be expected, our values show some scatter, but no systematic deviation is found from the results of low-frequency measurements.

Figures 4.5 C - 4.8 C and 4.9 B show Arrhenius plots of the obtained values of ν_0, together with the rate plots of the corresponding mono alcohols. The scatter, which appears to be somewhat larger for the measurements of the mixtures than those for the pure compounds, increases with increasing length of the carbon chain. This can be explained from the decrease of the amplitude of the main dispersion range with increasing chain length of the alcohols, leading to a rather low value of $\varepsilon(\infty) - \varepsilon(0)$ for the mixture heptanol with carbon tetrachloride.

It appears from Figures 4.5 B - 4.9 B that in the temperature range of the measurements, which varies from -15/40 ^{o}C for the methanol mixture to 31/64 ^{o}C for the heptanol mixtures, dilution by carbon tetrachloride leads to a decrease of the relaxation frequency for methanol and ethanol, and to an increase for heptanol. For the mixtures of propanol and butanol, it is found that the Arrhenius plot intersects the corresponding plot for the pure compounds within the temperature range of the measurements. This behaviour can be illustrated by plotting at one temperature (for which 30 ^{o}C is chosen) the values of $\Delta(\log \nu_0)$ against the number of carbon atoms of the alcohol chain, where $\Delta(\log \nu_0)$ is the difference between the interpolated values of ν_0 for the pure compound and for the mixture. The resulting graph is given in Figure 4.10. It appears that $\Delta(\log \nu_0)$ decreases monotonically from positive to negative values.

The values of the activation energies and the frequency factors, as determined from the results of Figures 4.5 - 4.9, are given in Table 4.4. It must be mentioned that some of these values are less accurate than those for the pure alcohols, due to the larger scatter of the results and due to the fact that the relaxation frequencies

of some of the materials are determined over a smaller temperature range.

TABLE 4.3

TDR-MEASUREMENTS ON 1:1 VOLUME MIXTURES OF ALCOHOL-CCl_4

Compound	T	ε_0	ε_∞	ν_0	τ_0	H/E	smoothed	$\Delta\varepsilon$
Methanol-CCl_4	-15	23.1	4.6	0.355	475	H		
	30.5	15.3	5.3	1.51	105	H	+	
	40.0	16.0	4.5	2.0	80	H	+	
Ethanol-CCl_4	1.0	15.5	4.8	0.27	589	H	+	
	19.5	11.8	3.6	0.515	309	H		
	26.0	12.65	3.2	0.61	261	H		
	34.0	11.7	3.6	0.75	212	H		
	39.0	10.4	3.5	1.13	141	H	+	
Propanol-CCl_4	5.0	11.7	3.4	0.2	796	H		
	15.0	9.95	3.15	0.28	568	H		
	20.0	10.4	3.9	0.36	442	H		
	22.3	11.05	3.45	0.41	388	H	+	
	41.0	9.0	3.53	0.85	187	H	+	
	42.0	7.95	3.05	0.94	169	H	+	
	46.0	7.75	3.4	0.9	177	H		
	64.0	7.12	3.75	1.66	96	H	+	
Butanol-CCl_4	16.0	7.85	3.35	0.233	683	H	+	-0.5
	17.0	7.86	2.95	0.248	642	H		
	20.0	8.58	2.8	0.29	549	H		
	32.0	6.5	3.15	0.57	279	H		
	48.0	5.85	2.8	0.87	183	H	+	
Heptanol-CCl_4	31.0	3.96	2.78	0.355	448	H		
	33.0	4.24	2.85	0.334	477	H	+	
	40.5	3.83	2.85	0.67	238	H	+	
	49.0	3.88	2.9	0.73	218	H		
	50.0	3.75	2.81	0.95	167	H	+	+1
	63.5	3.67	2.88	1.25	127	H	+	

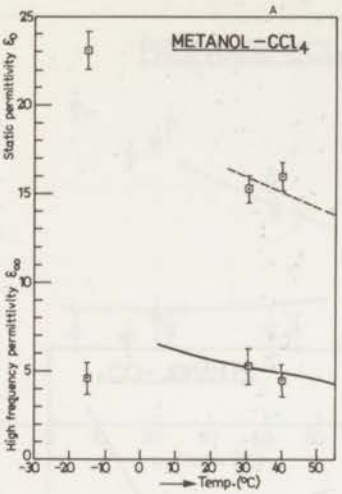

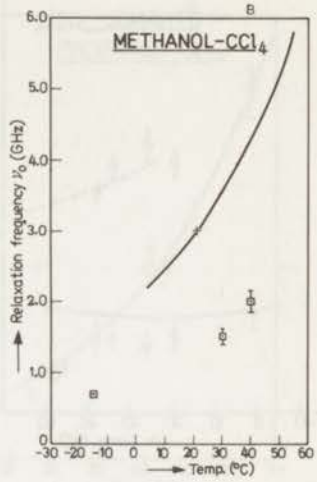

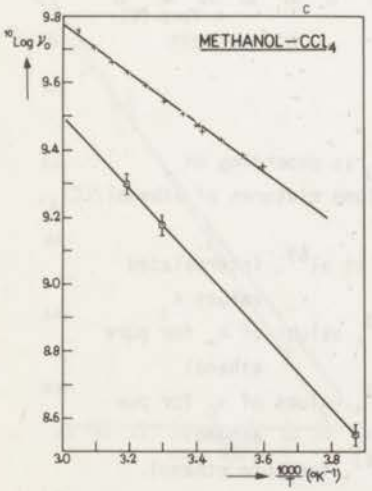

Figure 4.5

Values of ε_0, ε_∞ and ν_0 as depending on temperature for 1:1 volume mixtures of methanol/CCl_4.

⊡, This work.

A. – – – P. Huyskens et al[69] interpolated values of ε_0.

——— G. H. Barbenza[66], values of ε_∞ for pure methanol

B. ——— G.H. Barbenza[66], values of ν_0 for pure methanol.

\+ E.H. Grant, Proc. Phys. Soc., B70, 937, (1957).

C. — + — G.H. Barbenza[66], for pure methanol

* E.H. Grant, for pure methanol.

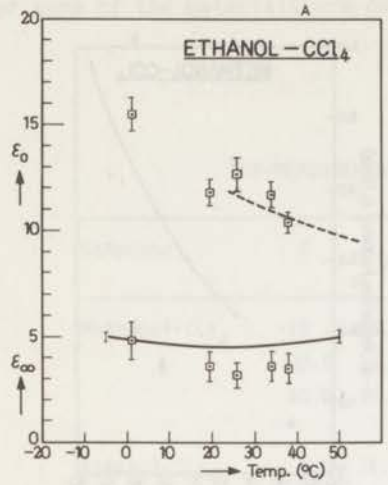

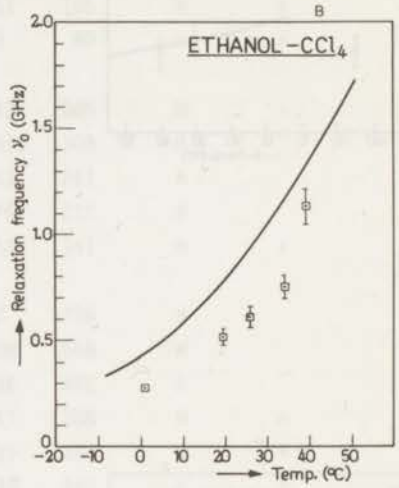

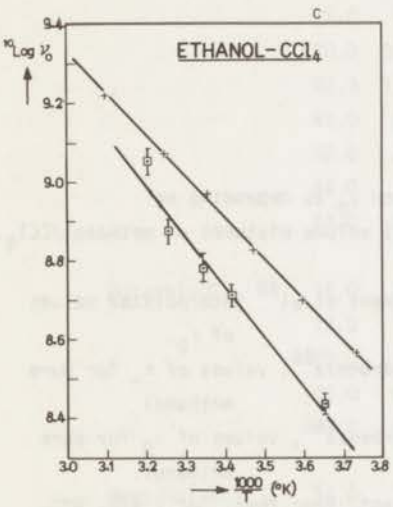

Figure 4.6

Values of ε_0, ε_∞ and ν_0 as depending on temperature for 1:1 volume mixtures of ethanol/CCl_4.

⊡, This work.

A. – – – P. Huyskens et al[69], interpolated values ε_0

——— M.W. Sagal[63], values of ε_∞ for pure ethanol

B. ——— M.W. Sagal[63], values of ν_0 for pue ethanol

C. — + — M.W. Sagal[63], for pure ethanol.

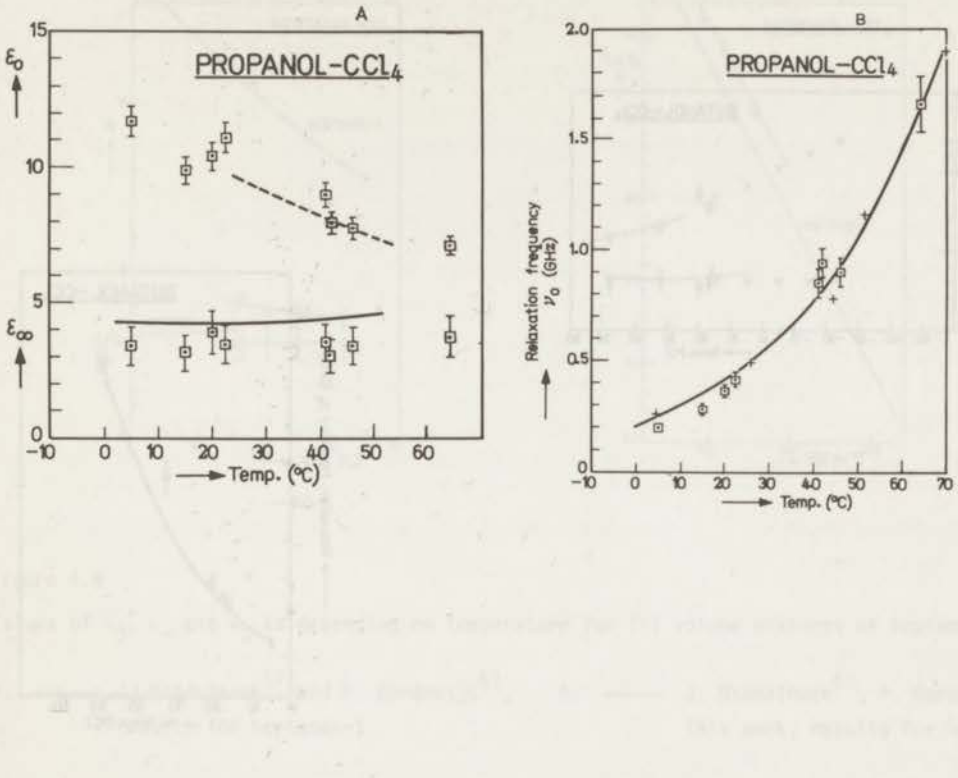

Figure 4.7

Values of ε_0, ε_∞ and ν_0 as depending on temperature for 1:1 volume mixtures of propanol-1/CCl_4.

⊡, This work

A. – – – P. Huyskens et al[69], interpolated values of ε_0

——— ε_∞ for pure propanol-1, this work

B. — + — ν_0 for pure propanol-1, this work

C. — + — results for propanol-1, this work

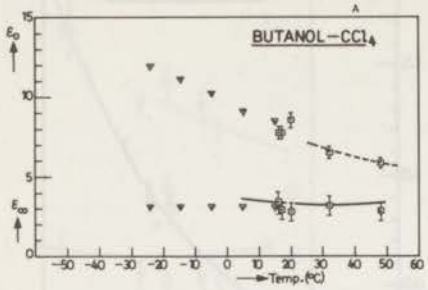

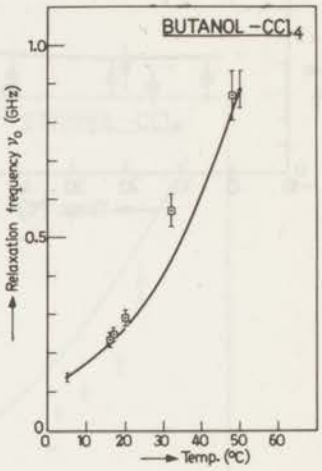

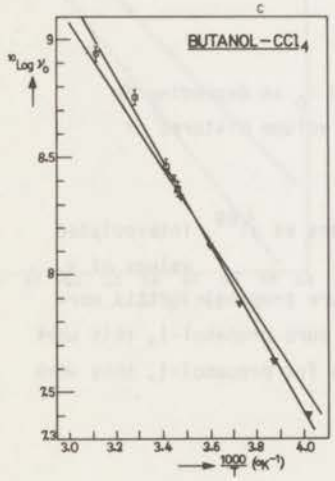

Figure 4.8

Values of ε_0, ε_∞ and ν_0 as depending on temperature for 1:1 volume mixtures of butanol-1/CCl_4.

⊡. This work

A. – – – P. Huyskens et al[69], interpolated valus of ε_0

▽, J.F. v.d. Berg[65], interpolated values of ε_0

——— M.W. Sagal[63], values of ε_∞ for pure butanol-1

B. ——— M.W. Sagal[63], values of ν_0 for pure butanol-1

C. ▽, J.F. v.d. Berg[65], interpolated values of ν_0

——— M.W. Sagal[63], results for butanol-1.

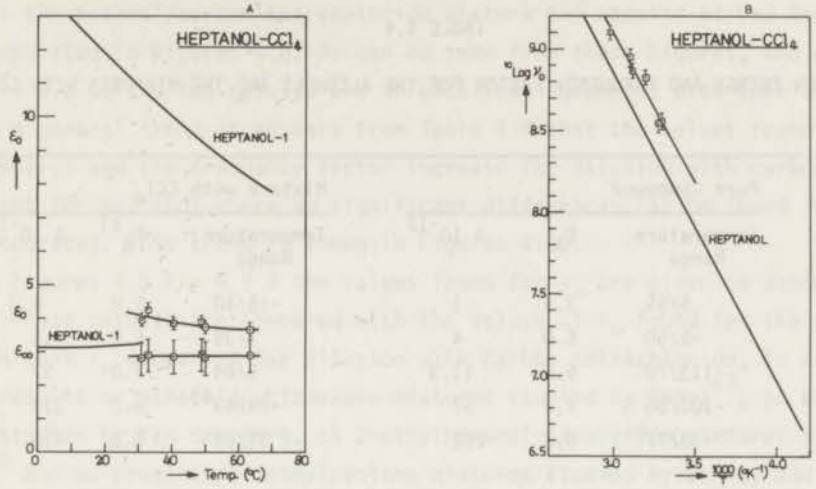

Figure 4.9

Values of ε_0, ε_∞ and ν_0 as depending on temperature for 1:1 volume mixtures of heptanol-1/CCl_4

A. —— J. Middelhoek[57] and P. Bordewijk[51], results for heptanol-1

B. —— J. Middelhoek[57], P. Bordewijk[51], This work, results for heptanol-1.

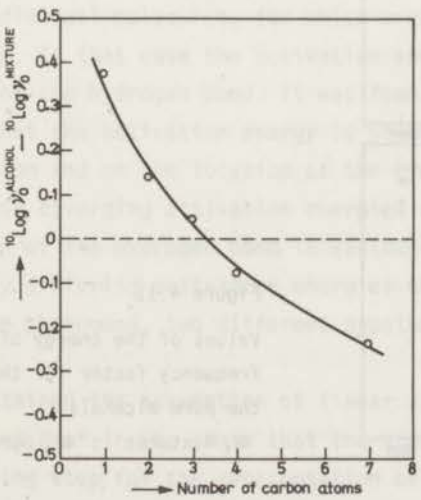

Figure 4.10 Values for $\Delta(\log \nu_0)$ for the mono alcohols diluted with carbon tetrachloride.

TABLE 4.4

ACTIVATION ENERGY AND FREQUENCY FACTOR FOR THE ALCOHOLS AND THE MIXTURES WITH CCl_4

Alcohol	Pure Compound			Mixture with CCl_4		
	Temperature Range	E_A	A 10^{-12}	Temperature Range	E_A a)	A 10^{-12} b)
Methanol	5/55	3.4	1	-15/40	5.0	6.3
Ethanol	-5/50	5.0	4	1/39	6.0	16
Propanol	-113/70	6.0	11.3	5/64	7.0	57
Butanol	-100/50	7.2	57	-24/48 c)	8.2	320
Heptanol	-33/77	8.6	262	31/64	8.5	420

a) Inaccuracy about 10%. b) Inaccuracy about 50%. c) J.F. van den Berg, -24/15, and this work 16/48.

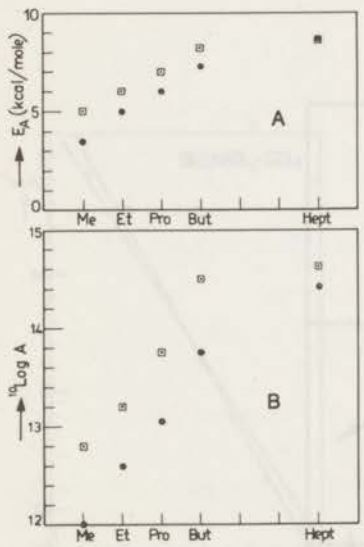

Figure 4.11

Values of the energy of activation and the frequency factor for the mixtures and for the pure alcohols.

⊡, Mixtures ; ●, pure Alcohols.

For the butanol/carbon tetrachloride mixture the results of Van den Berg have been incorporated in Figures 4.8. As can be seen from these Figures, and especially from Figure 4.8 C, the two results are in excellent agreement with each other.

As a general trend it appears from Table 4.4 that the values found for the activation energy and the frequency factor increase for dilution with carbon tetrachloride, except for heptanol where no significant differences can be found (within measurement accuracy). This trend is shown in Figures 4.11.

In Figures 4.5 A - 4.9 A the values found for ε_∞ are given in dependence on temperature. These results are compared with the values of ε_∞ found for the pure alcohols. It appears that ε_∞ decreases for dilution with carbon tetrachloride, in accordance with the results on ethanol/cyclohexane mixtures studied by Sagal[63], on butanol/hexane mixtures studied by Van den Berg, on 2-ethylhexanol-1/paraffin mixtures studied by Moriamez[62] and on propanol/2-methylpentane mixtures studied by Denney and Ring[64].

4.3,2 DISCUSSION

Although there is general agreement that H-bonding in the liquid mono alcohols is having a strong influence on the observed dielectric relaxation behaviour, alternative, and some of them at present equally acceptable, hypotheses exist concerning the likely relaxation mechanisms.

A theory has been developed by Bauer, Magat and Brot[70-74] in which it is assumed that the alcohols associate to linear multimers. The main dispersion range then arises from reorientation of individual molecules, for which breaking of the hydrogen bond is the rate determining step. In that case the activation energy would be of the order of the energy of formation of the hydrogen bond. It was found by Middelhoek[57] and by Dannhauser[75], however, that the activation energy is strongly dependent on the structure of the carbon skeleton and on the location of the hydroxyl group in this chain*. The possibility that these diverging activation energies are due to diverging values of the heat of formation of the hydrogen bond is excluded by the fact that mixtures of alcohols with strongly differing activation energies show only one main dispersion range[51]. To explain these phenomena, two different hypotheses have been introduced until now.

Dannhauser[55] maintained the assumption of linear association, and modified the theory of Bauer, Magat and Brot in the sense that the breaking of the hydrogen bond is not the rate determining step for the reorientation of the alcohol molecule, but only prerequisite. In this model it is assumed that a particular hydrogen bond breaks and reforms many times without reorientation of the molecules involved. The reorienta-

* Values of the activation energy, for many of the mono alcohols, are given by Bordewijk[51] page 43.

tion depends not only on the breaking of the hydrogen bond but also on the whole of interactions of a molecule with respect of its surroundings, and is thus a cooperative process. The degree of cooperativity for reorientation of a molecule then increases with increasing length and branching of the carbon chain, and also with increasing sterical hindrance of the hydroxyl group. In the case of methanol the reorientation after breaking of the hydrogen bond would be so easy that breaking of this bond remains the rate-determining step, whereas the influence of the alkyl group on the reorientation would become important for the higher alcohols.

In contrast to this theory, Bordewijk[51] assumes that the association of the normal alcohols in the pure state is dominated by cyclic multimers of one size which have, despite their cyclic structure, a high dipole moment because the oxygen and the hydrogen atoms are presumed not to lie in one plane. It is then suggested that the dielectric relaxation is due to the movements of a multimer and its surroundings whereas Dannhauser assumes that it is due to the cooperative movements of a single molecule and its surroundings. Again, the necessary amount of cooperation increases with increasing length and branching of the carbon chains.

In both views, the influence of the carbon tetrachloride on the dielectric relaxation frequency is caused by the influence of the CCl_4 molecule on the amount of coordination between the molecular movements in the liquid.

The results of the present work do not support some of the assumptions of Dannhauser since he states that for methanol the reorientation depends on the breaking of the hydrogen bond only and not on the surroundings of the molecule. For this compound we found, however, that the addition of carbon tetrachloride leads to a significant increase of the energy of activation.

With respect to the influence of carbon tetrachloride on the amount of coordination in the liquid, the following properties of the CCl_4-molecule are of importance:

(1) the CCl_4-molecule is rigid
(2) the CCl_4-molecule does not form associates
(3) the molar volume of CCl_4 is 96.5 cm^3/mole whereas the molar volumes for methanol, ethanol, propanol, butanol and heptanol are 40.5, 58.4, 77.1, 91.4 and 141.4 cm^3/mole respectively.

The result of the measurements, as presented in Table 4.4 and in Figure 4.11, show the general trend that the energy of activation and the frequency factor increase when the alcohols are diluted by carbon tetrachloride. This trend is most evident for methanol, ethanol, propanol and butanol whereas it seems to disappear for heptanol. The observations can be explained from the assumption that addition of carbon tetrachloride tends to a higher degree of coordination in the liquid when the molar volume of CCl_4 is large with respect to the molar volumes of these alcohols. The inverse statement may also hold as is presumably the case for heptanol.

Although the results of the measurements, described in this work, cannot give a final conclusion concerning the dielectric relaxation mechanism for the mono alcohols, it shows in principle that an extension of this investigation to a greater temperature range, also applied to other alcohols and other non-polar solvents[76], would give valuable information. For these applications TDR-measurements are particularly useful because of the relatively small amount of time necessary for the determination of the relaxation frequencies.

CHAPTER 5

GENERAL DISCUSSION ON TDR-MEASUREMENTS AND SUGGESTIONS FOR FURTHER WORK

In this thesis, the time domain reflectometry technique is considered as a possible method to examine dielectric relaxation phenomena in polar liquids. The first measurements, by Fellner-Feldegg, were not sufficiently accurate but due to the introduction of "know how" from the field of network analysis, rather accurate results have now been obtained by Suggett, Quickenden, Loeb and Young[12,13].

One important remark has to be made at this stage. The TDR-equipment, as delivered by Hewlett-Packard has not been constructed for the examination of dielectric relaxation phenomena. Two features of the equipment are a consequence of this. First, in many TDR-equipments (but not for all) the characteristic impedance of the sampling system is larger than 50 Ω resulting in the unwanted step voltage, which determines the low-frequency limit of the measurement technique. Second, the time base of the oscilloscope is non-linear. The latter property is of great importance when automatic data processing aquisition is available. A correction for this non-linearity is then necessary[44].

The high-frequency limit is at the present state of art determined by the time reference procedure. This procedure, as discussed in Chapter 3, is disputable since it is not based upon a mathematical exact relation; but as can be inferred from the error analysis, and also from the experimental results, it is a surprisingly good approximation.

Although the experimental results confirm that the TDR-method is a very promising one, a disadvantage of the method should be mentioned as well. This disadvantage refers mainly to the present situation and it is believed that it can be solved within reasonable time.

Due to the deficiencies of TDR (jitter, internal reflections, different characteristic impedance of the sampling system, time reference procedure, uncertanties in the last samples) the constructed Cole-Cole plot may not have a satisfactorily shape a priori and subsequently the curves $R(\omega)$ and $\theta(\omega)$ may contain oscillations, while $\theta(\omega)$ may also need a phase correction. When frequency domain results are established, as for instance the normal alcohols, the corrections are known to be necessary. When, however, the shape of the Cole-Cole plot is not known, the corrections may not be necessary and therefore the possibility exists that a "correct but strange-looking" Cole-Cole plot is corrected into an "incorrect but good-looking" Cole-Cole plot. Such a situation may for instance occur when two separate dispersion ranges with the same amplitudes are present.

As a suggestion for further work, it should therefore be pointed out that one

of the first things to work on, in TDR-experiments, is the improvement of the equipment (if possible) and of the method of analysis in order to be certain that the final, Fourier transformed, results do not need further corrections. It is then necessary that

(1) the time reference method, as discussed in Chapter 3, is replaced by a mathematical correct procedure (for instance by Suggett's pulse reference method or, alternatively, by recording the full TDR-curves and using the points H of Figure 3.7 as the reference points.

(2) XY-recording of the data is replaced by an automatic data processing method. Then, very fast scan times can be used which minimize the influence of the jitter[12,13], while also the full TDR-curves can be recorded with still a sufficient number of samples per unit time.

(3) the TDR-curves have to be very smooth (eventually after computer corrections), which means that the unwanted reflections have to be removed. This can be obtained by an improvement of the TDR-equipment itself, constructing it for the special purposes of dielectric measurements (this should be done by Hewlett-Packard of course), and/or correcting the TDR-traces for all types of all possible reflections. This latter procedure requires a detailed quantitative knowledge of the TDR-equipment. Some first remarks in this field have been given by Loeb et al[13].

When these suggestions for further work have been carried out, the accuracy of dielectric measurements, by TDR-experiments, will certainly be improved with respect to the TDR-measurements described in this work. The low-frequency limit may then be extended to $\nu_0 \simeq 10^7$ or 10^6 Hz by for instance using the spiral coaxial line (length about 20 m) as discussed by Fellner-Feldegg and also by Bagozzi[8,9] or using the "thin-cell" method (or a variant) as has recently been proposed by Fellner-Feldegg[46,45]. The high-frequency limit may in that situation be extended to the natural limit caused by the finite rise time of the step voltage.

It is recalled, however, that dielectric measurements, even when they are carried out with a TDR-technique as described in this work, are approximately as accurate as measurements performed with the present frequency domain techniques. This refers especially to the determination of the relaxation frequency in the range

$$0.2 < \nu_0 < 3 \text{ GHz}$$

To finish this Chapter, a comparison is made between the TDR-method in the present state of development and the present frequency domain techniques for measurements in the frequency range $5\ 10^6 < \nu < 10^{10}$ Hz.

TDR- MEASUREMENTS	FREQUENCY DOMAIN-MEASUREMENTS
Not expensive equipment (apart from computer and C.A.T., about $ 4000,-- in 1972)	Expensive equipment
Measurements not time consuming for microwave frequencies (apart from sampling by hand and computer time, about 5 minutes)	Time consuming experiments for microwave frequencies
Accuracy comparable with frequency domain methods $\frac{\Delta\varepsilon_0}{\varepsilon_0} \simeq 5\%$, $\frac{\Delta\varepsilon_\infty}{\varepsilon_\infty} \simeq 20\%$, $\frac{\Delta\tau_0}{\tau_0} \simeq 7.5\%$	$\frac{\Delta\varepsilon_0}{\varepsilon_0} \simeq 1\%$, $\frac{\Delta\varepsilon_\infty}{\varepsilon_\infty} \simeq 10\%$, $\frac{\Delta\tau_0}{\tau_0} \simeq 7.5\%$
Works very good for $0.2<\nu_0<2$ GHz	Very difficult to obtain data for $0.2<\nu<1$ GHz
Indirect estimation of ε' and ε'' from Fourier analysis	Direct measurement of ε' and ε''
Computer is necessary	Computer not necessary a priori
No absolute certainty about the obtained Cole-Cole plot	Within measurement accuracy in ε', ε'' ($\simeq 5\%$) absolutely certain about the shape of the Cole-Cole plot obtained
The influence of any error, involved in the measurement, is spread out over all frequencies	Any error involved in the measurement gives an error in ε' and ε'' for one frequency only (provided that the error is not systematic)
High-frequency limit, in principle due to the finite rise time of the step voltage, but at this stage, due to the time reference method	No high-frequency limit a priori

Low-frequency limit due to the necessity to obtain a "complete" TDR-curve (This limit can be extended by using methods analogous to Fellner-Feldegg's thin cell technique)	No low-frequency limit a priori

APPENDIX A

SOME REMARKS ON THE COLE-COLE EQUATION IN CONNECTION WITH CAUSALITY[77]

INTRODUCTION

In 1941, Cole and Cole published equation (2.3), for the present purposes written as

$$\psi(i\omega) = \frac{\varepsilon(i\omega) - \varepsilon_\infty}{\varepsilon_0 - \varepsilon_\infty} = \frac{1}{1 + (i\omega\tau_0)^\alpha} \quad , \quad 0<\alpha<1 \qquad (A.1)$$

This function, which has a branch point at the origin, is important for experimental purposes since many dielectric experiments are analysed in terms of values of ε_0, ε_∞, τ_0 and α.

Without proof, Cole and Cole stated explicitely that the real and negative imaginary parts of equation (A.1) satisfy the Kramers-Kronig relations, which is necessary if $\varepsilon(i\omega)$ is to be used to describe the behaviour of a causal system[78].

In 1956, in an important paper on integral relations of linear systems, MacDonald and Brachman[22] stated that equation (A.1) is not an analytic function for $0<\alpha<1$ and therefore the $\varepsilon'(\omega)$ and $\varepsilon''(\omega)$ functions would not represent a causal system. They also stated, however, that the situation may be saved by putting in the necessary $|\omega|$ and sign (ω) factors to force them to have the proper parity. But then, the resulting $\varepsilon'(\omega)$ and $\varepsilon''(\omega)$ are not the real and negative inmaginary parts from $\varepsilon(i\omega)$ as given by equation (A.1). Unfortunately they did not give the corrected relations.

When dielectric permittivity is studied by transient methods, as for instance in this thesis, the corresponding transient behaviour of a Cole-Cole dielectric material is calculated by using equation (A.1) and not the "corrected functions" as is suggested by MacDonald and Brachman. It is therefore clear that when the Cole-Cole equation would not represent a causal system, large deviations may be expected between the calculated and observed transient behaviour. Since the deviating asymptotic behaviour of P(t), as predicted in Chapter 2, has not (yet) been observed experimentally for Cole-Cole materials, it will be shown in this Appendix that this feature will indeed be observed (when dielectric materials exist behaving exactly according to equation (A.1), since equation (A.1) does represent a causal system albeit with limitations in terms of the branch to be used.

THE KRAMERS-KRONIG RELATIONS. Consider the function

$$\psi(s) = \frac{1}{1 + s^{\alpha}} \quad , \quad 0<\alpha<1 \tag{A.2}$$

of the complex variable s. The quantity s^{α} is defined as

$$s^{\alpha} = |s|^{\alpha} e^{i\alpha \arg(s)}, \quad -\pi<\arg(s)\leq\pi \tag{A.3}$$

Due to the definition of s^{α} on the branch $-\pi<\arg(s)\leq\pi$, $\psi(s)$ defines a single valued function. It also defines an analytic function since the poles of equation (A.3), given by $|s| = 1$ and $\arg(s) = (\pi + k\,2\pi)/\alpha$ for $k = 0, \pm 1, \ldots$, are outside the branch.

It is therefore clear that the Cole-Cole equation, extended over the entire complex s-plane, defines a single valued and analytic function for $-\pi<\arg(s)\leq\pi$. For our purposes, however, it is sufficient that $\psi(s)$ is analytic for $\mathrm{Re}(s)>0$ since this is necessary (but not sufficient) for any equation to represent a causal system[78-80]

In order to prove the existence of the Kramers-Kronig relations for the real and negative imaginary parts of equation (A.2), for the line $\mathrm{Re}(s) = 0$, Cauchy's integral relation, defined by[81]:

$$\frac{1}{2\pi i}\int_C \frac{\psi(s)}{s - s_0}\,ds \quad \begin{cases} = \psi(s_0) & s_0 \in C \\ = 0 & s_0 \notin C \end{cases} \tag{A.4}$$

is applied to $\psi(s)$, for s on the contour C shown in Figure A,1.

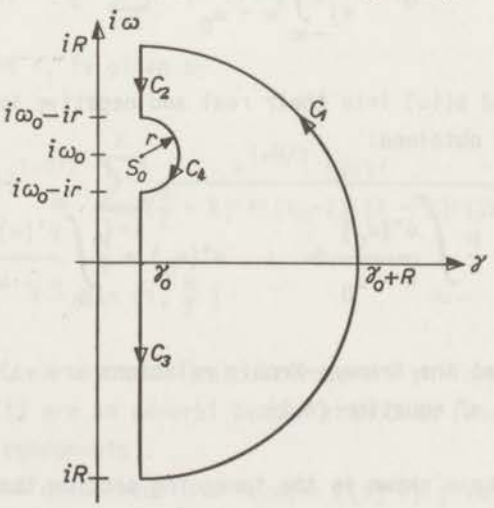

Definition of the contour C. The quantity s_0 is given by $s_0 = \gamma_0 + i\omega_0$.

The avaluation of equation (A.4), for $r \to 0$ and $R \to \infty$, is standard mathematics, resulting into:

$$\tfrac{1}{2}\psi(\gamma_0 + i\omega_0) = \frac{P}{2\pi i}\int_{\gamma_0 - i\infty}^{\gamma_0 + i\infty} \frac{\psi(\gamma + i\omega)}{i\omega - i\omega_0}\, d(\gamma + i\omega) +$$

$$+ \lim_{R\to\infty} \frac{1}{2\pi i}\int_{C_1} \frac{\psi(s)}{s - s_0}\, ds \qquad (A.5)$$

where P denotes the principal value of the integral. The second integral on the right hand side of equation (A.5) vanishes since[82]:

$$\lim_{R\to\infty} \int_{C_1} \frac{\psi(s)}{s - s_0}\, ds \leqslant \lim_{R\to\infty} \quad \mathrm{Max}\left| \frac{\psi(Re^{i\phi})}{Re^{i\phi} - \omega_0} \right| 2\pi R =$$

$$= \lim_{R\to\infty} \frac{2\pi R}{\mathrm{Min}\,|1 + R^{\alpha} e^{i\alpha\phi}|\,|Re^{i\phi} - \omega_0|} = 0 \qquad (A.6)$$

Taking the limit of $\psi(\gamma_0 + i\omega_0)$ for $\gamma_0 \to 0$, equation (A.5) can be written as

$$\psi(i\omega_0) = \frac{P}{\pi i}\int_{-\infty}^{\infty} \frac{\psi(i\omega)}{\omega - \omega_0}\, d\omega \qquad (A.7)$$

Separating $\psi(i\omega_0)$ and $\psi(i\omega)$ into their real and negative imaginary parts, the Kramers-Kronig relations are obtained:

$$\psi'(\omega_0) = \frac{P}{\pi}\int_{-\infty}^{\infty} \frac{\psi''(\omega_0)}{\omega - \omega_0}\, d\omega \quad ; \quad \psi''(\omega_0) = \frac{P}{\pi}\int_{-\infty}^{\infty} \frac{\psi'(\omega)}{\omega - \omega_0}\, d\omega \qquad (A.8)$$

It is thus proved that the Kramers-Kronig relations are valid for the real and negative imaginary parts of equation (A.1).

CONCLUSIONS. It has been shown in the foregoing section that the permittivity equation of Cole and Cole satisfies the requirements for a causal (and hence physically realizable) system of a dielectric material, when the complex frequency plane is defined on the branch $-\pi < \arg(s) \leqslant \pi$ only. It is therefore proved that the behaviour of P(t) for $t \to \infty$,

as given in Chapter 2 for a Cole-Cole dielectric material, cannot be attributed to the use of the non-causal character of equation (A.1)

APPENDIX B

NUMERICAL EVALUATION OF THE INVERSE LAPLACE TRANSFORM

Evaluation of the inverse Laplace transform, i.e. calculating f(t) for $0 \leq t \leq \infty$ from known analytical behaviour of F(s), is not always an easy task. Recently, however, numerical techniques have been developed by Bellman, Kalaba and Lockett[83], Zakian[84-86], Stehfest[87] and Singhal and Vlach[88]. All inverse Laplace transforms, discussed in this thesis, have been calculated by the procedure XLAPLINV written by De Graan according to the algorithm of Stehfest. This algorithm is given below.

The functions f(t) and F(s) are given by the equation

$$f(t) = \frac{1}{2\pi i}\int_{c-i\infty}^{c+i\infty} ds \quad F(s)\, e^{st} \equiv \mathcal{L}^{-1}\{F(s)\} \tag{B.1}$$

This equation can be approximated by

$$f(t) \approx \frac{\ln 2}{t} \sum_{i=1}^{N} V_i \, F\left(i \frac{\ln 2}{t}\right) \tag{B.2}$$

where N has to be even and V_i is given by

$$V_i = (-1)^{1+N/2} \sum_{k=1}^{X} \frac{k^{i+N/2}\,(2k)!}{\left(\frac{N}{2}-k\right)!\, k!\,(k-1)!\,(i-k)!\,(2k-i)!} \tag{B.3}$$

$$X = \text{Min}\left(i, \frac{N}{2}\right) \tag{B.4}$$

For the CDC 3200 computer, on which all calculations are performed, N = 12 is advisable[89]. The results of f(t) are in general better than 0.1% (when f(t) does not contain very high-frequency components).

For all applications described in this work F(s) is given by

$$F(s) = \Phi(s)\,\rho(s) = \Phi(s)\left(\frac{\sqrt{s} - \sqrt{s\,\varepsilon(s) + \sigma/\underline{\varepsilon}}}{\sqrt{s} + \sqrt{s\,\varepsilon(s) + \sigma/\underline{\varepsilon}}}\right) \tag{B.5}$$

where $\Phi(s)$ is given by 1/s when a heaviside input is considered or by equation (3.19) for a non-ideal step function. For the actual calculations equation (B.1) is rewritten as (using $\Phi(s) = 1/s$ for convenience)

$$f(t) = \frac{1}{2\pi i}\int_{c-i\infty}^{c+i\infty} \frac{1}{s}\left(\frac{\sqrt{s} - \sqrt{s\,\varepsilon(s) + \sigma/\underline{\varepsilon}}}{\sqrt{s} + \sqrt{s\,\varepsilon(s) + \sigma/\underline{\varepsilon}}}\right) e^{st}\, ds =$$

$$= \frac{1}{2\pi i}\int_{c-i\infty}^{c+i\infty} \frac{1}{s\tau_0}\left(\frac{\sqrt{s\tau_0} - \sqrt{s\tau_0\,\varepsilon(s\tau_0) + \sigma\tau_0/\underline{\varepsilon}}}{\sqrt{s\tau_0} + \sqrt{s\tau_0\,\varepsilon(s\tau_0) + \sigma\tau_0/\underline{\varepsilon}}}\right) e^{s\tau_0 t/\tau_0}\, d(s\tau_0)$$

Choosing $s\tau_0$ as a new variable of integration, the final result can be written as :

$$f(t/\tau_0) = \mathcal{L}^{-1}\left\{\frac{1}{s}\left(\frac{\sqrt{s} - \sqrt{s\,\varepsilon(s,\tau_0 = 1) + \sigma\tau_0/\underline{\varepsilon}}}{\sqrt{s} + \sqrt{s\,\varepsilon(s,\tau_0 = 1) + \sigma\tau_0/\underline{\varepsilon}}}\right)\right\} \qquad (B.6)$$

The algorithm, written in FORTRAN is as follows:

```
                                        VS FORTRAN (4.0)/MSOS          15/09/70

      FUNCTION XLAPLINV(P,N,T,J)
C
C     PURPOSE
C
C     COMPUTE APPROXIMATE INVERSE LAPLACE TRANSFORM OF FUNCTION P(S)
C     AT TIME-INSTANT T
C
C     TRANSLATED FROM ALGOL  ALGORITHM NO. 368  COMM. A.C.M.
C     VOL 13 , NO. 1 , JANUARY 1970   PAGES 47 - 49
C     N IS THE NUMBER OF TERMS USED IN APPROXIMATING THE INVERSE OF P(S)
C     N MUST BE EVEN
C     FOR THE CDC-3200  N = 12 IS ADVISED FOR OPTIMUM ACCURACY
C     ACCURACY WILL IN GENERAL BE BETTER THAN 0.1 PERCENT
C     COMPUTING TIME EQUALS N TIMES COMPUTING TIME OF P(S) , S = LN(2)*I/T
C
C     ON THE FIRST CALL A TABLE V(N) IS CONSTRUCTED
C     DIMENSION V(N), H(N/2), G(N+1)
      DIMENSION V(16),G(17),H(8)
C     H AND G ARE NEEDED ONLY DURING THE FORMATION OF TABLE V
C
      TYPE DEF(3) DUM,FB
      INTEGER SN,M
      DATA(M=-1)
C     ERROR CHECK ON N
      IF( N.LT. 2 .OR. N.GT. 16) STOP
      IF(N .NE.2*(N/2)) STOP
C
C     CHECK IF TABLE V MUST BE CALCULATED
      IF(M-N) 1,6,1
C
C     FORMATION OF TABLE V
    1 G(1)=OLDG=1. $ NH=N/2
      NK=NH+1
      N1=N+1
      DO 2 I=2,N1
```

```
      2 G(I)=OLDG=(I-1)*OLDG
        H(1)=2./G(NH)
        DO 3 I=2,NH
        NL=NK-I
      3 H(I)=FLOATF(I)**NH*G(2*I+1)/(G(NL)*G(I+1)*G(I))
        NHX=NH-(NH/2)*2
        SN=1
        IF(NHX .EQ. 0) SN=-SN
        DO 5 I=1,N
        DUM=0.
        KSTART=(I+1)/2
        KEND=I
        IF(I.GE. NH) KEND=NH
        DO 4 K=KSTART,KEND
        IK=I-K+1 $ KI=K-IK+2
      4 DUM=DUM+H(K)/(G(IK)*G(KI))
        IF(SN) 10,5,15
     10 V(I)=-DUM
        GOTO 5
     15 V(I)=DUM
      5 SN=-SN
        R=ALOG(2.)
        M=N
C
C                                                    N
C
C     COMPUTE APPROXIMATE INVERSE OF P(S) = SUM V(I)*P( LN(2)*I/T )
C                                           I=1
C
      6 FB=0. $ A=R/T
        DO 9 I=1,N
        AI=A*I
        DUM=P(AI,J)*V(I)
      9 FB=FB+DUM
        XLAPLINV=A*FB
        RETURN
        END

                FORTRAN DIAGNOSTIC RESULTS FOR    XLAPLINV

NO ERRORS
LOAD,56
RUN,5,NM
```

APPENDIX C

COMPUTER PROGRAM SHANTDR

In this Appendix the listning of the computer program used for the calculations of $\varepsilon'(\omega)$ and $\varepsilon''(\omega)$ from $V_0(m)$ and R(n) is given. It is based on the equations (3.14), (3.12) and (3.1).

```
                                        *** NSOS V4.2 EDITION=10 DATE=20/12/71.
$EQUENCE,045
!EQUENC
JOB,2090,GFME  VAN GEMERT 361, 4 ,ND
FFT,RVOTNO,SUBROUTINEPACK,500,00,0000,0000
OPEN,10
AUX,10
FORTRAN,L,X
```

MS FORTRAN (4.2)/MSOS 20/12/71

```
      PROGRAM SHANTDR
      COMMON IMEET(1024),PHIE(101),AMPE(101)
      COMMON IBEGIN,IEIND
      COMMON T(1024)
      COMMON TAU
      REAL NU,NUNUL
      REAL IMEET
      NUNUL=0.05
      TIMEFAC=0.0593472
      INDEX=1
      IBEGIN=1
      PI=3.14159265
      TAU=TIMEFAC*0.1
    1 READ 2,N
    2 FORMAT(I5)
      IEIND=IBEGIN+N-1
      READ 3,DIST,ZEROD
    3 FORMAT(2F10)
      PRINT 4,N,DIST,ZEROD,TIMEFAC
    4 FORMAT(X,I5,3F15.5)
      TREF=DIST*TIMEFAC
      TZERO=ZEROD*TIMEFAC
      DO 15 I=IBEGIN,IEIND
      T(I)=I*TAU-TREF+TZERO
   15 CONTINUE
      READ 10, (IMEET(I),I=1,IEIND)
   10 FORMAT(8F10.6)
      ITOT=100
      DO 100 J=1,ITOT
      NU=NUNUL*J
      JJ=J
      CALL SHANNON(AMP,PHI,NU)
      IF (INDEX.EQ.2) GOTO 101
      AMPE(J)=AMP $ PHIE(J)=PHI
      GOTO 100
  101 CALL EPSILON(EPSR,EPSIM,AMP,PHI,JJ)
      QUOT=AMP/AMPE(J)
      PHASE=(PHI-PHIE(J))*(180./PI)
      PRINT 200,NU,EPSR,EPSIM,AMPE(J),PHIE(J),AMP,PHI,QUOT,PHASE
  200 FORMAT(X,3(F15.5),6(E15.5))
  100 CONTINUE
      INDEX=INDEX+1
      IF (INDEX.GT.2) GOTO 105
          GOTO 1
      105 END
```

FORTRAN DIAGNOSTIC RESULTS FOR SHANTDR

NO ERRORS

```
                                MS FORTRAN (4.2)/MSOS          20/12/71

    SUBROUTINE SHANNON(AMP,PHI,NU)
    COMMON IMEET(1024),PHIE(101),AMPE(101)
    COMMON IBEGIN,IEIND
    COMMON T(1024)
    COMMON TAU
    REAL IMEET
    REAL NU
    TYPE COMPLEX(4) CI,CG,CSOM,CMPLX,CEXP,CSHAN
    INTEGER EIND
    PI=3.14159265
    CI=CMPLX(0.,1.)
    OMEGA=2*PI*NU
    CG=1./(1.-CEXP(-CI*OMEGA*TAU))
    CSOM=CMPLX(0.,0.)
    EIND=IEIND-1
    DO 10 I=IBEGIN,EIND
    CSOM=CSOM+(IMEET(I+1)-IMEET(I))*CEXP(-CI*T(I+1)*OMEGA)
 10 CONTINUE
    CSHAN=TAU*CG*CSOM
    RE=REAL(CSHAN)
    XIM=AIMAG(CSHAN)
    AMP=SQRTF(RE**2+XIM**2)
    PHI=ATANF(XIM/RE)
    RETURN
    END

          FORTRAN DIAGNOSTIC RESULTS  FOR    SHANNON

NO ERRORS
                                MS FORTRAN (4.2)/MSOS          20/12/71

    SUBROUTINE EPSILON(EPSR,EPSIM,AMP,PHI,JJ)
    COMMON IMEET(1024),PHIE(101),AMPE(101)
    COMMON IBEGIN,IEIND
    COMMON T(1024)
    REAL IMEET
    TYPE COMPLEX(4) CI,CMPLX,CEXP,CRE,CRT,CEPS
    J=JJ
    CI=CMPLX(0.,1.)
    CRE=AMPE(J)*CEXP(CI*PHIE(J))
    CRE=-1.*CRE
    CRT=AMP*CEXP(CI*PHI)
    CEPS=((CRE-CRT)/(CRE+CRT))**2
    EPSR=REAL(CEPS)
    EPSIM=AIMAG(CEPS)
    RETURN
    END

          FORTRAN DIAGNOSTIC RESULTS  FOR    EPSILON


NO ERRORS
LOAD,56
RUN,5
```

APPENDIX D

Some Cole-Cole plots of the TDR-measurements. Indicated frequencies are in GHz.

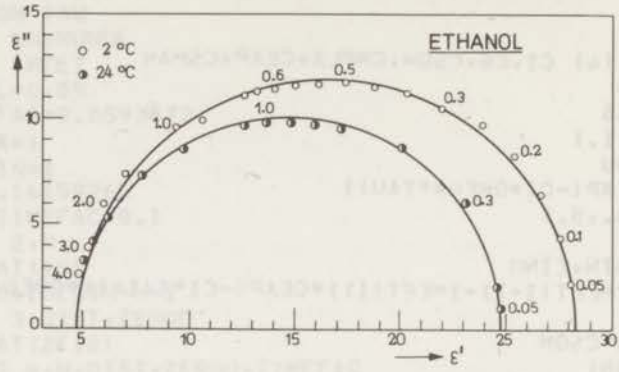

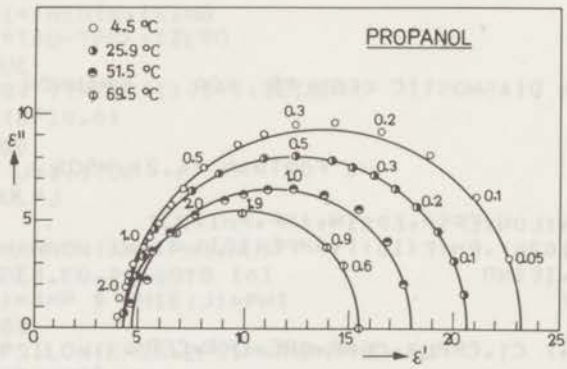

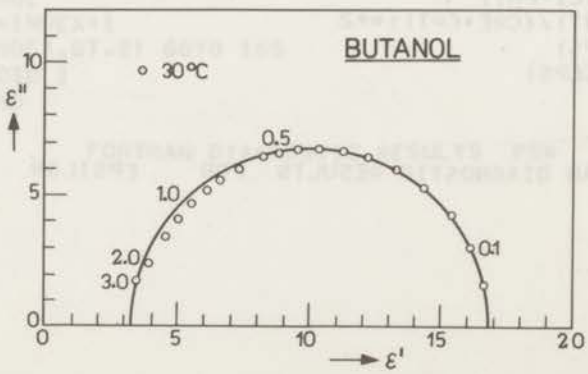

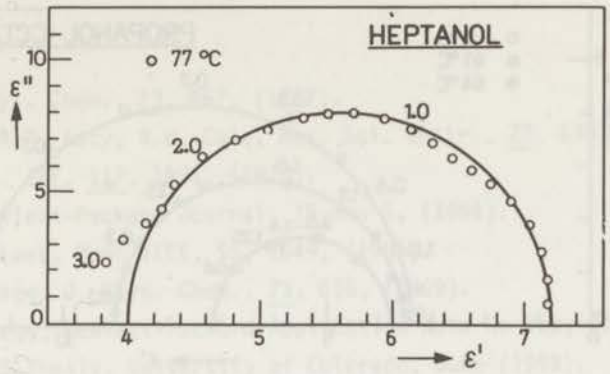
HEPTANOL
77 °C
ε''
ε'
1.0
2.0
3.0
10
5
0
4
5
6
7

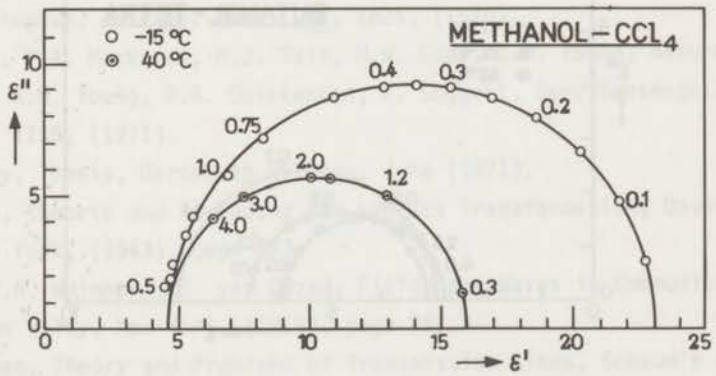
METHANOL – CCl4
-15 °C
40 °C
ε''
ε'
0.4
0.3
0.2
0.75
1.0
2.0
1.2
3.0
4.0
0.1
0.5
0.3
10
5
0
0
5
10
15
20
25

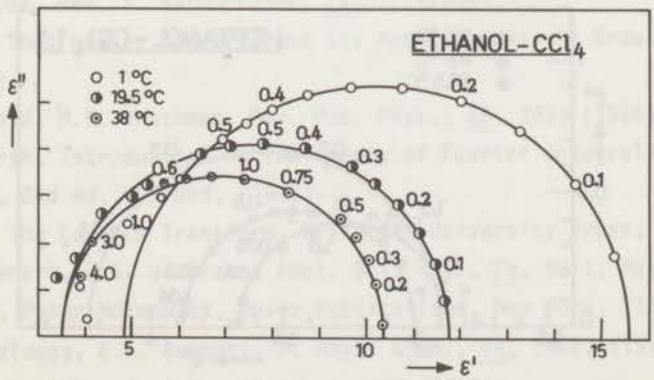
ETHANOL – CCl4
1 °C
19.5 °C
38 °C
ε''
ε'
0.4
0.2
0.5
0.5
0.4
0.3
0.6
1.0
0.75
0.1
0.5
0.2
1.0
3.0
0.3
0.1
4.0
0.2
5
10
15

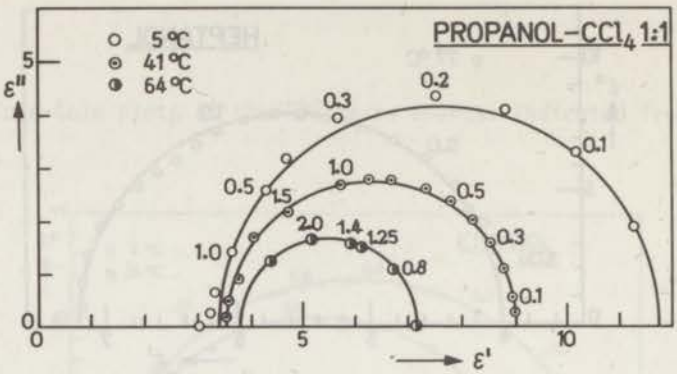
PROPANOL–CCl4 1:1
5 °C
41 °C
64 °C
ε''
ε'
0.3
0.2
0.1
0.5
1.5
1.0
0.5
2.0
1.4
1.25
0.3
1.0
0.8
0.1
0
5
10

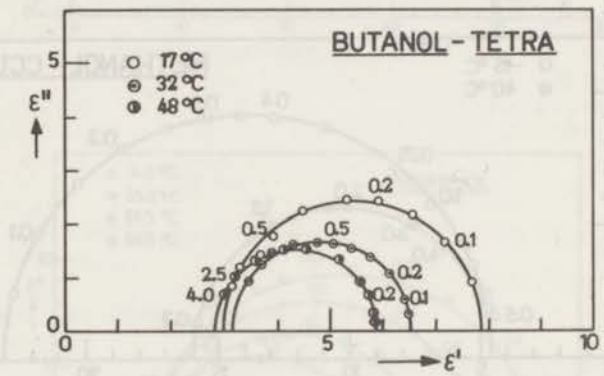
BUTANOL – TETRA
17 °C
32 °C
48 °C
ε''
ε'
0.2
0.5
0.5
0.1
2.5
0.2
4.0
0.2
0.1
0
5
10

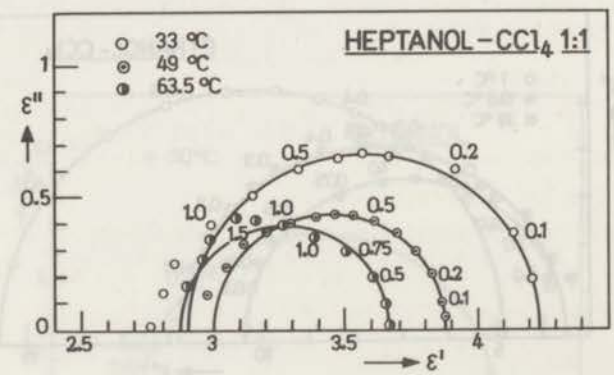
HEPTANOL–CCl4 1:1
33 °C
49 °C
63.5 °C
ε''
ε'
0.5
0.2
1.0
1.0
0.5
0.1
1.5
1.0
0.75
0.5
0.2
0.1
1
0.5
0
2.5
3
3.5
4

REFERENCES

1. P. Drude, Z. Phys. Chem., 23, 267, (1897).
2. D.W. Davidson, R.P. Auty, R.H. Cole, Rev. Sci. Instr., 22, 678, (1951).
3. P.J. Hyde, Proc. IEE, 117, 1891, (1970).
4. B.M. Oliver, Hewlett-Packard Journal, 15, No 6, (1964).
5. F. Davis, H.W. Loeb, Proc IEEE, 53, 1649, (1965).
6. H. Fellner-Feldegg, J. Phys. Chem., 73, 616, (1969).
7. H. Fellner-Feldegg, Hewlett-Packard Application Note No 118, (1970).
8. R.P. Bagozzi, MS Thesis, University of Colorado, June (1969).
9. R.P. Bagozzi, W.R. Ives, N.S. Nahman, Progress in Radio Science 1966-1969, 2, 257, (1971).
10. A.M. Nicolson, G.F. Ross, IEEE transactions on Instrument. Measurement, IM-19, 377, (1970).
11. T.A. Whittingham, J. Phys. Chem., 74, 1824, (1970).
12. A. Suggett, P.A. Mackness, M.J. Tait, H.W. Loeb, G.M. Young, Nature, 228, 456, (1970).
13. H.W. Loeb, G.M. Young, P.A. Quickenden, A. Suggett, Ber. Bunsenges. Phys. Chem., 75, 1155, (1971).
14. S.C. Harvey, Thesis, Dartmouth College, June (1971).
15. G. Doetsch, Theorie und Anwendung der Laplace Transformation, Dover Publications, New York, (1943), page 373.
16. S. Ramo, J.R. Whinnery, T. van Duzer, Fields and Waves in Communication Electronics, John Wiley, New York, (1965), page 292.
17. R.A. Chipman, Theory and Problems of Transmission Lines, Schaum's Outline Series, Mc Graw Hill, New York, (1968), page 77.
18. H.A. Kramers, Phys. Z., 30, 522, (1929).
19. R. Kronig, J. Opt. Soc. Am., 12, 547, (1926).
20. N.G. van Kampen, Ned. T. Natuurkunde, 24, 1, (1958).
21. A. Papoulis, The Fourier Integral and its Applications, Mc Graw Hill, New York, (1962).
22. J.R. Mac Donald, M.K. Brachman, Rev. Mod. Phys., 28, 393, (1956).
23. E.C. Titchmarsh, Introduction to the Theory of Fourier Integrals, Oxford University Press, 2nd ed., Oxford, (1948).
24. D.V. Widder, The Laplace Transform, Princeton University Press, Princeton, (1946).
25. M.J.C. van Gemert, J.G. de Graan, Appl. Sci. Res., 26, No 1, May (1972).
26. P.J.W. Debye, Polar Molecules, Dover Publications, New York, (1929).
27. H. Fellner-Feldegg, E.F. Barnett, J. Phys. Chem., 74, 1962, (1970).
28. K.S. Cole, R.H. Cole, J. Chem. Phys., 9, 341, (1941).

29. D.W. Davidson, R.H. Cole, J. Chem. Phys., 18, 1417, (1951).
30. D.W. Davidson, R.H. Cole, J. Chem. Phys., 19, 1481, (1952).
31. M.J.C. van Gemert, J. Phys. Chem., 75, 1323, (1971).
32. M.J.C. van Gemert, P. Bordewijk, Appl. Sci. Res., to be published.
33. P. Bordewijk, M.J.C. van Gemert, Advances in Molecular Relaxation Processes, in the press (1972).
34. J.P. Schouten, Operatorenrechnung, Springer Verlag, Berlin, (1961), page 152.
35. M. Abramowitz, I.A. Stegun, Handbook of Mathematical Functions, N.B.S., (1964), page 255.
36. G. Doetsch, Guide to the Application of Laplace Transforms, Van Nostrand, (1961), page 210.
37. C.J.F. Böttcher, Theory of Electric Polarisation, Elsevier, Amsterdam, (1952).
38. C.P. Smyth, Dielectric Behaviour and Structure, Mc Graw Hill, New York, (1955).
39. V.V. Daniel, Dielectric Relaxation, Academic Press, London, (1967).
40. N.E. Hill, W.E. Vaughan, A.H. Price, M. Davies, Dielectric Properties and Molecular Behaviour, Van Nostrand Reinhold, London, (1969).
41. Reference 35 page 377.
42. H.A. Samulon, Proc. IRE, 39, 175, (1951).
43. C. Shannon, Proc. IRE, 37, 10, (1949).
44. P.A. Quickenden , A. Suggett, Private communication.
45. A. Suggett, Chem. Soc. Specialist Periodical Reports, 31, (1972).
46. H. Fellner-Feldegg, Hewlett-Packard Application Note, 153, (1972).
47. Handbook of Chemistry and Physics, 49th ed, The Chemical Rubber Co., (1968).
48. D. Hadzi, Hydrogen Bonding (Papers presented at the Symposium on Hydrogen Bonding held at Ljubljana, 29 July - 3 August 1957), Pergamon, (1959).
49. G.C. Pimentel, A.L. McClellan, The Hydrogen Bond, W.H. Freeman, (1960).
50. S.N. Vinogradov, R.H. Linell, Hydrogen Bonding, Van Nostrand Reinhold, (1971).
51. P. Bordewijk, Thesis, Leiden, (1968).
52. J. Crossley, Adv. Mol. Rel. Proc., 2, 69, (1970).
53. R.H. Cole, D.W. Davidson, J. Chem. Phys., 20, 1389, (1952).
54. C. Brot, Ann. de Phys., 13-2, 714, (1957).
55. W. Dannhauser, A.F. Flueckinger, Phys. Chem. Liquids, 2, 37, (1970).
56. J. Middelhoek, C.J.F. Böttcher, Molecular Relaxation Processes, Chem. Soc. Spec. Publ., 20, 69, (1966).
57. J. Middelhoek, Thesis, Leiden, (1967).
58. P. Bordewijk, F. Gransch, C.J.F. Böttcher, J. Phys. Chem., 73, 3255, (1969).
59. J. Crossley, J. Phys. Chem., 75, 1790, (1971).
60. J. Crossley, Can. J. Chem., 49, 712, (1971).
61. J. Crossley, L. Glaser, C.P. Smyth, J. Chem. Phys., 55, 2197, (1971).

62. M. Moriamez, Thesis, Lille, (1959).
63. M.W. Sagal, J. Chem. Phys., 36, 2437, (1962).
64. D.J. Denney, J.W. Ring, J. Chem. Phys., 39, 1268, (1963).
65. J.F. van den Berg, Thesis, Amsterdam, (1972).
66. G.H. Barbenza, J. Chim. Phys., 65, 906, (1968).
67. S.K. Garg, C.P. Smyth, J. Phys. Chem., 69, 1294, (1965).
68. S. Glastone, K.J. Laidler, H. Eyring, The Theory of Rate Processes, Mc Graw Hill, (1941).
69. P. Huyskens, G. Gillerot, Th. Zeegers- Huyskens, Bull. Soc. Chim. Belg., 72, 666, (1963).
70. E. Bauer, Cah. de Phys., 20, 1, (1944).
71. E. Bauer, Cah. de Phys., 21, 21, (1944).
72. E. Bauer, M. Magat, Bull. Soc. Chim. F., D341, (1949).
73. C. Brot, M. Magat, L. Reinisch, Koll. Zs., 134, 101, (1953).
74. C. Brot, M. Magat, J. Chem. Phys., 39, 841, (1963).
75. W. Dannhauser, J. Chem. Phys., 48, 1918, (1968).
76. M.J.C. van Gemert, G.P. de Loor, P. Bordewijk, P.A. Quickenden, A. Suggett, in preparation.
77. M.J.C. van Gemert, Chem. Phys.Lett., to be published, (1972).
78. B. Gross, Nuovo Cimento Suppl. III, series X, 235, (1956).
79. J.S. Toll, Phys. Rev., 104, 1760, (1956).
80. Reference 23 page 128.
81. F. Sommer, Mathematics Applied to Physics, E. Roubine ed., Springer Verlag, Berlin, (1970).
82. E.T. Whittaker, G.N. Watson, A Course of Modern Analysis, 4th ed., Cambridge, (1962).
83. R.E. Bellman, R.E. Kaleba, J. Lockett, Numerical Inversion of the Laplace Transform, American Elsevier, New York, (1966).
84. V. Zakian, Electron. Lett., 5, 120, (1969).
85. V. Zakian, Electron. Lett., 6, 677, (1970).
86. V. Zakian, D.R. Gannon, Electron. Lett., 7, 70, (1971).
87. H. Stehfest, Comm. of the ACM, 13, 47, (1970).
88. K. Singhal, J. Vlach, Electron. Lett. 7, 413, (1971).
89. J.G. de Graan, unpublished results, (1970).

SUMMARY

In this thesis, the use of Time Domain Reflectometry (TDR) is discussed as a technique for measuring the permittivity of polar liquids. Originating from the field of electronics and communication engineering (1960) this method has been applied to dielectric spectroscopy by Fellner-Feldegg (1968). Improvements in terms of the measuring technique and the mathematical analysis have been introduced by Suggett, Quickenden-Mackness, Tait, Loeb and Young (1969-1971). Due to these improvements, a rather accurate measurement technique is available now.

After an introduction to transmission line theory and linear system theory, in Chapter 1, some theoretical results are presented in Chapter 2. These results refer to the case of an ideal step function. In section 2.1 the TDR-step response is calculated numerically for three current descriptions of dielectric permittivity, including low-frequency conductivity. It is concluded that an evaluation of the dielectric parameters in the time domain, as was suggested in the early papers on TDR, is not possible since the response curves do not show enough characteristic features which enables such a time domain evaluation.

In section 2.2, an investigation has been carried out to the similarity of the asymptotic behaviour of the TDR-step response (in the time domain) and to the asymptotic behaviour of the permittivity, represented by a Cole-Cole plot, in the frequency domain. One of the main conclusions is that for dielectric materials of which the low-frequency side of the Cole-Cole plot does not cut the ε'-axis perpendicularly, as for instance for a Cole-Cole type of material, the TDR-decay is extremely slow in reaching its asymptotic value at $t = \infty$. This means that, in general, a material with a Cole-Cole behaviour cannot successfully be examined by means of the TDR-method described in this work. The results of the asymptotic calculations for $t \to 0$ suggest the possibility to determine the value of τ_0, in the case of a single relaxation time, from the derivative of the step response at $t = 0$. This method may be applicable when materials with very large values of τ_0 are involved (it will not be a very accurate one). The results of the asymptotic calculations for $t \to \infty$ suggest the possibility to determine the low-frequency conductivity, when this quantity is very large compared with dipolar losses.

In Chapter 3 an error analysis is presented, based upon TDR-measurements by means of an XY-recording system and the use of the time reference procedure as described in this thesis. The result is that the inaccuracy in the values of ε_0, ε_∞ and τ_0 (or ν_0) is approximately

$$\frac{\Delta\varepsilon_0}{\varepsilon_0} \simeq 5\% \quad , \quad \frac{\Delta\varepsilon_\infty}{\varepsilon_\infty} \simeq 20\% \quad , \quad \frac{\Delta\nu_0}{\nu_0} \simeq 7.5\%$$

for the relaxation frequency range

$$0.2\ \ 10^9 < \nu_0 < 3\ \ 10^9$$

In Chapter 4 the results of the experiments are presented. Dielectric measurements, by TDR, have been carried out for the mono alcohols ethanol, propanol-1, butanol-1 and heptanol-1. These measurements, although intended as a test procedure to confirm the applicability and accuracy of TDR-measurements, contain some new data for propanol-1, at room temperatures, and for heptanol-1, at temperatures above 40^o C.

In section 4.3 the results of measurements on 1:1 volume mixtures of the mono alcohols with carbon tetrachloride are presented. Although the values found for the activation energy and the frequency factor are not very accurate (which is also true for frequency domain measurements), the results show that the values of E_A and of A for the mixtures tend to be larger than for the pure compounds. This effect is most pronounced for methanol, while it decreases (in percentages) with increasing length of the carbon chain. From the results of heptanol-1/carbon tetrachloride it seems that the values for E_A and A tend to be smaller than those of the pure compounds when the length of the chain is large.

The changes in the relaxation frequency, energy of activation and the frequency factor, after dilution of the pure alcohol by carbon tetrachloride are discussed in terms of a change in the amount of coordination in the polar liquid when an alcohol volume is replaced by the same non-polar CCl_4 volume.

The results on methanol are in contradiction to the statement of Dannhauser that for this compound breaking of the hydrogen bond would still be the rate determining step for the reorientation.

Finally, in Chapter 5, a general discussion of the TDR-method is presented, incorporating suggestions for further work.

SAMENVATTING

Dit proefschrift is gewijd aan de toepassing van Time Domain Reflectometry (TDR) voor het meten van dielektrische eigenschappen van polaire vloeistoffen. Deze methode, die afkomstig is uit het vakgebied van de kommunikatie techniek, is het eerst toegepast op dielektrische spectroskopie door Fellner-Feldegg (1968). Verbeteringen van de meettechniek en van de mathematische verwerking, door Suggett, Quickenden-Mackness, Tait, Loeb en Young (1969-1971), hebben ertoe geleid dat nu een tamelijk nauwkeurige meetmethode beschikbaar is.

Na een inleiding in transmissie lijn theorie en lineaire systeem theorie, in Hoofdstuk 1, worden in Hoofdstuk 2 de resultaten besproken van responsie berekeningen voor een ideale stap funktie. In sektie 2.1 wordt de TDR-stap responsie numeriek berekend voor drie veel gebruikte beschrijvingen van de dielektrische permittiviteit, waarbij ook laag frequent geleiding in rekening wordt gebracht. De konklusie is dat een bepaling van de dielektrische parameters in het tijdsdomein, zoals was voorgesteld in de eerste artikelen over TDR, onmogelijk is omdat de responsie curven te weinig kenmerken bevatten voor zo'n bepaling.

In sektie 2.2 is een studie gemaakt van de overeenkomsten in het asymptotisch gedrag van de TDR-stap responsie (in het tijdsdomein) en de permittiviteit, in de Cole-Cole plot representatie (in het frequentie domein). Een van de belangrijkste konklusies is dat voor een dielektrisch materiaal waarvan de laagfrequent kant van het Cole-Cole plot de ε'-as niet loodrecht snijdt, zoals b.v. voor een "Cole-Cole materiaal", de TDR-decay extreem langzaam is in het bereiken van de asymptotische waarde op $t = \infty$. Dit betekent dat een dielektrisch materiaal met een "Cole-Cole gedrag" met de hier beschreven TDR-techniek in het algemeen niet onderzocht kan worden. De resultaten van de asymptotische berekeningen voor $t \to 0$ suggereren de mogelijkheid om voor een Debye dispersie de waarde van τ_0 te bepalen uit de afgeleide van de stap responsie op $t = 0$. Deze methode zou toegepast kunnen worden wanneer de waarde van τ_0 erg groot is, maar het zal geen erg nauwkeurige methode zijn. De resultaten van de asymptotische berekeningen voor $t \to \infty$ suggereren de mogelijkheid om de laagfrequent geleiding te bepalen, wanneer deze veel groter is dan de dipolaire verliezen.

In Hoofdstuk 3 wordt een fouten analyse gegeven welke geheel gebaseerd is op de TDR-techniek zoals hier beschreven, dus op het gebruik van een XY-rekorder en de besproken tijd referentie procedure. Het resultaat is dat de onnauwkeurigheden in de waarden van ε_0, ε_∞ en ν_0 (of τ_0) globaal gegeven worden door

$$\frac{\Delta\varepsilon_0}{\varepsilon_0} \simeq 5\% \quad , \quad \frac{\Delta\varepsilon_\infty}{\varepsilon_\infty} \simeq 20\% \quad , \quad \frac{\Delta\nu_0}{\nu_0} \simeq 7.5\%$$

in het relaxatie frequentie gebied

$$0.2\ \ 10^9 < \nu_0 < 3\ \ 10^9$$

In Hoofstuk 4 worden de resultaten van de metingen gegeven. Dielektrische metingen m.b.v. TDR zijn verricht aan ethanol, propanol-1, butanol-1 en heptanol-1. Hoewel deze metingen bedoeld zijn als een test procedure ter bevestiging van de toepasbaarheid en nauwkeurigheid van TDR-experimenten, bevatten zij nieuwe gegevens voor propanol-1 bij kamertemperatuur en voor heptanol-1 bij temperaturen boven 40^oC.

In sektie 4.3 zijn de resultaten weergegeven van metingen aan 1:1 volume mengsels van de mono alkoholen met tetrachloorkoolstof. Hoewel de gevonden waarden voor de aktiveringsenergie en de frequentie faktor niet zeer nauwkeurig zijn (dit is echter eveneens het geval voor frequentie domein metingen) , tonen de resultaten aan dat de waarden voor E_A en A groter zijn voor de mengsels dan voor de pure alkoholen. Dit effekt is het duidelijkst voor methanol terwijl het afneemt (procentueel) bij toenemende lengte van de koolstof keten. Uit de resultaten aan heptanol-1/CCl_4 kan echter de trend worden afgeleid dat de waarden voor E_A en A kleiner worden dan die van de pure alkoholen wanneer de koolstof keten erg lang is.

De verandering in de relaxatie frequentie, aktiverings energie en frequentie faktor, wanneer de alkoholen met CCl_4 worden verdund, worden besproken door de veranderingen die optreden in de hoeveelheid koordinatie in de polaire vloeistof wanneer een volume eenheid van een alkohol wordt vervangen door een gelijke volume eenheid CCl_4.

De resultaten aan methanol zijn in tegenspraak met de aanname van Dannhauser dat voor deze vloeistof het breken van de waterstof binding de snelheidsbepalende stap is voor reorientatie.

Tot slot is in Hoofdstuk 5 een algemene diskussie gegeven over de TDR-methode, waarbij ook suggesties voor voortgezet onderzoek zijn opgenomen.

Dit proefschrift zou niet tot stand gekomen zijn zonder de bijdragen van anderen.

In de eerste plaats geldt dit Dr. Ir. G.P. de Loor, die de TDR-methode heeft geintroduceerd op het Physisch Laboratorium TNO en die het werk in alle stadia op een plezierige en zeer intensieve manier heeft begeleid en gestimuleerd. Behalve het oplossen van wetenschappelijke problemen heeft hij ook vele buiten ons om gegenereerde (minder wetenschappelijke) problemen tot een oplossing weten te brengen. Ook Dr. P. Bordewijk heeft tot het ontstaan van dit proefschrift op vele manieren een wezenlijke bijdrage geleverd, waaronder het suggereren van het in Hoofdstuk 4 beschreven onderzoek en z'n bijdragen aan de asymptotische berekeningen. H. Gravesteijn heeft door vele diskussies over signaal verwerking en Fourier analyse, en door een deel van het komputerwerk voor z'n rekening te nemen eveneens belangrijk bijgedragen. Wat betreft het numerieke werk hebben Ir. J.G. de Graan en J. de Vries belangrijk werk verricht. Een deel van de testexperimenten zijn uitgevoerd door D.L.A. Osseman en de experimenten beschreven in Hoofdstuk 4 zijn uitgevoerd door A.J. van der Lugt, die voor dit doel enige maanden in ons groepje heeft meegewerkt. De gegevens van de experimenten werden geponst door Mej. E.M. Bouman (40 keer 600 punten) terwijl de destillaties van de vloeistoffen door Mej. J. Kouwenhoven werden verricht. Met elektronika problemen werd ik geholpen door J.F.C. Baesjou, J. van Reenen en J. de Stigter, terwijl de mechanische problemen door P. Leemans werden opgelost. De tekeningen van de Hoofdstukken 1 en 2 zijn vervaardigd door de tekenkamer van het Physisch Laboratorium TNO terwijl de tekeningen van de Hoofdstukken 3 en 4 door de heer P. Vissers (Philips Natuurkundig Laboratorium) gemaakt zijn.

Aan de direktie van het Physisch Laboratorium TNO betuig ik mijn dank voor het feit dat ik na mijn militaire dienst nog drie maanden lang in de gelegenheid bengesteld (wetenschappelijk en financieel) dit werk af te ronden, waarbij verder het bekostigen van het werkbezoek aan Dr. A. Suggett en Mevr. P.A. Quickenden van zeer grote invloed is geweest.

De direktie van het Philips Natuurkundig Laboratorium ben ik zeer erkentelijk voor het feit dat zij mij na mijn militaire dienst nog drie maanden verlof heeft gegeven om het hier beschreven werk af te maken. Verder wil ik gaarne memoreren dat zij het mij financieel mogelijk heeft gemaakt om tijdens mijn militaire diensttijd de in Oxford gehouden Advanced Summer School in Theoretical Chemistry, o.l.v. Prof. C.A. Coulson, bij te wonen; en dat zij de kosten, verbonden aan het offset drukken van dit proefschrift, voor haar rekening heeft genomen.

I am very indepted to Dr. A Suggett and to Mrs. P.A. Quickenden for their hospitality and quidence during my stay at the Unilever Research Laboratories. This stay has been of great importance for learning how to work out TDR-experiments. The numerous discussions during this stay and also before and afterwards, by telephone, have contributed much to my knowledge.

I am also very grateful to Mr. and Mrs. R.E. Turvey for their hospitality during all my visits to England and to Mr. Turvey for his careful reading of the entire manuscript.

Ik ben mijn vrouw zeer dankbaar voor het vele werk dat zij voor mij gedaan heeft, waaronder het uittypen van het manuscript en het (gezamenlijk) digitaliseren van ca. dertig XY-curven.

Na het behalen van het einddiploma HBS-B, aan de Gemeentelijk HBS te Delft in 1962, werd datzelfde jaar begonnen met de Natuurkunde studie aan de Technische Hogeschool te Delft. Het P2 examen werd in 1966 behaald. Het vierdejaars werk (een onderzoek naar de ESR-spektra van instabiele fenoxy radikalen) en het vijfdejaars werk (een ESR-studie naar lijnbreedte effekten en temperatuurafhankelijkheid van koppelingskonstanten van enige fenoxy radikalen) werd verricht in de werkgroep Magnetische Resonantie o.l.v. Prof. Dr. Ir. J. Smidt. In het vierde studiejaar bezocht ik bovendien de Summer School in Theoretical Chemistry, o.l.v. Prof. C.A. Coulson te Oxford, hiebij financiel gesteund door het Delftse Lipkensfonds. Na het afstuderen op 24 juni 1969 bleef ik nog tot 5 januari 1970 bij de werkgroep M.R. Vanaf 16 januari 1970 ben ik verbonden aan het Natuurkundig Laboratorium van de N.V. Philips' Gloeilampen Fabrieken.

Mijn militaire dienst periode, welke 5 januari 1970 aanving, heb ik vanaf maart 1970 doorgebracht op het Physisch Laboratorium TNO te Den Haag, in de groep van Dr. Ir. G.P. de Loor. Het daar verrichte onderzoek aan TDR is in dit proefschrift vastgelegd. In september 1971 werd ik in de gelegenheid gesteld om drie dagen op het Unilever Research Laboratorium te werken bij Mevr. P.A. Quickenden en Dr. A. Suggett. In juli 1971 bezocht ik opnieuw de cursus Advanced Summer School in Theoretical Chemistry in Oxford, o.l.v. Prof. C.A Coulson, nu financieel gesteund door de N.V. Philips.

Sinds januari 1972 ben ik daadwerkelijk verbonden aan het Philips Natuurkundig Laboratorium, in de groep Gasontladingen.